OREGON HEALTH & SCIENCE UNIVERSITY
SCHOOL OF MEDICINE – GRADUATE STUDIES

SPATIOTEMPORAL DISTRIBUTION OF THE ANTI-
DIABETIC DRUG, METFORMIN, IN THE LOWER
COLUMBIA RIVER AND ITS EFFECT ON
PHYTOPLANKTON GROWTH

By

Brittany M. Cummings

A THESIS

Presented to the Institute of Environmental Health
and the Oregon Health & Science University
School of Medicine
in partial fulfillment of
the requirements for the degree of

Master of Science

March 2018

School of Medicine

Oregon Health & Science University

Certificate of Approval

This is to certify that the Master's Thesis of

<u>Brittany M. Cummings</u>

*"Spatiotemporal Distribution of the Anti-Diabetic Drug,
Metformin, in the Lower Columbia River and its Effect on
Phytoplankton Growth"*

Has been approved

_____
Thesis Advisor

_____
Committee Member

_____
Committee Member

_____
Committee Member

TABLE OF CONTENTS

ACKNOWLEDGMENTS

ABSTRACT

Water quality impacts both human and ecosystem health. Many pharmaceuticals and personal care products are considered contaminants of emerging concern (CEC) due to their bioactive properties. Among these, metformin—the most commonly prescribed drug for treatment of type 2 diabetes—has been reported at high concentrations (μg L^{-1}) in stream, lake, and estuary surface waters in the United States. However, a propensity for broad-scale CEC surveys has prevented seasonal and spatial monitoring of metformin in river systems. Moreover, the effect of metformin in river food webs remains poorly explored, despite its known action on conserved eukaryotic enzymes (AMPK/SnRK1/SNF1). This project comprised the first spatiotemporal characterization of metformin in a high-discharge river system and examined the effects of metformin on aquatic primary producers. Monthly water samples were taken at eight year-round sites and five additional summer-sites in the lower Columbia River from October 2016-September 2017. Metformin and its breakdown product, guanylurea, were determined from water samples using direct injection with liquid chromatography coupled to tandem mass spectrometry (LC-MS/MS). Laboratory toxicity assays using PAM fluorometry and environmentally or sewage relevant doses (50-500 μg L^{-1}) probed for effects of metformin on photosynthetic efficiency in green algae (*Chlorella vulgaris*) and diatom (*Thalassiosira weissflogii*) cultures. Metformin and guanylurea were successfully detected and quantified in the lower Columbia River (MET$_{AVG}$ = 67.4 ng L^{-1}, GUAN$_{AVG}$ = 32.6 ng L^{-1}). High variation in metformin concentrations was only partially explained by seasonal river discharge and riverine sources; but possible sorption effects suggested additional physicochemical influence. Metformin effects on algae depended on exposure

time, dose, and species, with reduced photosynthetic efficiency of *C. vulgaris* cultures

within 24 h of high dose exposure (500 µg L^{-1}), and within 72 h of sewage effluent-

equivalent exposure (50 µg L^{-1}). Overall, these results are consistent with the expected

behavior of a polar basic cation species in a high-flow river system and a SnRK1-

activator in algae. This study illustrates the importance of investigating individual CECs

in water systems in order to elucidate fine-scale processes governing distributions,

behavior, and, ultimately, environmental risk.

LIST OF TABLES

Chapter 3

Appendix

LIST OF FIGURES

xiii

LIST OF ABBREVIATIONS

1. CEC = contaminant of emerging concern

2. PPCP = pharmaceutical and personal care product

3. WWTP = wastewater treatment plant

4. MET = metformin

5. GUAN = guanylurea

6. G:M = guanylurea:metformin ratio

7. USGS = United States Geological Survey

8. EPA = U.S. Environmental Protection Agency

9. LC-MS/MS = liquid chromatography coupled with tandem mass spectrometry

10. K_{ow} = octanol-water partition coefficient

11. pK_a = an index of acid dissociation constant K_a

12. K_{oc} = organic carbon-water partition coefficient

13. K_d = adsorption-desorption coefficient

14. AMPK = AMP-activated protein kinase

15. SnRK1 = SNF1-related kinase 1

CHAPTER 1: INTRODUCTION

1.1. Chemicals of Emerging Concern in the Environment

Water quality impacts both human and ecosystem health. As a result, there is a growing concern over the occurrence of trace organic contaminants in water systems around the world. These so-called "contaminants of emerging concern" (CECs) are distinguished from priority pollutants (e.g. polycyclic aromatic hydrocarbons, polychlorinated biphenyl) by lack of monitoring/regulation and poorly described or unknown environmental fate and toxicity.[1,2] Analysis of waste suggests that CEC compounds ultimately originate from human activities, including, for example, hospitals, households, farmland, and industry.[3–5] Examples of CECs include medicinal drugs, industrial compounds (e.g. polybrominated diphenyl ethers, perfluorinated compounds), household chemical, and agricultural pesticides.[3] CECs have most recently been identified as "agents of global change" since their production currently outpaces rising atmospheric CO_2 concentrations, nutrient pollution, habitat destruction, and biodiversity loss.[6]

Much recent research is devoted to tracking the distribution and fate of CECs in the environment.[7–14] CECs enter and move through the environment via pathways that depend on the compound's physicochemical properties in relation to its respective surroundings.[15–19] For instance, a polar, hydophilic compound will likely exhibit high mobility in the environment, while a nonpolar, hydrophobic compound will tend to bioaccumulate and/or adsorb to surfaces.[15,20] These chemical characteristics determine the overall degree of degradation, persistence, and bioavailability of the compound in the environment and, thus, overall environmental risk.[21–23] However, oversimplification of

physicochemical properties by compound types have led to mispredictions of CEC behavior in different environments.[24–26]

Concerns over CECs are built around human and wildlife toxicity. By the United States Geological Survey (USGS) definition, CECs are foreign agents in the environment with the potential to harm living organisms.[27] Effects of CECs on humans, plants, and other organisms range from no effect to chronic or acute toxicity.[28–34] Possibly the first and most iconic example of a publicly recognized CEC was the pesticide dichlorodiphenyltrichloroethane (DDT), which was eventually recognized as a priority pollutant and banned as a result of poignant observations regarding DDT-associated bird mortality in Rachel Carson's 1962 book "Silent Spring".[35] While there is considerable interest in CEC effects in drinking water due to its obvious connections with public health,[36–38] perhaps of greater concern are non-human organisms that are exposed to CECs over their entire life, such as aquatic and sediment-dwelling organisms.[3] Many aquatic organisms may uptake CECs through filtering or direct ingestion of water during oxygen exchange or feeding, while sediment-dwellers may similarly uptake CECs by ingestion of sediment during nutrient acquisition.[2] Constant exposure to CECs in water or sediment may lead to detrimental effects on, for example, macroinvertebrate community composition,[39] algal growth,[40–42] and fish reproduction or behavior.[43–45] Furthermore, these organisms are exposed to CECs over their entire life cycle for multiple generations which could result in slow cumulative physiological or ecological alterations over time that remain undetected.[3]

1.2. Pharmaceuticals as Emerging Contaminants

1.2.1. Rise of PPCPs in the Environment

Pharmaceuticals and personal care products (PPCPs) have gained attention as CECs due to advances in analytical instrumentation (liquid chromatography/tandem mass spectrometry, or LC-MS/MS) that allow low-level detection of polar organic compounds in aquatic and sediment environments.[46,47] Pharmaceutical compounds include synthetic and semi-synthetic compounds that are used to treat medical conditions in humans or animals (e.g., painkillers, statins, hormone supplements, antibiotics). Personal care products (PCPs) include compounds that improve quality of hygiene, health, or appearance through preventative or cosmetic function (e.g., lipstick, sunscreen, shampoo, toothpaste, deodorant). Numerous studies have detected PPCPs in wastewater, freshwater, seawater, and groundwater around the world.[9,13,26,46,48–50]

The environmental presence of PPCPs is correlated with an increasing reliance on manufactured pharmaceuticals for improved health and quality of life. It has been shown that increased consumption of PPCP products is directly linked to their presence as CECs in the environment.[51] Due to improvements in living conditions, education, and medical treatments over the past century, populations are now living longer and spending more on healthcare, which exceeds 10% of GDP on average in many countries.[52–55] Regarding improvements in medical treatments, pharmaceutical drug development has greatly increased over the past century to increase treatment options and efficacy;[56] for example, the National Institutes of Health (NIH) recently issued a new wave of "precision medicine" which will tailor pharmaceuticals to individual patients and increase the production of novel therapeutic compounds.[57] Furthermore, healthcare access (and,

therefore, access to pharmaceuticals) is improving around the world,[58] and there has been

a steep increase in non-medical pharmaceutical use.[59,60] As a result of a growing human

population with an increasing reliance on personal care, PPCPs, and pharmaceuticals in

particular, are now ubiquitous in the environment,[61] being found in even the most remote

locations.[62]

1.2.2. *Sources and Sinks of Pharmaceutical CECs*

Pharmaceuticals enter the environment through excretory waste or direct

disposal.[63–65] Specifically, most human or veterinary drugs pass through the body and

into the sewage waste stream, which enters a municipal wastewater treatment plant

(WWTP) for removal of contaminants and nutrients before release into local surface

waters. Hospital and manufacturer waste streams, which are treated either in a separate

treatment process or combined with municipal wastewater, also comprise major sources

of pharmaceuticals in the environment, in addition to leachate from pharmaceuticals

directly disposed to landfill.[66–69] Additionally, the use of recycled biosolids from

wastewater treatment plants for agricultural fertilizer also creates a source of

pharmaceuticals to the environment.[70]

Wastewater treatment often does not completely remove pharmaceuticals from

influent. Treatment strategies vary by plant, and typically consist of primary treatment

which filters out solids, secondary treatment which removes dissolved or suspended

particles, and, in advanced WWTPs, tertiary treatment which removes nutrients.[71]

Adsorption to suspended solids (sludge) and biodegradation by microbes in the

secondary, and sometimes tertiary, steps may break down pharmaceutical compounds

into metabolites.[64] The tertiary step may also (or alternatively) utilize additional treatment steps such as UV disinfection, microfiltration, ion exchange, and activated carbon adsorption,[71] which may increase pharmaceutical breakdown.[72] The specific chemical properties of each pharmaceutical compound determine its propensity for degradation[64,73] and many are resistant to complete degradation during wastewater treatment due to high solubility and low sorption to sludge.[4,74] As a result, wastewater breakdown varies with pharmaceutical type in wastewater and ranges from 6-98% removal efficiency of the parent compound.[65,75]

Pharmaceutical compounds ultimately end up in surface water or groundwater after passing through the waste stream. Surface water consists of water that has not penetrated the ground, such as streams, rivers, lakes, and oceans, while groundwater is surface water or precipitation that has been pulled by gravity into soil pore spaces and bedrock fractures to form underground aquifers. PPCPs enter surface water directly through wastewater effluent, land runoff, or contact with contaminated groundwater.[3,76] The groundwater zone receives PPCPs leached from landfill or biosolids[77] (likely enhanced by precipitation[78,79]) or transferred from surface water contact.[76] PPCP research indicates that pharmaceutical compounds are continually released into one of these two sinks at diluted, but detectable, concentrations relative to the waste stream (ng L^{-1} to μg L^{-1}) (Figure 1.1).[46,47]
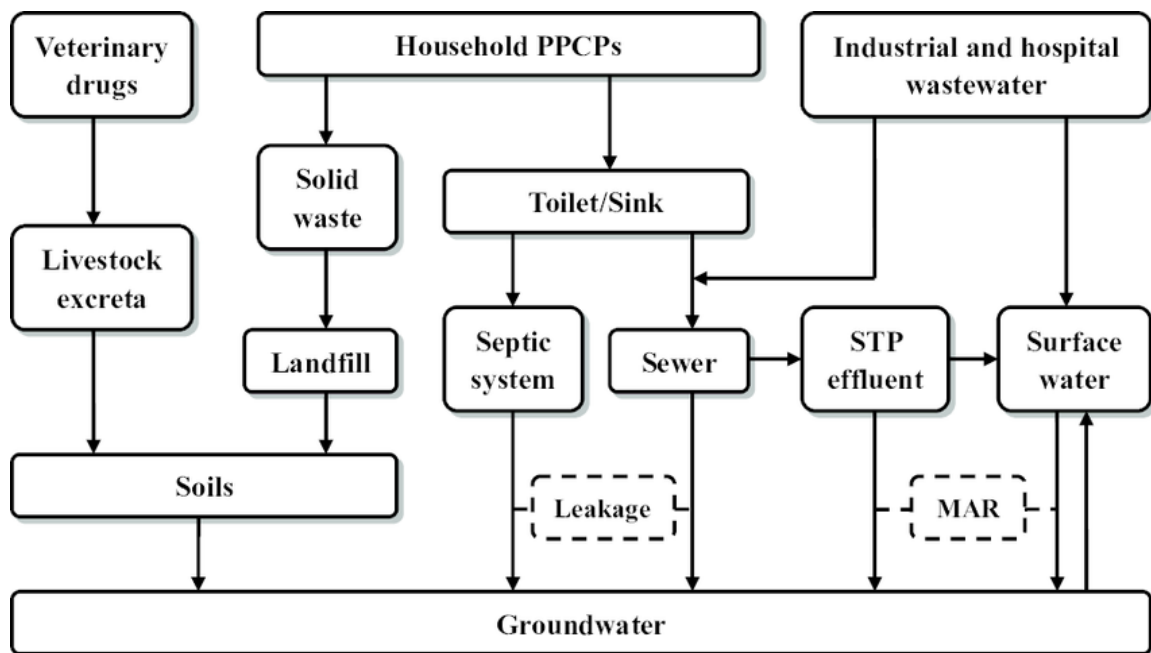
Figure 1.1. PPCP pathways from source to sink in the environment. Figure extracted from Sui et al 2015.[14]

1.2.3. *Pharmaceutical Activity in the Environment*

Pharmaceuticals comprise an extremely diverse class of chemical compounds.[80–82] With over 4000 molecules with different chemical structures,[80] each pharmaceutical drug has unique biochemical functions and physicochemical interactions in human or animal patient. These compounds can be natural, synthetic, or semi-synthetic and are designed for any number of treatments to combat microorganisms, destroy abnormal cells, replace deficits, or alter cellular function.[83,84] In order to function in their medical capacity, the drug must be chemically stable and delivered in active form to the target site in the body.[85] Since many parent pharmaceuticals are large, lipophilic, unionized or partially ionized species, drug metabolization in the body converts these drugs to more polar (water soluble) species for excretion by the kidneys.[86,87] Thus, based on the specific properties of a compound, some pharmaceuticals may remain unchanged,[88,89] and others

pharmaceuticals may be enzymatically broken down whereby a certain fraction of the parent compound exits the body as secondary metabolites;[90,91] either way, the parent compound is usually polar upon excretion.[86,87]

Many pharmaceuticals and personal care products are considered CECs due to their potential to affect non-target living tissue after excretion. Urinary excretion containing pharmaceutical compounds enter the waste stream where WWTP processes may further breakdown unchanged parent compounds and/or metabolites.[4,92,93] However, wastewater plants are not completely effective at breaking down the pharmaceutical compounds during treatment and many compounds enter the environment in their bioactive form.[4,92,93] Natural breakdown processes (e.g. photochemistry, radical reactions, biotic activity) may further degrade parent pharmaceutical concentrations in the environment but at a comparably slower rate than during wastewater treatment.[94] Since these compounds are typically polar and, therefore, have a low bioaccumulation factor, the "pseudo-persistence"[95] of pharmaceuticals in the environment is a result of higher input vs. degradation rates.[94]

As a result of continuous exposure and bioactivity at low doses,[96] medicinal drugs in surface waters have been linked to ecotoxicological effects. While acute toxicity has been observed,[97,98] chronic toxicity[44,99–102] is of particular concern due to the continual low dose exposure experienced by aquatic- and/or sediment-dwelling organisms.[103] It many cases, drugs with specific physiological functions interact with the same tissue of non-target organisms as they do with the intended recipient. The most obvious example is steroid hormones and their endocrine-disrupting effects on fish.[44,100,104,105] Additional examples include antibiotics reducing algae growth,[106,107] and behavioral drugs (e.g.

antidepressants, anti-anxiety medication) altering foraging strategies (i.e., risk/reward tradeoff) in crabs[108] and nesting behavior in fish.[109,110] Thus, pharmaceuticals can have far-reaching consequences reaching from individual mortality to population-wide ecosystem function.[102]

Due to the possibility of harmful ecological effects, regulations have been put into place regarding environmental risk assessment of pharmaceuticals.[111–116] Regulations are generally determined from the chemical properties of the parent compound (typically the octanol-water partition coefficient, K_{ow}, as a predictor of bioaccumulation) in conjunction with growth inhibition or toxicity assays. The measured level of toxicity is compared against the predicted environmental concentration (PEC), which is calculated from known sales, dosage, and dilution values, in order to determine the environmental risk associated with the pharmaceutical compound. However, since freshwater matrices are complex mixtures constantly influenced by environmental and chemical variables, pharmaceutical compounds may behave in unpredictable manners in the environment.[24–26] A more parsimonious method for understanding pharmaceutical risk in the environment is direct measurement of compound distribution and behavior relative to individual variables within a multi-variate model.

1.3. The Antidiabetic Drug Metformin as an Emerging Contaminant

1.3.1. Type 2 Diabetes & Pharmaceutical Treatment

One of the most common chronic medical conditions requiring pharmaceutical treatment is the hyperglycemic condition of diabetes mellitus type 2 (i.e., Type 2 diabetes). According to the Centers for Disease Control and Prevention (CDC), ~30% of

the U.S. population were estimated to have Type 2 diabetes in 2015.[117] On a global scale,

an estimated 8.5% of the world population suffers from Type 2 diabetes, and is increasing

at relatively higher rates in low and middle income countries.[118] As a result of this rapid

increase in disease occurrence, Type 2 diabetes has been labeled a global epidemic

(Figure 1.2).[119–121]

2013 Diagnosed Diabetes Prevalence

Percentage in quintiles
0–7.83
7.84–8.80
8.81–9.96
9.97–11.65
≥11.66

Puerto Rico
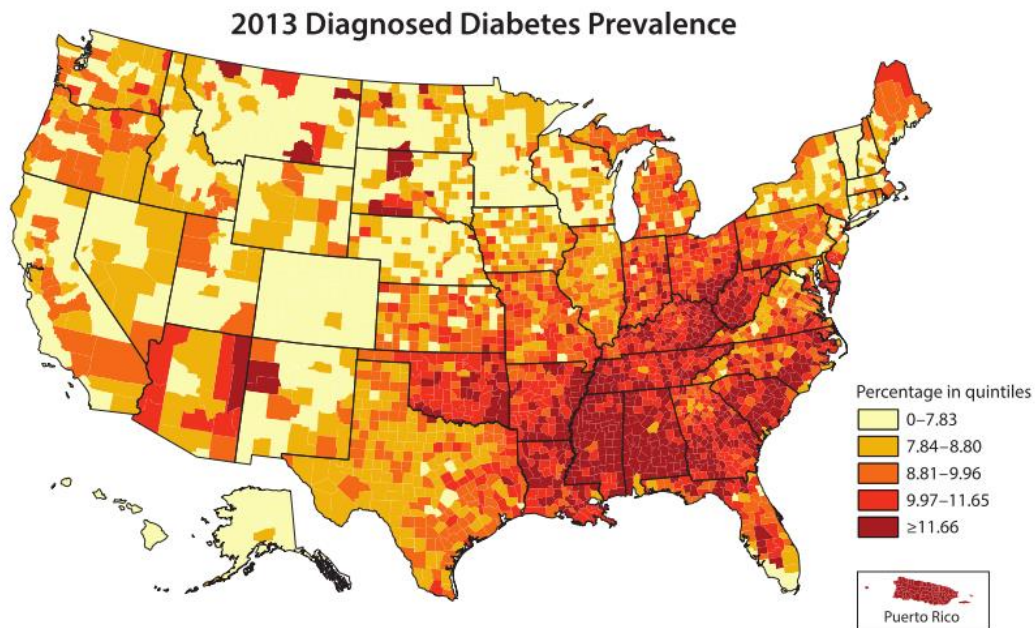
Figure 1.2. Percentage of U.S. adults ≥20 years diagnosed with Type 2 diabetes in 2013. Figure extracted from 2014 Centers for Disease Control and Prevention (CDC) National Diabetes Statistics Report (US Department of Health and Human Services).[117]

Type 2 diabetes is a state of insulin resistance which reduces the body's ability to

take up glucose from the bloodstream and stop the production of glucose in the

liver.[122,123] Insulin is produced by beta cells in the pancreas in response to glucose and

released into the bloodstream for delivery to tissue cells.[124] In a normal functioning body,

insulin binds to receptors on muscle, brain, liver and fatty tissue cells which open

transmembrane channels that uptake glucose from the bloodstream.[124] In response to

insulin binding, liver cells increase glycolysis (i.e., breakdown of glucose) and reduce

9

gluconeogenesis (i.e., production of glucose) which provides a negative feedback loop to reduce glucose levels in the blood.[124,125] The Type 2 diabetes condition is associated with insulin desensitization, where cells lose or reduce their ability to bind insulin.[122] The result is a continual state of hypoglycemia from inhibited glycolysis and an excess of glucose in the blood.[126] Moreover, pancreatic beta cells lose their ability to function and lower the production of insulin over time.[127,128] Thus, complications from high blood sugar are chronic and range from retinopathy, kidney disease, neuropathy, and macrovascular problems.[129] While genetics may increase predisposition to insulin resistance, Type 2 diabetes is largely determined by lifestyle factors, including excess weight, unhealthy diet, low physical activity, and substance abuse.[130]

Since Type 2 diabetes is a progressive disease, doctors treat the condition based on a step-wise diagnostic procedure.[131] Pre-diabetes or early-stage Type 2 diabetes is first treated with diet and exercise in order to manage hyperglycemia.[131,132] If lifestyle changes are not enough to manage elevated blood glucose levels, an oral medication is prescribed.[131] These oral medications typically utilize one of three strategies for reducing glucose in the body: inhibiting carbohydrate metabolism, stimulating insulin release, or increasing insulin sensitivity.[131] Insulin injections are used to treat Type 2 diabetes if lifestyle changes combined with oral medication is still not effective in blood sugar management (Figure 1.3).[131]
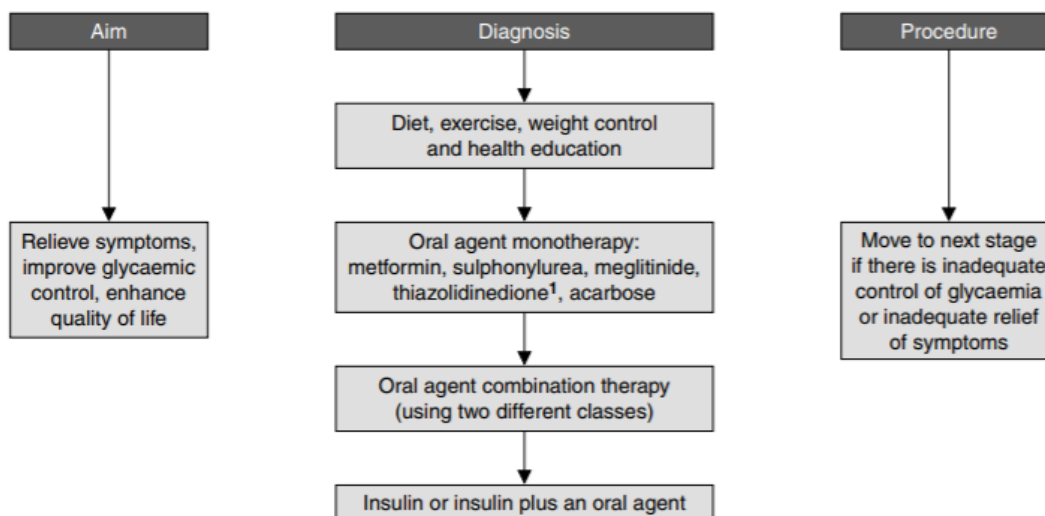
Figure 1.3. A step-care approach to Type 2 diabetes treatment. Figure extracted from Krentz and Bailey 2005.[131]

The biguanide drug, metformin, is the most commonly prescribed oral medication for Type 2 diabetes.[133] The origin of metformin traces back to medieval medicine and the use of extracts (i.e., "Goat's Rue") from the French lilac plant, *Galega officinalis*, to treat diabetic-like symptoms.[134] These extracts contained guanidine compounds which were first linked to blood sugar effects in 1918.[135] However, attempts at using guanidine derivatives, including biguanides, for treatment of Type 2 diabetes often induced lactic acidosis in patients.[136] Specifically, lactate (an anion from lactic acid dissociation) is the end product of glycolysis which is partially recycled for glucose production; in guanidine-treated patients, activated glycolysis increased production of lactate while decreasing gluconeogenesis and removal of lactate, thereby stimulating lactic acidosis.[137] Unlike other biguanides of the time, metformin was a guanidine derivative which was able to lower blood glucose levels with much lower lactate production.[136] The antidiabetic properties of metformin were first discovered in the mid-20th century when the drug was successfully used to combat influenza by glucose starvation.[136] However,

metformin as a pharmaceutical drug did not catch on in the U.S. until the 1990's due to the poor reputation of biguanide drugs associated with lactic acidosis.[136] After FDA approval and many years of research on the mechanisms and pathways of metformin activity clarifying risk-benefits of using the drug, metformin is now the primary choice for oral treatment of Type 2 diabetes.[136,138]

1.3.2. Metformin Chemistry & Biochemistry

Metformin (1,1-Dimethylbiguanide) is a semi-synthetic biguanide compound with the chemical formula $C_4H_{11}N_5$ (Table 1.1). Two methyl groups attached to the guanidine side chain form a structure with polar basic properties and high stability.[139] As a pharmaceutical drug, metformin is commonly distributed as a colorless white hydrochloride salt for oral administration.

Metformin exists in solution as a freely soluble cation (Figure 1.4). Due to high polarity, metformin has a low K_{ow} (< 0) and is highly soluble in water/polar solvents (Table 1.1). With predicted acid dissociation constant (pK_a) values of 10.27 and 12.33, metformin exists as a double charged cation species at physiological pH (e.g. 7.4 in humans) and environmental pH (e.g. ~7.8-8.4 in the Columbia River) (Figure 1.4). Calculated and predicted values for metformin organic carbon-water partition coefficients (K_{oc}, or the adsorption-desorption coefficient, K_d, normalized to organic carbon content of a substrate) in soil and sediment are not well established, ranging from as low as 39.2 to as high as 3209 $L\,kg^{-1}$,[140,141] indicating possible sorption interactions under certain conditions (Table 1.1).[142]

Table 1.1. Relevant chemical information for metformin. Values obtained from www.chemicalize.com (accessed 26 Feb 2018) or EPI-Suite™ (U.S. Environmental Protection Agency, 2000-2012).

Common Name	Metformin
Molecular Structure	
IUPAC Name	3-(Diaminomethylene)-1,1-dimethylguanidine
Molecular Formula	$C_4H_{11}N_5$
CAS #	657-24-9
Average Mass	129.167 g mol^{-1}
pK$_a$ (ionization)	10.27, 12.33
Solubility (logS)	1.81
LogK$_{ow}$	-2.64
K$_{oc}$	3.05-3209 L kg^{-1}
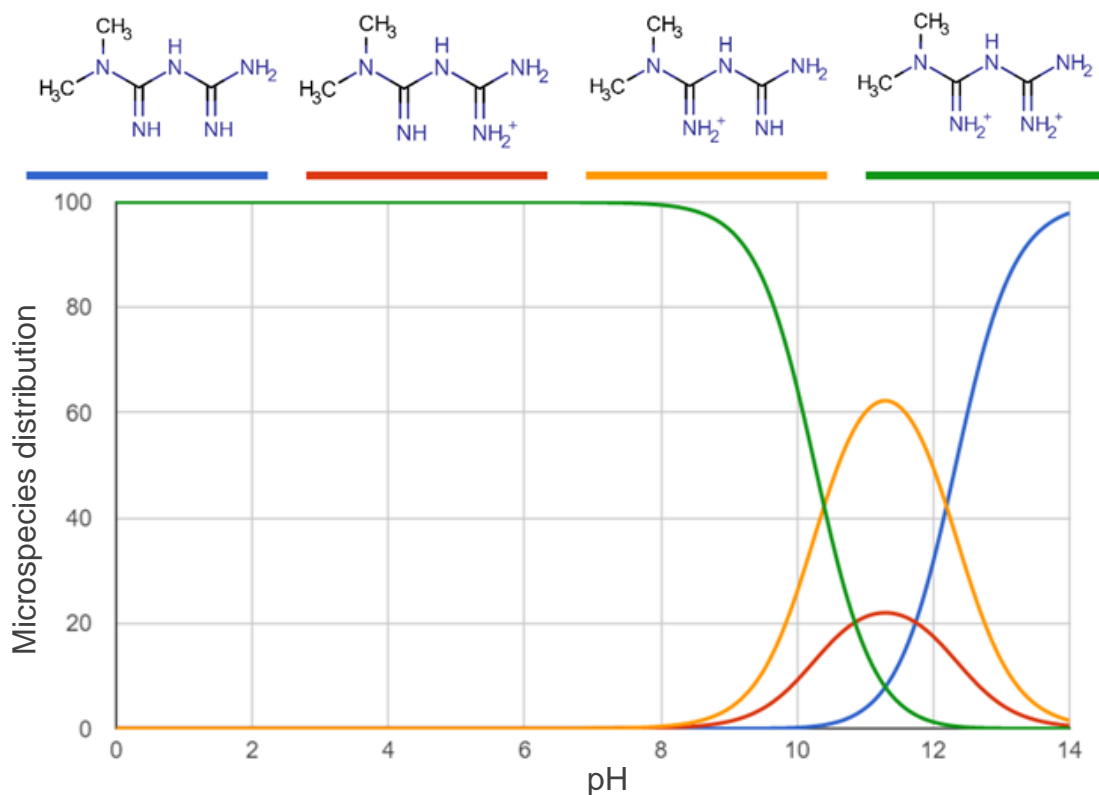
Figure 1.4. Metformin species distribution at different pH values. Intersection points represent where pH equals pKa (i.e., points with equal amounts of protonated and deprotonated metformin species). Graph obtained from www.chemicalize.com (accessed 26 Feb 2018).

While the mechanism of metformin antihyperglycemic activity is still an area of active research,[143–145] a primary pathway of metformin action is through activation of the cellular energy sensing enzyme, AMP-activated protein kinase (AMPK).[146] AMPK belongs to a class of energy-sensing enzymes responsible for maintaining energy homeostasis; specifically, AMPK promotes energy-releasing (catabolic) processes and downregulates energy-depleting (anabolic) processes in response to increasing adenosine monophosphate (AMP) levels relative to adenosine triphosphate (ATP) levels.[147] Thus, the stress response of a cell (i.e., reaction of a cell to reduced energy availability) is partially induced by AMPK activity.[148]

Metformin allosterically activates AMPK and induces a stress response in the cell to reduce blood glucose levels (Figure 1.5).[146,149] Research indicates that metformin may bind to Complex I of the mitochondrial electron transport chain by an unconfirmed mechanism and disrupt oxidation of NADH to NAD^+, thereby disrupting redox reactions within Complex I that normally generate the current responsible for transport of protons across the membrane.[150–152] Thus, metformin breaks down the proton gradient of the electron transport chain and reduces ATPase activity.[143] AMPK then senses the increase in AMP relative to ATP in the cell and signals a decrease in gluconeogenesis and increase in glycolysis.[143,146]
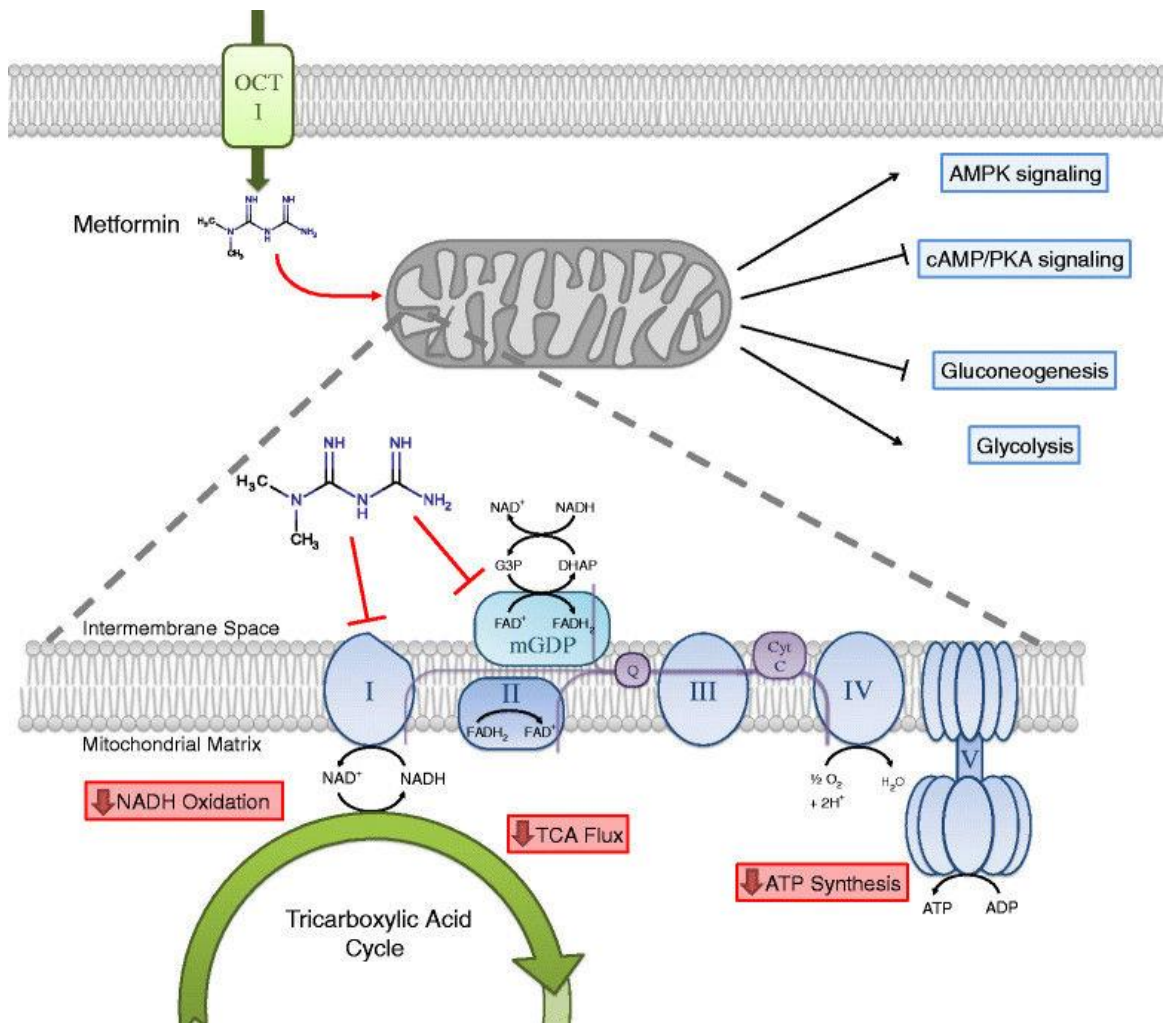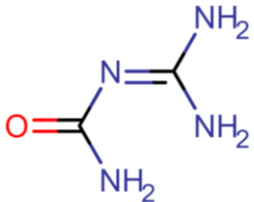
Figure 1.5. The AMPK pathway of metformin. Metformin inhibits Complex I of the mitochondrial electron transport chain, disrupting the transmembrane proton gradient which powers the production of ATP by ATPase. Sensing the increasing AMP:ATP ratio, AMPK promotes glycolysis and decreases gluconeogenesis. Figure extracted from Luengo et al 2014.

1.3.3. *Guanylurea as a Breakdown Product*

Degradation of metformin primarily occurs after excretion. Metformin remains largely unmetabolized by the body (>90% recovery) since the highly soluble compound does not readily bind to plasma proteins.[153,154] Upon exiting the body, metformin may remain in its parent form or break down by aerobic (and possibly anaerobic[155]) biodegradation into guanylurea.[156]

Guanylurea (Amidinourea, Dicyandiamidine) is the end-product of metformin degradation[156–158] with the chemical formula $C_2H_6N_4O$ (Table 1.2). The chemical structure of guanylurea consists of both urea and guanidine which, like metformin, lends polar basic properties and high stability. Guanylurea exists primarily as a single cation at physiological pH (e.g. ~7.4 in humans) and environmental river pH (e.g. ~7.8-8.4 in the Columbia River), based on predicted pKa values (Figure 1.6). Like metformin, guanylurea is highly soluble (low K_{ow}) and stable.[156] Values of K_{oc} are estimated to be low (~109 L kg^{-1}), but the physicochemical properties of guanylurea are poorly explored.

Table 1.2. Relevant chemical information for the breakdown product of metformin, guanylurea. Values obtained from www.chemicalize.com (accessed 26 Feb 2018) or EPI-Suite™ (U.S. Environmental Protection Agency, 2000-2012).

Common Name	Guanylurea
Molecular Structure	
IUPAC Name	diaminomethylideneurea
Molecular Formula	$C_2H_6N_4O$
CAS #	10310-28-8
Average Mass	102.097 g mol-1
pK$_a$ (ionization)	9.79, 13.62
Solubility (logS)	2.28 (pH 7.4), 2.08 (pH 8.0)
LogK$_{ow}$	-3.57
K$_{oc}$	109 L kg^{-1}

Figure 1.6. Guanylurea species distribution at different pH values. Intersection points represent the points where pH equals pKa, or the point where there are equal amounts of protonated and deprotonated guanylurea species in solution. Graph obtained from www.chemicalize.com (accessed 26 Feb 2018).

1.3.4. *Metformin in the Environment*

Due to chemical stability and high prescription rates, metformin has been reported at high concentrations in wastewater (μg L^{-1}) and surface waters (ng L^{-1}) around the world.[13,46,50,159–167] Metformin in the waste stream is only partially removed by biodegradation from wastewater treatment.[156,159] As a result, metformin in sewage effluent has been measured at concentrations ranging from ~1-150 μg L^{-1},[13,50,51,67,160,164,167,168] and in diluted surface waters at concentrations of ~0.001 to 8 μg L^{-1}.[13,50,160,162,165] Metformin has also been measured in groundwater at 3.0 μg L^{-1} and sediments up to 140 ng g^{-1},[160,168] thus illustrating the ubiquity of metformin as a PPCP in

17

the environment. Such wide ranges of distributions and concentrations between studies suggest that it is necessary to understand specific water systems (well-mixed vs poorly-mixed, closed vs open system, fresh vs saltwater) and pharmaceutical sources (i.e., local population demographics, local hospital abundance and treatment strategies, wastewater treatment) in relation to measured concentrations of metformin in order to better characterize and predict metformin as a CEC in the environment.

The breakdown product of metformin, guanylurea, co-occurs with metformin in wastewater and the environment. Studies reporting high metformin levels have measured guanylurea concentrations ranging from 48-67.2 µg L^{-1} in sewage effluent,[13,51] and ~0-50 µg L^{-1} in surface waters,[13,162] indicating a possible connection between metformin degradation and environmental guanylurea levels. However, there are multiple chemicals that may be in the environment that are known to break down into guanylurea, such as munition compounds[169] and chemotherapeutic compounds;[170] additionally, guanylurea is the base of the dicyandiamide component used in the manufacturing of melamine plastics[171,172] and fertilizer.[173,174] Thus, guanylurea in the environment may be a function of multiple compound breakdown processes and it is unknown whether measured levels accurately reflect metformin degradation.

Metformin in the environment has raised questions about ecotoxicological effects. The non-human toxicity of metformin is poorly explored, but limited research has shown potential endocrine disrupting effects in fathead minnows at sewage-relevant concentrations[31] and antimicrobial effects in microbiomes.[175] OECD toxicity assays have also revealed acute toxicity in zooplankton, juvenile zebrafish, and chironomids, but only at extremely high concentrations (mg L^{-1} and mg kg^{-1}).[140] Since the metformin parent

compound is bioactive with effects on a highly conserved enzyme, metformin may have unknown chronic effects on other members of the food web.

1.4. The Columbia River

1.4.1. Geography & Hydrology of the Columbia River

The Columbia River is the fourth largest river by discharge in North America[176] and comprises a major transport system for compounds in the environment.[177–179] The river drains an area of ~ 670,000 km^2 and forms a basin that encompasses 5 U.S. states and 1 Canadian province (Figure 1.7).[176] The Columbia stretches almost 2000 km, originating in the Rocky Mountains of British Columbia, Canada, and flowing northwest before turning south into the United States through Washington and then west on the border of Oregon. The river ends at the Pacific Ocean where it unloads water at an average rate of ~7730 m^3 s^{-1}.[180] The dominant climates of the watershed are largely determined by mountain range topography, with wetter and cooler climates west of the Cascades, and drier and warmer climates east of the Cascades.[181]

The large volume of water carried by the Columbia River is largely driven by a snowmelt-dominant watershed.[182,183] Freezing winter temperatures build snowpack in the mountains which annually melts from rising temperatures or rainfall on snow and causes an influx of water (i.e., freshet) into the mainstem during spring and early summer. Surprisingly, much of the Columbia watershed consists of arid/semi-arid climate; the Columbia Plateau (i.e., Columbia Basin), which comprises the southern area of the Columbia watershed east of the Cascades, receives less than 12 inches of precipitation each year.[184] Thus, precipitation and snowmelt from Canada supply ~44 percent of water

runoff east of the Cascade Mountains, while water runoff west of the Cascade Mountains (i.e., the lower Columbia River) is supplied by the Cascade Mountains and precipitation from southwestern Washington and the Willamette Valley.[184] Thousands of tributaries deliver water to the mainstem, but the two largest tributaries, the Snake River and Willamette River, supply ~32 percent of the average Columbia discharge rate.[180]

Seasonal river discharge and precipitation is critical to ecosystem function in the Columbia River. High flow creates pools and habitat for juvenile salmon and invertebrates along the river,[185,186] and may also limit fish predation by enabling downstream transportation, increasing turbidity, and regulating water temperature.[187] Moreover, strong river flow carries sediment downstream along with organic matter from detritus and sediment-based material which provides nutrients for phytoplankton growth after peak flow recedes.[187,188] Thus, seasonal river discharge largely dictates both hydrological and ecological processes in the Columbia River.
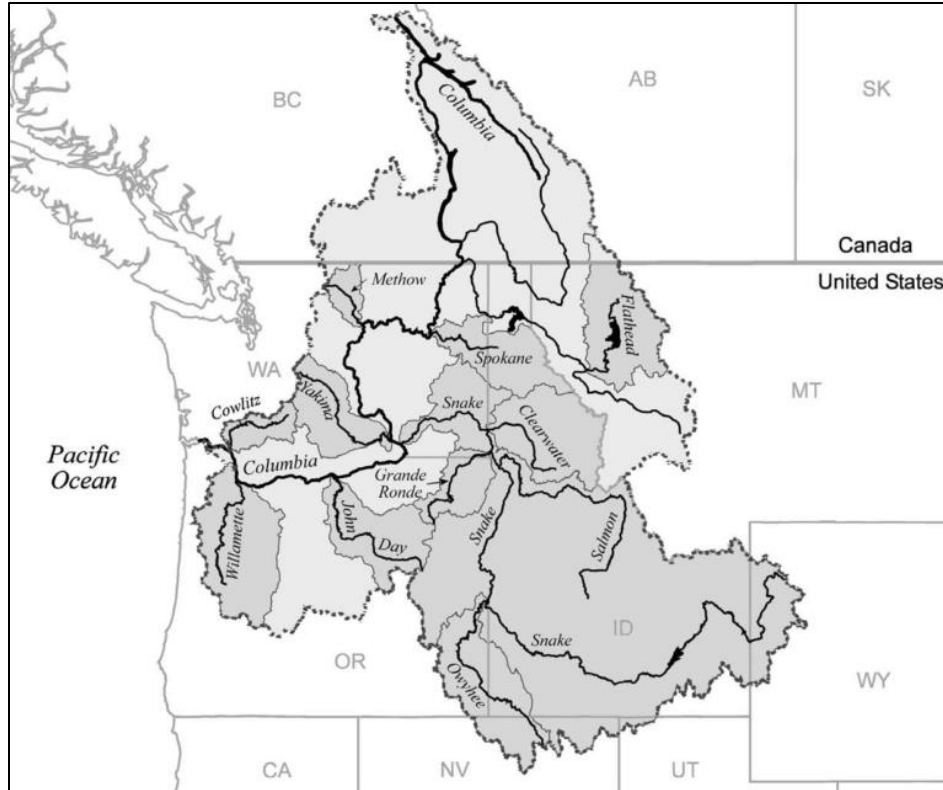
Figure 1.7. The Columbia River watershed. Map extracted from Benke and Cushing 2005.[180]

1.4.2. CECs in the Lower Columbia River Basin

The discovery of CECs in water systems around the world has led to the investigation of CECs in the lower Columbia River. As a historically important source of fresh water, abundant food resources,[189,190] energy,[191] and transportation, the Columbia River provides critical support for human populations and development in the region. The Columbia watershed has witnessed a steady increase in population growth from 1930 to present, a trend that is expected to continue until 2030.[192] Such a large population relying on one water system has influenced dramatic change on the river;[192,193] for instance, a number of hydroelectric dams have reduced the daily discharge of the annual freshet by ~30-50% percent,[194] overfishing and flow alteration have reduced salmon runs dramatically,[193,195] and urban development has altered riparian zones and ecosystem

21

functions.[196] More importantly, human waste and runoff have introduced numerous pollutants and CECs that are now being detected in the Columbia River.[47,197–202]

Most CEC research in the Columbia River is focused on the lower reach west of the Cascades.[47,197,199–202] This focus is a direct result of population distribution along the river; the lower Columbia River supports the highest population densities with large urban centers and industry,[192] and, therefore, likely experiences the highest diversity (and, perhaps, concentration) of waste input relative to a dominantly agricultural watershed. Reflecting this high density of contaminant input, numerous CECs in wastewater, surface water, and sediment ranging from PBDEs (flame retardants) to pesticides have been detected in the lower Columbia River at levels comparable to less dilute water systems.[47,197,199,201] Pharmaceuticals comprise a number of these CECs in the lower Columbia River[47,201] and are associated with toxicological effects on resident largescale sucker fish.[203,204]

Emerging contaminant studies in the lower Columbia River have mostly been limited to large-scale USGS[47,197,202] or U.S. Environmental Protection Agency (EPA)[205,206] surveys which prohibit a detailed analysis of single CECs in a high-volume river. As a result, CECs, which are known to be abundant in other systems, such as the pharmaceutical drug, metformin, remain uncharacterized in the Columbia River. Due to transport processes dictated by flow, it is expected that seasonal river discharge in a snowmelt-dominant system like the Columbia River would strongly influence individual CEC distribution. Thus, smaller-scale research is required to efficiently ascertain CEC patterns in relation to annual river variation.

1.5. Research Objectives

The aims of this study were (1) to characterize the spatiotemporal distribution of the antidiabetic drug, metformin, as a CEC in the lower Columbia River, and (2) to determine the effects of metformin on algae supporting the river food web.

In order to achieve these aims:

1. I measured the monthly concentrations of metformin and its breakdown product, guanylurea, at eight sites along the lower Columbia River over a one-year period using a direct-injection LC-MS/MS method.

2. I calculated the explained variation in metformin and guanylurea concentrations by (a) river condition and (b) geographic site in the lower Columbia River.

3. I measured the cell growth and photosynthetic activity of freshwater alga (*Chlorella vulgaris*) and marine diatom (*Thalassiosira weissflogii*) cultures in response to environmentally relevant and sewage relevant doses of metformin using Coulter counting and PAM fluorometry.

1.6. Significance of the Study

This study attempts to characterize the distribution and toxicology of a ubiquitous bioactive CEC in an economically and ecologically important high-volume river system. A better understanding of the amount, variation, and effects of metformin in relation to seasonal river conditions and geographic river location has relevance for CEC research in other snowmelt-dominant water systems and for predicting water quality concerns associated with rising rates of Type 2 diabetes around the world.

Furthermore, this study is a direct answer to members of the United States EPA and USGS who are urgently calling for more CEC research in U.S. waters.[207,208] The U.S.

contains numerous high-volume water systems which present a laborious and expensive task for future CEC assessments. This research demonstrates the scientific and financial efficacy of focusing on single contaminants in these dynamic high-volume systems in order to acquire more informative distribution data of a physiochemically complex compound.

CHAPTER 2: DISTRIBUTION OF METFORMIN & GUANYLUREA IN THE LOWER COLUMBIA RIVER

2.1. Introduction

There is a distinct paucity of pharmaceutical and personal care product (PPCP) data for high-volume river systems. As primary sources of freshwater and gateways to the ocean, large rivers provide an important backdrop for urban development, agriculture, fisheries and hydropower. North America contains four of the 25 largest rivers in the world,[209] most of which are of increasing interest to PPCP research.[34,104,200,210] Outside of China,[10,211,212] few studies have characterized PPCPs in the surface waters of high-volume river systems,[104,213] with the majority of CEC research conducted in estuaries,[50,214,215] lakes,[13,160,216] and comparatively small rivers or tributaries.[9,13,46,217–220] Moreover, the majority of this PPCP research consists of temporally static analyses which do not capture seasonal variation in river conditions beyond simplified summer/winter comparisons.[9,13,46,50,104,160,213–221] The water quality of mainstem rivers in North America is particularly relevant to ecological disturbance and human health concerns; therefore, a spatial and temporal assessment of pharmaceutical compounds in high-volume rivers is necessary to fully evaluate ecotoxicological risks.

As the second largest river by volume in the United States and an important source of freshwater habitat to Pacific Northwest ecosystems, the Columbia River has great potential to affect the environment through water quality. Numerous PPCPs have been measured in the Columbia River, but the sheer number of PPCPs renders the elucidation of their ecological effects intractable.[47,197–201,222] A reasonable strategy is to focus on those that are (i) likely to have strong biological effects, or (ii) present at

relatively high concentrations. Metformin—the most commonly prescribed drug for treatment of Type II diabetes[133]—is a candidate PPCP that meets these two criteria.

Metformin is an unmetabolized, bioactive, antidiabetic drug that is being detected at high concentrations (ng L^{-1}) in wastewater, streams, and lakes around the world.[13,46,50,160,216] Despite concerning environmental concentrations and increasing rates of Type 2 diabetes, metformin remains poorly explored in surface waters. Much metformin PPCP data originates from broad-spectrum CEC surveys which do not thoroughly explore spatial and temporal trends in compound distribution.[46,50,160] For instance, there were only three field studies found by this author that singly focused on characterizing metformin in surface waters, all based out of Germany.[13,159,223] Other broad CEC studies have focused on metformin in natural water systems,[165] but only over short time periods.

There is also sparse data concerning transformation of metformin in surface waters.[156] As the dead-end transformation product of metformin, guanylurea is a compound that could potentially track the degradation of metformin as it enters and moves through the environment. However, guanylurea is also a component in plastics,[172] fertilizers,[173,174], chemotherapeutics,[170] and munitions compounds[169] which might also be in the environment through separate breakdown processes.

A focused assessment of metformin and its breakdown product in a high-volume river may reveal seasonal patterns, transport processes, and overall environmental bioavailability associated with an increasingly prevalent CEC. Therefore, the first objective of this project was to detect and characterize the seasonal and spatial distribution of metformin and guanylurea in the high-volume Columbia River. This was

accomplished by measuring monthly water samples along the lower river for a one-year period using direct injection LC-MS/MS. From a preliminary CEC analysis of a Columbia River water sample detecting metformin at 55 ng L^{-1},[224] and due to high population density along the lower river with strong seasonal flow, it was expected that metformin in the lower Columbia River would be detected at levels comparable to other studies in less dilute water systems and vary in both space and time. Specifically, it was expected that periods of high discharge, and thus high dilution effects, would be associated with lower metformin and guanylurea concentrations. Additionally, sites relative to sewage effluent pipes and larger tributaries such as the Willamette were expected to be elevated in both metformin and guanylurea due to proximity to concentrated input. It was also expected that guanylurea concentrations would inversely related to metformin concentrations. By revealing the processes governing metformin concentrations in the environment, this field study was relevant to a prediction framework for future environmental risk assessments.

2.2. Methods

2.2.1. Chemicals and Materials

Glass sampling and filtering equipment was used to minimize contact with potential plasticizers that often contain guanylurea. All equipment was cleaned according to the USGS National Water-Quality Assessment (NAWQA) protocol in order to eliminate trace organic and inorganic contaminants.[225] Sampling equipment consisted of 1 L amber wide-mouth glass jars, 40 mL Thermo Scientific™ amber glass VOA vials, and 60 mL VWR® TraceClean® straight-sided wide mouth jars with un-lined caps. Filtering equipment consisted of EMD Millipore™ borosilicate glass 125 mL vacuum flasks, 15

mL funnels, and bases with a silicon plug and aluminum clamp. Samples were filtered using Whatcom™ 0.7 µm GF/F filters that had been combusted at 450 °C for 4 h.

All standards were prepared in 20 mL VWR® TraceClean® clear borosilicate glass vials and 1.5 mL (12x32mm) Thermo Scientific™ amber borosilicate glass SUN-SRI™ standard opening autosampler vials. Stock standards of metformin (1,1 - dimethylbiguanide hydrochloride) and guanylurea (carbamoyl-guanidine amidino urea hydrochloride), and stock internal standards of deuterated metformin (metformin-d6 hydrochloride) and ^{15}N-labelled guanylurea (guanylurea-^{15}N$_4$ hydrochloride) were purchased from Toronto Research Chemicals (North York, ON, Canada). All standards were diluted to working solutions using Evian© mineral water. Filtered micropipette tips were used whenever possible during preparation of standards to minimize contamination, while standard autoclaved micropipette tips were used to transfer river water samples to autosampler vials.

Separation of metformin and guanylurea was attained using a Synergi™ Hydro-RP LC Column (250 x 4.6 mm, 4 µm, 80 Å; Phenomenex, Torrance, CA). All mobile phase solvents were made in lab: Solvent A consisted of 0.1% formic acid in water, and Solvent B consisted of 0.1% formic acid in acetonitrile. A ThermoFisher™ (Waltham, MA) BetaBasic™ C8 Javelin guard column (10 x 2.1 mm, 1.5 µm) minimized column contamination from the sample matrix.

2.2.2. *Water Sample Collection and Processing*

From October 2016 to January 2018, monthly samples were taken at nine sites along the lower Columbia River from Hood River (River km 261) to Beaver Army

Terminal (River km 79) (Figure 2.1). Four sites captured river water concentrations downstream of the Willamette-Columbia confluence (River km 156), while five sites capture river water concentrations upstream of the confluence (Figure 2.1). Samples were most often collected from docks, shoreline rocks, or beaches, but were collected in the main channel when possible. Geographic locations and sampling site abbreviations are summarized in Table 2.1.

A pair of sampling sites at Kalama and Hood River were chosen for capturing the influence of wastewater treatment plants. Kalama samples were taken upstream and downstream of a sewage effluent pipe that projected into the water on a local beach. Hood River samples were taken outside and inside The Hook, a spit into the Columbia River that creates an offshore protected area shielded from a local effluent pipe.
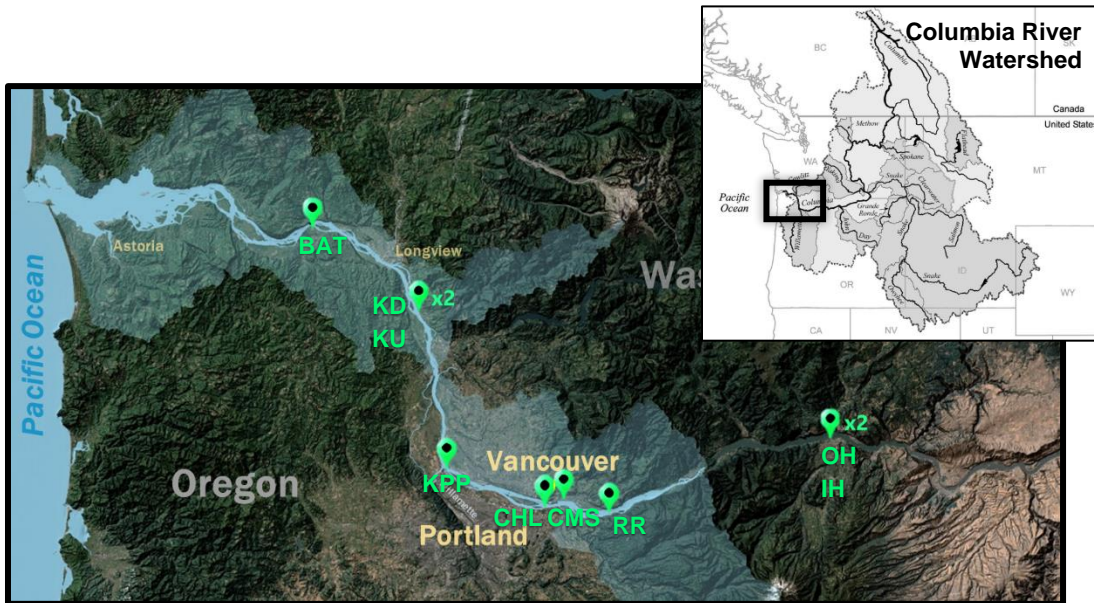
Figure 2.1. Water sampling sites along the lower Columbia River. Image provided by Kirstyn Pittman using ArcGIS® software.

Table 2.1. Geographic summary of sampling sites along the lower Columbia River. River kilometer is a measure of the distance (km) from the mouth of the river. Sites were sampled from October 2016 to September 2017. Four sites captured river water concentrations downstream of the Willamette-Columbia confluence, while five sites captured river water concentrations upstream of the confluence.

Site	Site Abbrev	US/DS of Willamette	River km	Geographic location
Beaver Army Terminal	**BAT**	Downstream	79	46.185° N, -123.188° W
Kalama (downstream of sewage pipe)	**KD**	Downstream	114	46.003° N, -122.847° W
Kalama (upstream of sewage pipe)	**KU**	Downstream	114	46.002° N, -122.846° W
Kelley Point Park	**KPP**	Downstream	156	45.649° N, -122.760° W
Chinook Landing	**CHL**	Upstream	183	45.561° N, -122.444° W
Camas	**CMS**	Upstream	187	45.577° N, -122.381° W
Rooster Rock	**RR**	Upstream	200	45.546° N, -122.247° W
Outer Hook (main channel)	**OH**	Upstream	261	45.717° N, -121.527° W
Inner Hook (shielded from channel)	**IH**	Upstream	261	45.716° N, -121.526° W

During each sampling event, three river water samples were taken by subsampling into 40 mL glass vials from a cleaned 1 L glass jar. For each sample, the jar was rinsed three times with river water and the sample vial was rinsed three times with river water from the jar. In August 2017, field blanks were also collected using a 1 L glass jar of Milli-Q in order to verify minimal field contamination. Each vial was transported on ice and refrigerated at 20 °C until filtering. Sample water was filtered through a standard glass filtering apparatus using 0.7 µm GF/F filters within 72 h of collection. Filtered river water was frozen at -20 °C in 60 mL glass jars until analysis. On the morning of LC-MS/MS analysis, frozen solutions were thawed under running tap water and pipetted into standard 1.5 mL autosampler vials.

Water sample data were complemented by real-time river condition data from in situ sensors along the lower Columbia River. Specifically, river discharge data were acquired from the U.S. Geological Survey (USGS) National Water Information System at

Beaver Army Terminal (Site 14246900) to correspond with sites downstream of the

Willamette-Columbia confluence and from The Dalles (Site 14105700) to correspond to

sites upstream of the Willamette-Columbia confluence. Temperature, turbidity,

chlorophyll, chromophoric dissolved organic matter (CDOM), and oxygen saturation data

were obtained from SATURN-03 near Astoria, OR, and SATURN-08 near Camas, WA,

through the Center for Coastal Margin Observation & Prediction (CMOP) SATURN

Observation Network. In order to complement river discharge data, precipitation data

averaged over WA and OR weather stations at Longview (USC00454769), Portland

(USC00356750), Bonneville (USC00350897), and Hood River (USC00354003) were

obtained through the NOAA National Centers for Environmental Information.

2.2.3. Sorption Experiment

A brief metformin sorption experiment was performed on Columbia River

sediment in order to explore additional sources of metformin variation. Three sets of

triplicate sediment samples were analyzed for metformin recovery. Negative and positive

control samples consisted of sieved sediment that had been baked at 450 °C overnight,

and aliquoted into 20 mL vials with an equivalent weight of filtered river water.

Treatment samples consisted of sieved unbaked sediment with an equivalent weight of

filtered river water. Each vial received 1 µg L^{-1} metformin and was extracted by shaking

overnight with 10 mL acetonitrile (ACN). The extracted ACN-metformin solution was

filtered and pipetted into HPLC vials for LC-MS/MS analysis.

2.2.4. Instrumentation

All LC-MS/MS conditions are summarized in Table 1. A Shimadzu Prominence®

HPLC system using two binary pumps (Shimadzu LC-20AD XR Prominence® LC

pumps) was used to separate metformin and guanylurea in unconcentrated river water

samples. Separation was optimized using gradient elution on the reverse-phase column

with a flow rate of 0.75 mL min^{-1} and an injection volume of 50 µL. A column oven kept

the column operating at 35 °C. Mobile phase composition started at 5% Solvent B and

ramped up to 95% Solvent B over the first seven min. A long re-equilibration period of

~8 min with 5% Solvent B ensured minimal carryover between samples. Total

acquisition duration was 15.6 min for each sample.

Material separated on the HPLC system was identified, detected, and confirmed

using an AB Sciex® QTRAP 5500 mass spectrometer (Applied Biosystems/MDS Sciex

Instruments, Concord, ON, Canada) in conjunction with Analyst 1.6.2 software. The

mass analyzer system was set to scan for precursor and product ions in multiple reaction

monitoring (MRM) mode using a positive ionization turbospray ion source. Mass

transitions between the parent compound and two different fragments were used to

quantify and verify metformin and guanylurea analytes, respectively (Table 2.2).

Table 2.2. LC-MS/MS conditions used for the analysis of metformin (MET) and guanylurea (GUAN) in river water samples. HPLC conditions are shown in white boxes and mass spectrometer conditions are shown in grey boxes.

Chromatographic column	Synergi™ Hydro-RP, 80 Å, 250x4.6 mm, 4 µm
Solvent A	Water (0.1% formic acid)
Solvent B	Acetonitrile (0.1% formic acid)
Mobile phase	Gradient elution: 5% to 95% Solvent B over 7 min
Total run time	15.6 min (7 min elution, 8.6 min re-equilibration)
Flow rate	0.75 mL/min
Column temperature	35 °C
Injection volume	50 µL
Ion source	Turbospray
Ionization mode	Positive
Scanning mode	Multiple Reaction Monitoring (MRM)
MET quantifier transition	130.038 → 60.000 (mass to charge ratio)
MET qualifier transition	130.038 → 42.900 (mass to charge ratio)
GUAN quantifier transition	103.000 → 60.000 (mass to charge ratio)
GUAN qualifier transition	103.000 → 43.056 (mass to charge ratio)

2.2.5. LC-MS/MS Analysis of River Water Samples

Chromatographic analysis was performed using MultiQuant™ Software (Version 3.0). Metformin and guanylurea were quantified based on peak integration of chromatograms using the internal standard (IS) method. A "valley-to-valley" linear baseline fit was used for all peak integrations with a Gaussian smoothing factor of 1.0.

The concentrations of metformin and guanylurea were calculated from standard curves of measured area ratios (analyte area/IS area) versus expected concentration ratios (analyte concentration/IS concentration). The standard curve encompassed the predicted range of analyte concentrations in river water (0–300 ng L^{-1}). Standard solutions

capturing this concentration range were processed with each sample batch to establish a standard curve with each run. Data from a standard sample was used in the standard curve if the concentration calculated from the measured area ratio was within 20% of expected values. A triplicate seven-point linear standard curve was established during the first LC-MS/MS run, and a singlet standard curve in each run thereafter.

Standards were made from dilutions of metformin and guanylurea prepared within 36 h of the LC-MS/MS run. Primary stock solutions of 60 mg mL^{-1} metformin and guanylurea in mineral water were made in separate 1.5 mL autosampler vials. A three-step serial dilution of the stock solutions in clean 20 mL glass scintillation vials yielded working stock solutions of 600 ng L^{-1}. To establish a standard curve, the working solution was diluted with mineral water to make triplicates of at least seven calibration solutions ranging from 0-600 ng L^{-1} in 20 mL scintillation vials. Final standard solutions ranging from 0-300 ng L^{-1} were made by combining 0.5 mL metformin and guanylurea calibration solutions in 1.5 mL autosampler vials on the day of the LC-MS/MS run.

During each LC-MS/MS run, procedural blanks were used to verify signal response. Prior to running the standard curve, a Milli-Q blank and mineral water blank without internal standard were used as negative controls for general instrument response. At the beginning of the standard curve and at random intervals in between long sets of samples, mineral water blanks spiked with internal standard were used for the zero standard point and used to verify minimal carryover between samples.

Due to unexpected contamination on scintillation vial caps between July and September 2017, standard curves during these months were prepared via combined serial dilution in 1.5 mL autosampler vials. Originally, metformin and guanylurea primary

34

stock solutions were kept separate before analysis in order to minimize possible

interaction effects; however, due to the relative stability of standards in solution (R.

Kilpatrick, unpublished data), metformin and guanylurea stock solutions were combined

and diluted in tandem to minimize contamination from extraneous sample prep steps.

Specifically, a primary stock solution of 10 mg/mL 1:1 metformin/guanylurea in mineral

water was diluted to working stock solutions of 1250 ng L^{-1}. Calibration solutions

ranging from 0-300 ng L^{-1} were made by pipetting appropriate amounts of working stock

solution into mineral water to reach a final volume of 1 mL calibration solution for each

concentration.

Internal standard (IS) solutions of deuterated metformin and ^{15}N-labelled

guanylurea were prepared the day of each LC-MS/MS run. Solid stock material of 1 mg

was previously dissolved in 1 mL Milli-Q, sealed, and frozen at -20 °C, up to 8 months.

On the day of the run, a serial dilution of the 1 mg mL^{-1} stock solution in mineral water

yielded an IS working solution of 100 ng mL^{-1}. All samples and standard solutions

received 2 µL each of metformin and guanylurea IS working solution just before LC-

MS/MS injection to get a final IS concentration of 200 ng L^{-1}.

2.2.6. Detection Limits

Detection and quantification limits were based on established U.S. Environmental

Protection Agency (EPA) and U.S. Geological Survey (USGS) protocol (Table 2).

Specifically, the lower limit of detection was based on the estimated method detection

limit (MDL) and was calculated as three times the standard deviation of seven IS-spiked

blank mineral water samples.[226] The lower limit of quantification (LOQ) was set as 10

standard deviation units above the average blank response.[227] The minimum reporting

level (MRL) was set at the MDL.[227]

2.2.7. Method Performance

All chromatograms, standard curves, and corresponding linear equations and test

statistics were obtained from MultiQuant™ Software (Version 3.0). Method performance

values were calculated from concentration values obtained from MultiQuant™ using

Microsoft® Excel® 2016.

The linearity, sensitivity, recovery, and precision of standard samples were

calculated to evaluate LC-MS/MS method performance. Standard curves were fitted with

linear regression models without weighting and evaluated for fit of linearity (R^2).

Sensitivity was calculated as the signal to noise ratio (S/N) associated with the lowest

standard point. Percent recovery was determined relative to a known addition in a river

water sample (corrected for blank river water metformin or guanylurea levels); recovery

was calculated for duplicate 10 ng L^{-1}, 50 ng L^{-1}, and 200 ng L^{-1} spikes and averaged

together to get final average percent recovery for each compound, if the individual

recoveries were within 20% variation of each other. Precision was estimated by the

relative percent difference between field duplicate samples (collected from the same site

to minimize the influence of site variability), averaged over each LC-MS/MS run.

Instrument precision was estimated from the relative percent difference between

reinjections of the same sample. Peak retention time and shape were also compared

between and within LC-MS/MS runs to determine general peak precision. The standard

deviation between runs for predicted values from standard curves was used as a proxy for

intermediate precision (i.e., precision among runs). During the final LC-MS/MS run, a larger standard curve spanning 0-1000 ng L^{-1} was used to estimate the accuracy and intermediate precision of values predicted to be beyond 300 ng L^{-1}.

Internal standard precision was based on within-run variation of IS response (i.e., peak area). Samples with IS responses that exceeded 60% of the mean IS response of all samples in the corresponding run were noted as potentially overestimated or underestimated and excluded from data analysis.

Average peak retention time was 3.6-3.7 minutes for metformin and 3.4-3.5 minutes for guanylurea. Linear models were successfully fitted to both metformin and guanylurea standards, with $R^2 > 0.99$ for each standard curve. Significant baseline noise was consistently observed with guanylurea peaks, however, the average signal to noise ratio (S/N) for both metformin and guanylurea standards was ≥ 9 (Figure 2.2A). Matrix effects were determined to be minimal based on average recovery of 106% ($\pm$9%) for metformin and 106% ($\pm$7%) for guanylurea. Minimal matrix effects were confirmed by precision values, which were <30%. Limits of detection, precision, and sensitivity are summarized in Table 2.3.

Vial cap contamination issues were present in standard samples used for two of five LC-MS/MS runs. Vials normally used for standard solution dilution were used in a separate metformin-spiked sediment experiment in July 2017. Despite extensive cleaning by the NAWQA protocol, many standards prepared with vial caps used in the sediment experiments showed extremely high metformin contamination and caused a shift in the standard peak shape of accurate standards. As a result, the peak shapes of standards used in calibration curve calculation was consistent within LC-MS/MS runs (Figure 2.2A) but

varied more between runs: peak width at half maximum showed $\leq 6\%$ variance within runs for metformin peaks and $\leq 14\%$ variance for guanylurea peaks, and between-run variance in peak width at half maximum was 9% for metformin standards and 21% for guanylurea standards.

The standard curve linear regression models varied among runs but the intermediate precision was acceptable for estimating relative metformin and guanylurea levels in river water samples. Metformin standard curve variation was primarily due to the August vial cap contamination, which limited the number of acceptable standard points for the two respective August LC-MS/MS runs. Guanylurea standard curve variation was likely due to noisy chromatogram baselines (Figure 2.2B). A comparison of predicted values from each model indicated standard deviations of 5-7 ng L^{-1} between runs for actual metformin values of 0-100 ng L^{-1}, and standard deviations of 5-25 ng L^{-1} between runs for actual metformin values of 100-300 ng L^{-1}. Similarly, there were standard deviations of 0-12 ng L^{-1} between runs for actual guanylurea levels of 0-100 ng L^{-1}, and standard deviations of 12-40 ng L^{-1} between runs for actual guanylurea levels of 100-300 ng L^{-1}. Comparison against a larger standard curve spanning 0-1000 ng L^{-1} revealed high standard deviations of 25-97 ng L^{-1} and 66-135 ng L^{-1} among runs for actual metformin and guanylurea values of 300-1000 ng L^{-1}, respectively. However, only 6% of the total river water data (3% of the year-round data), exceeded 300 ng L^{-1}.

Table 2.3. Limit of detection (MDL), limit of quantification (LOQ), correlation coefficients (R^2), recovery, and precision for metformin and guanylurea in river water. Limit of detection was based off the estimated MDL as established by EPA protocol (CITE). The correlation coefficient (R^2) corresponds to the standard curve used for MDL and LOQ calculations. Precision is based on the average relative percent difference between field duplicates over each LC-MS/MS run.

Compound	Method Detection Limit (MDL)	Limit of Quantification (LOQ)	Correlation coefficient (R^2)	Recovery (%)	Precision (%)
Metformin (ng L^{-1})	0.42	1.80	0.993	106%	26.0%
Guanylurea (ng L^{-1})	4.83	20.91	0.998	106%	21.1%

A. Standard Peaks
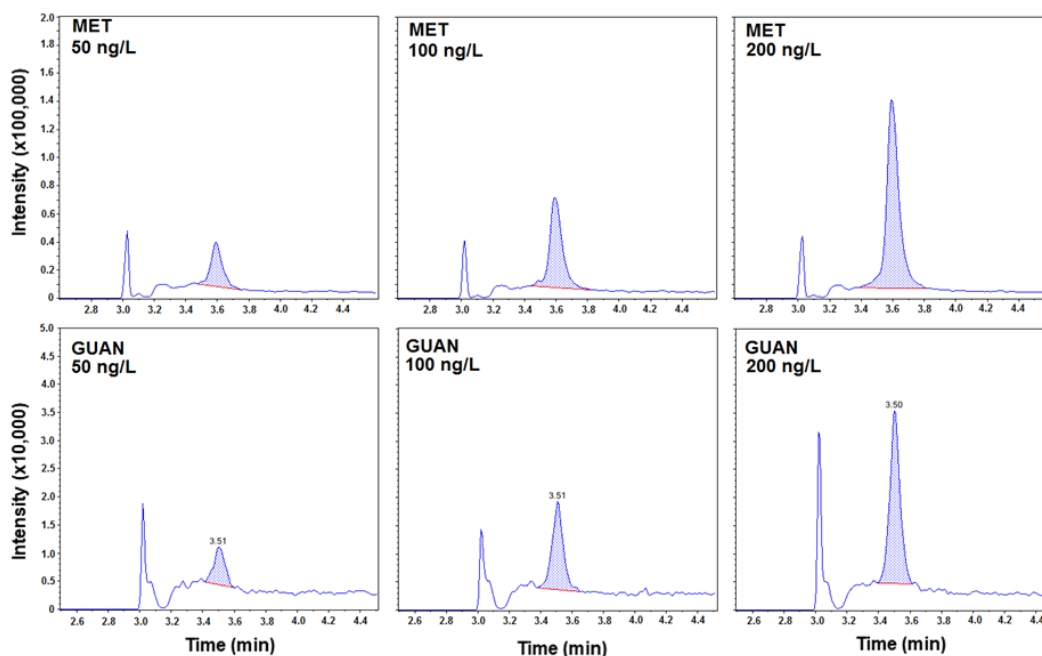
Figure 2.2A. LC-MS/MS chromatograms showing representative standard peaks. Each group of peaks were taken from the same run, except the largest guanylurea peak which was taken from a different run to represent a high concentration.

B. Sample Peaks
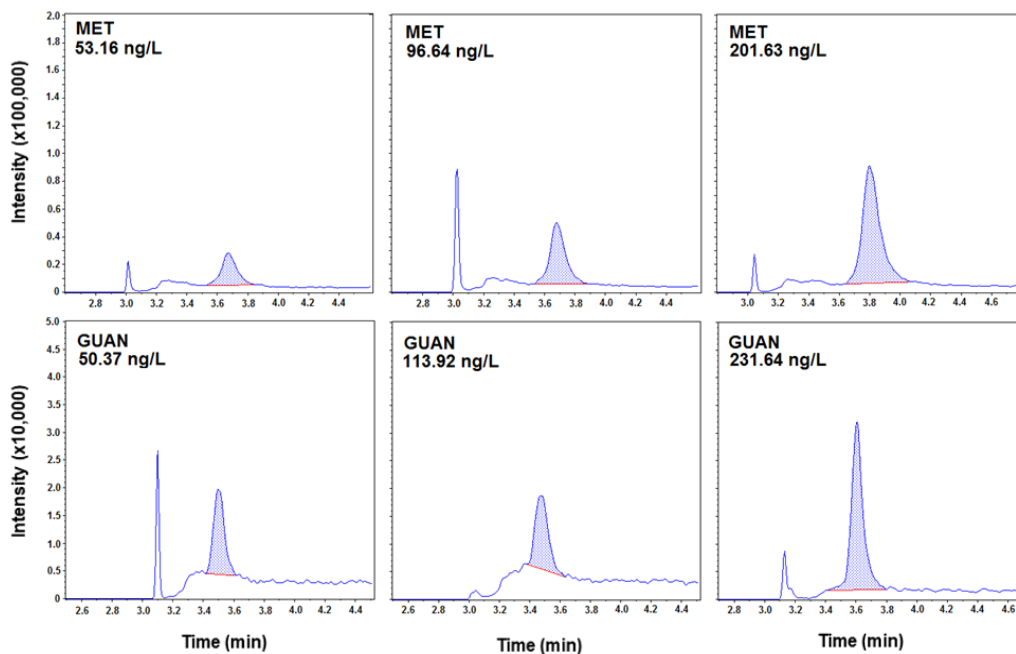
Figure 2.2B. LC-MS/MS chromatograms showing representative sample peaks.

2.2.8. *Sample Variance*

Internal standard response in river water samples exhibited high variation during two of the five LC-MS/MS runs. Specifically, samples from each of these runs exceeded 60% mean IS response. As a result, ~4% of metformin data and ~5% of guanylurea data from river water samples were noted as potentially overestimated or underestimated and excluded from data analysis.

High standard deviations of analyte concentrations were often observed between triplicates of river water samples (Table 2.4), but could not be definitely attributed to field methods or environmental variation. Field blanks with Milli-Q showed minimal guanylurea contamination (<12 ng L^{-1}), but indicated possible metformin field contamination ranging from ~11-27 ng L^{-1} and, in one case, ~80 ng L^{-1}. Contamination of field blanks could have arisen from contamination of caps from jars used in metformin-

spike experiments with sediments. This is possible since the 1 L glass jars used for water sampling in Milli-Q field blank prep were used to collect sediment during the sediment experiments; however, since metformin spikes were not added to the 1 L jars, contamination from the caps could only have occurred if there was a source of metformin in the natural sediments collected from Columbia River habitats.

Table 2.4. Standard deviations of triplicate river water samples at year-round sites for each month of the sampling period.

Site	Oct	Nov	Dec	Jan	Feb	Mar	Apr	May	June	July	Aug	Sept
BAT	74.2	34.7	17.5	10.4	4.9	1.1	1.3	6.2	16.7	46.5	40.9	5.2
KD	14.2	46.4	1.3	19.0	0.7	2.4	2.2	43.2	149.8	113.1		0.6
KU	6.0	2.3	1.7	21.4	2.0	0.7	2.7	14.5	2.7	27.2	14.9	15.3
KPP	7.2	5.0	2.1	11.4	3.4	3.1	38.7	29.2	76.7	280.0	4.0	366.6
CHL	12.6	3.2	1.8	15.0	3.8	15.0	6.5	34.6	3.1	536.2	37.1	68.2
CMS	1.9	3.2	40.0	2.0	0.9	0.9	4.7	306.5	8.4	201.0	1.1	206.2
RR	33.1	3.1	1.6	1.8	5.9	1.2	4.7	71.7	279.1	5.9	63.5	20.3
OH	3.8	81.7	83.0	3.2	8.4	1.3	8.3	73.8	2.1	704.8	150.1	1.5
IH	7.3	71.2	2.4		1.4	1.0	2.2	121.2	3.0	105.6	41.9	5.4

Shapiro-Wilk tests on concentration data found that metformin and guanylurea concentrations were not normally distributed (MET: $W=0.769$, $p<0.0001$; GUAN: $W=0.765$, $p<0.0001$). A $\ln(1+x)$ transform was applied to metformin and guanylurea concentration data in order to make response variables more normal prior to constructing GAM models (Shapiro-Wilk, MET: $W=0.986$, $p=0.721$; GUAN: $W=0.948$, $p=0.011$). Ratio data was also non-normal (Shapiro-Wilk, $W=0.690$, $p<0.0001$), so a cube root transformation was applied to make normally distributed data for GAM models (Shapiro-Wilk, $W = 0.978$, $p=0.333$).

Since metformin and guanylurea concentration data were not normally distributed, outlier tests could not be performed. Only one sample point was excluded from data analysis (Outer Hook, Sept #2) due to likely contamination inferred from a

peak response that exceeded 300x that of the other two replicates. All other samples with acceptable internal standard responses were included in data analysis.

2.2.9. Data Analysis

All multi-variate analyses, graphs, and statistics were performed using R Studio (Version 1.1.383) or Microsoft® Excel® 2016. Boxplots were used to show the mean, standard deviation, and outliers of metformin and guanylurea concentrations by site and by month. The ratio of guanylurea to metformin (G:M) was treated as an additional variable for approximation of metformin transformation. Heat maps were used to simultaneously visualize compound concentrations relative to site location and sampling month.

Principal component analyses (PCA) of river condition measurements corresponding to each sample point (i.e., average of triplicates) were used to reduce data dimensionality to principal components that explained ≥75% cumulative variation in the dataset. Two separate PCAs were performed on river condition data obtained from sensors located upstream and downstream of the Willamette-Columbia confluence (River km 156) in order to account for estuarine and riverine influence. River variables with ≥50% correlation with the first or second principle components were considered as possible explanatory variables for metformin and guanylurea data. PCAs were evaluated and visualized using eigenvector summaries and biplot functions from the R package 'factoextra' and 'FactoMineR'.

In order to account for the effect of multiple independent variables on metformin and guanylurea, generalized additive models (GAMs) were used for regression analysis

of compound concentrations relative to river conditions. GAM models were constructed using the R package 'mgcv' with P-spline smooth classes (Eilers and Marx 1996). Optimum smooth term combinations were selected based on initial p-value significance and overall lowest model AIC (Akaike Information Criterion) values. The basis dimension of each smooth term (k) was optimized by trying different values until a visual inspection of the model object checked against overfitting and k-index ≥0.9 (k-index is the estimated residual variance divided by the residual variance, where the estimated residual variance is the difference in near neighbor residuals according to the covariates of the smooth). GAM models were validated by comparing AIC, Generalized Cross Validation (GCV), and R^2 values to other plausible GAM models from the permutation selection process and linear models containing the same variables. Resulting smooths of each component were graphed with partial residuals to visualize the multi-variate relationships of the GAM models. While single independent variable scatterplots indicate the relationship between a single predictor and response variable, partial residual plots take into account the effect of all independent variables in the model by letting a single predictor vary while holding other predictors at their mean. The partial residuals of a component represent the part of the response not explained by other terms in the model and are ideally distributed within a 95% confidence interval around the component smooth function. Extensive deviations of partial residuals from this boundary were noted as poor smooth term fit with low predictive power.

Collinear variables were approximated by concurvity assessments of significant smooth terms after the selection process. If terms exhibited > 0.75 concurvity measure, the variables were considered collinear. High concurvity measures were calculated

between river discharge and CDOM (>0.9), and river discharge and oxygen saturation (>0.9), indicating strong collinearity between these environmental variables. Collinear terms were left in the model, but identified as potentially reducing the predictive power of independent variables. For these models, discussion was limited to overall predictive power of the multiple regression model, considering only the combined effect of the variables on the response with the possibility of redundant predictors.

2.3. Results

2.3.1. River Conditions

Monthly river conditions are summarized in Figure 2.3. Overall, river discharge was higher during sampling events associated with sites downstream of the Willamette-Columbia confluence. Precipitation was lower during sampling events at these downstream sites. Downstream river water was associated with higher turbidity, higher salinity, and lower oxygen saturation. Since the downstream sensor was located closer to the mouth of the river than the downstream sampling area, salinity levels at the downstream sampling sites were likely lower than the sensor observations.

River discharge varied by season as expected from annual fluctuations in precipitation and temperature. Discharge peaked from March to May corresponding to the annual freshet (i.e., spring thaw). Discharge started to increase in January until May and then decreased from June until September, corresponding to the beginning and end of the freshet. Discharge was lowest ($<7000 \text{ m}^3 \text{ s}^{-1}$) from July through December at sites upstream of the Willamette River and from July through September in sites downstream of the Willamette River (Figure 2.3A1, A2).

Trends in river discharge corresponded to trends in precipitation, chlorophyll, CDOM, and turbidity. Sampling events at sites upstream of the Willamette River were generally associated with high precipitation events in all months, except May through August (Figure 2.3D1). Increasing precipitation from January through March corresponded with the increase in river discharge, and a peak in chlorophyll, CDOM, and turbidity during the same time period (Figure 2.3A1, B1, E1, F1). While little precipitation was observed during sampling events at sites downstream of the Willamette

River, similar trends were observed between river discharge and chlorophyll, river discharge and CDOM, and river discharge and turbidity (Figure 2.3A2, B2, E2, F2). Chlorophyll concentrations decreased or were low during months associated with decreasing or low river discharge (generally, July through November), and peaked during periods of increasing river discharge (December through February for upstream sampling events, and January through February for downstream sampling events), and peak river discharge (May through July for upstream sampling events, and April through May for downstream sampling events) (Figure 2.3B1, B2). Furthermore, CDOM increased from January to April, before decreasing after peak river discharge (Figure 2.3E1, E2). Turbidity increased during periods of high river discharge, but also showed elevated levels from October through January during sampling events downstream of the Willamette River.

Fluctuations in temperature and dissolved oxygen saturation were also observed during the sampling period. Trends in river temperature followed fluctuations in river discharge and expected seasonal air temperature (Figure 2.3A1, A2, C1, C2). River temperature steadily increased from January until July (Figure 2.3C1, C2). Trends in dissolved oxygen saturation tracked patterns of primary productivity which are expected to increase in the spring when nutrients and light are increasing relative to winter months. The increase in oxygen saturation levels from January to May corresponds to an increase in chlorophyll during the same period. Likewise, the decrease in oxygen saturation levels following May corresponds to a decrease in chlorophyll.
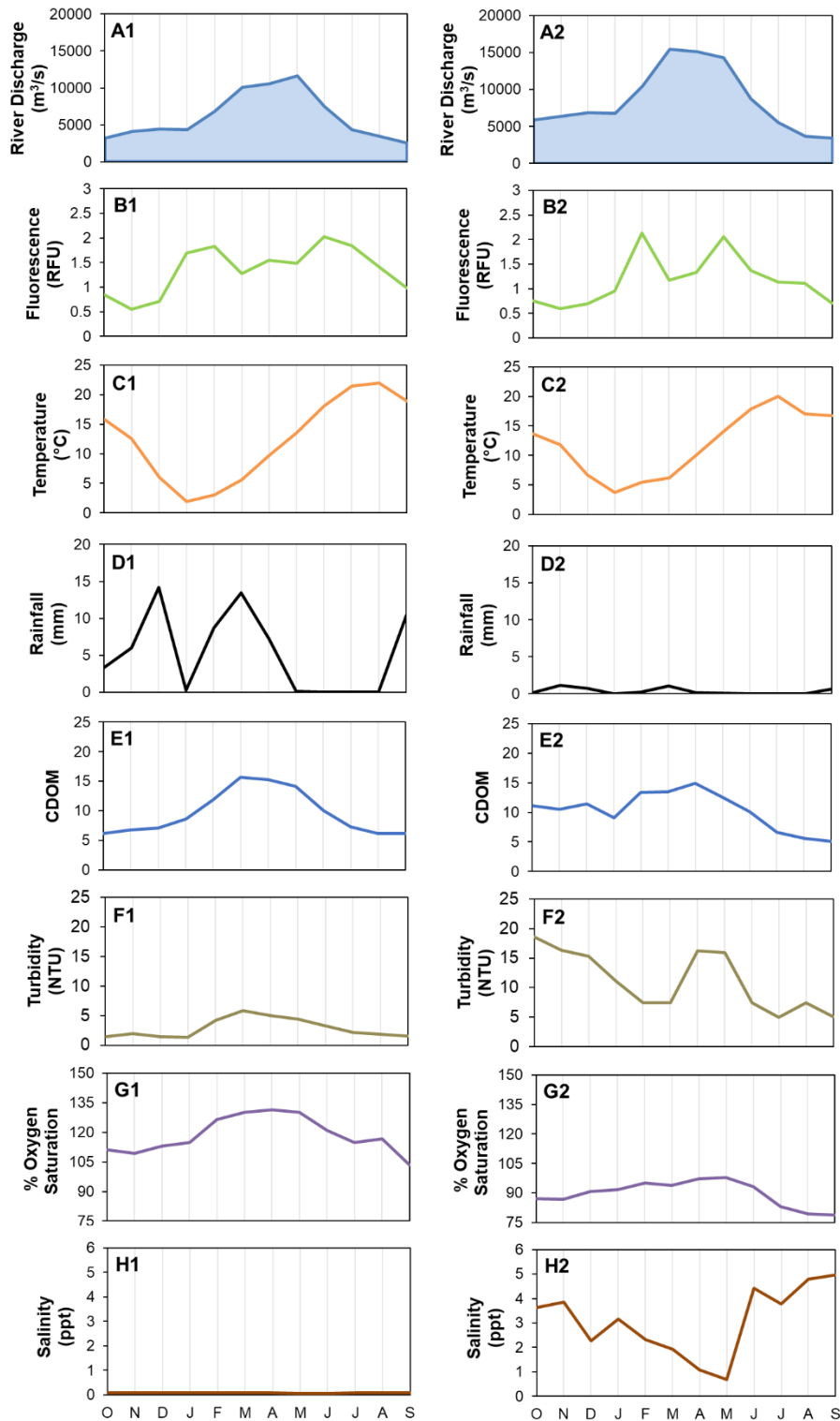
Figure 2.3. Average monthly river conditions upstream (A1-H1) and downstream (A2-H2) of the Willamette-Columbia confluence (River km 156) associated with times of river water sampling from October 2016 to September 2017. Graphs show river discharge (A), chlorophyll fluorescence (B), temperature (C), precipitation (D), CDOM (E), turbidity (F), oxygen saturation (G), and salinity (H).

47

2.3.2. *Overview of Metformin and Guanylurea in the Columbia River*

A total of 308 river water samples were successfully analyzed for metformin, 307 of which were also successfully analyzed for guanylurea. River water had an overall average metformin concentration of 67.4 ng L^{-1} (*SD*=127) and an overall average guanylurea concentration of 32.6 ng L^{-1} (*SD*=65.2).

Metformin and guanylurea concentrations are summarized by month in Figure 2.4 and Appendix Table 2A, and by location in Figure 2.5 and Appendix Table 2B. Metformin at year-round sites varied by month (ANOVA, $F_{(2,11)}$=3.711, p=0.0002). Standard deviations for May to July and September were at least twice as high as the standard deviations of other months. July and September had the highest metformin concentrations while February to April had the lowest concentrations. A notable increase in metformin concentration in May was also observed.

Guanylurea also varied by month (Figure 2.4; ANOVA, $F_{(2,11)}$=6.454, p<0.0001). Highest guanylurea concentrations were found in October, with generally higher guanylurea levels occurring from September to November. Median guanylurea concentrations exceeded metformin in October, November, and December. Lowest guanylurea levels were found in May, June, and July. Standard deviations of guanylurea concentrations were larger relative to other months from September to November and, additionally, in March.

Overall, metformin (ANOVA, $F_{(2,8)}$=0.716, p=0.677) and guanylurea (ANOVA, $F_{(2,8)}$=0.533, p=0.829) did not vary by individual location (Figure 2.5). River water sampled from the downstream Kalama (River km 114) and Kelley Point Park (River km 156) locations exhibited the highest metformin concentrations among the year-round

sites, while the highest guanylurea concentration was observed at Chinook Landing (River km 183). Guanylurea concentration interquartile ranges were higher than metformin at the upstream Kalama (River km 114), Camas (River km 187) and Rooster Rock sites (River km 200); however, average guanylurea did not exceed metformin at any site. Standard deviations were consistently high at each site, generally twice that of the mean concentration, which likely contributed to the lack of significant differences.

General spatiotemporal patterns in metformin were observed along the river. A heat map of metformin concentrations at each location and month showed higher metformin concentrations at or downstream of River km 156 (73.9 $\pm$25 ng L^{-1}) versus upstream (60.2 $\pm$16 ng L^{-1}) (Figure 2.6A). A two-way ANOVA testing for differences among average concentrations upstream and downstream of River km 156 for each month confirmed the observed higher values downstream of this site with significant interaction effects with month ($F_{(2,11)}=1.985$, $p=0.0298$). River km 156 marks the location of Kelley Point Park and the confluence of the Willamette River with the Columbia River (Figure 1). Sporadically high metformin levels occurred from May to September at sites upstream of River km 156; however, these hotspots were caused by more metformin "outliers" (i.e., observations beyond 1.5x the interquartile range), rather than higher average values (Figure 4). Unlike metformin, guanylurea did not exhibit any apparent spatial trends (ANOVA, $F_{(2,8)}=0.711$, $p=0.682$), but rather showed a strong temporal increase from August to January (Figure 2.6B) (ANOVA, $F_{(2,1)}=278.930$, $p=<0.0001$).
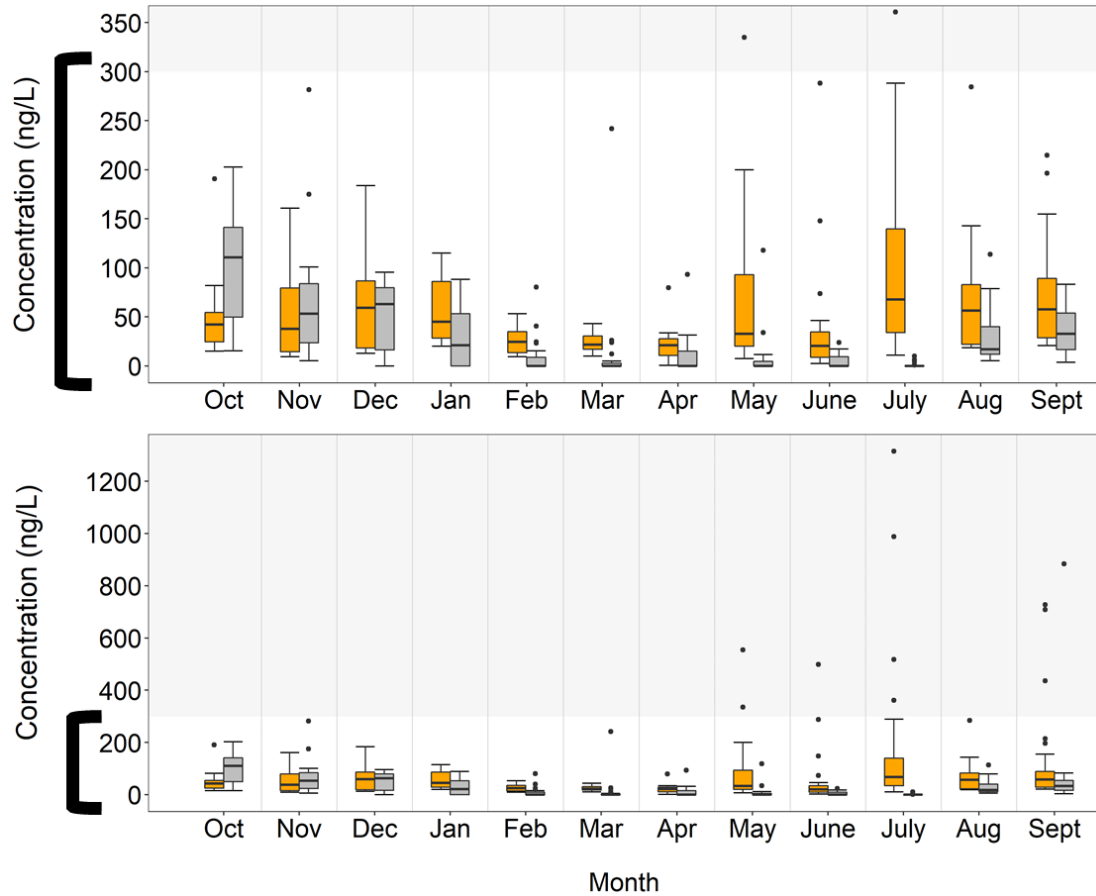
Figure 2.4. Temporal metformin and guanylurea distribution in the lower Columbia River. Compound levels for each month of the October 2016–September 2017 sampling period are shown (year-round sites only). Top plot is a close-up image of the 0–300 ng L^{-1} range of the bottom plot. Dots represent all averaged triplicate sample points outside 1.5 times the interquartile range. Everything in grey is outside the zoomed range.
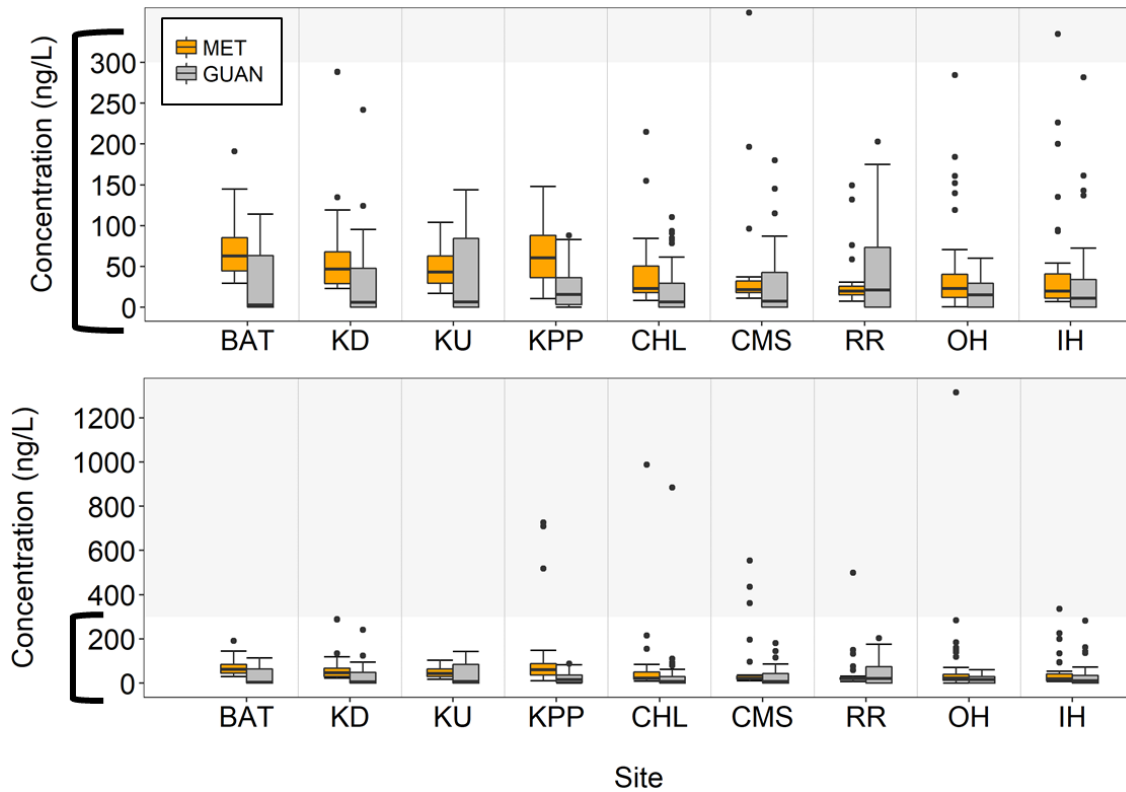
Figure 2.5. Spatial metformin and guanylurea distribution in the lower Columbia River. Compound levels at each sampling site are shown (year-round sites only). The top plot is a close-up image of the 0-300 ng L^{-1} range of the bottom plot. The average of triplicate samples was considered one sample point. Dots represent all sample points outside 1.5 times the interquartile range. Everything in grey is outside the zoomed range.
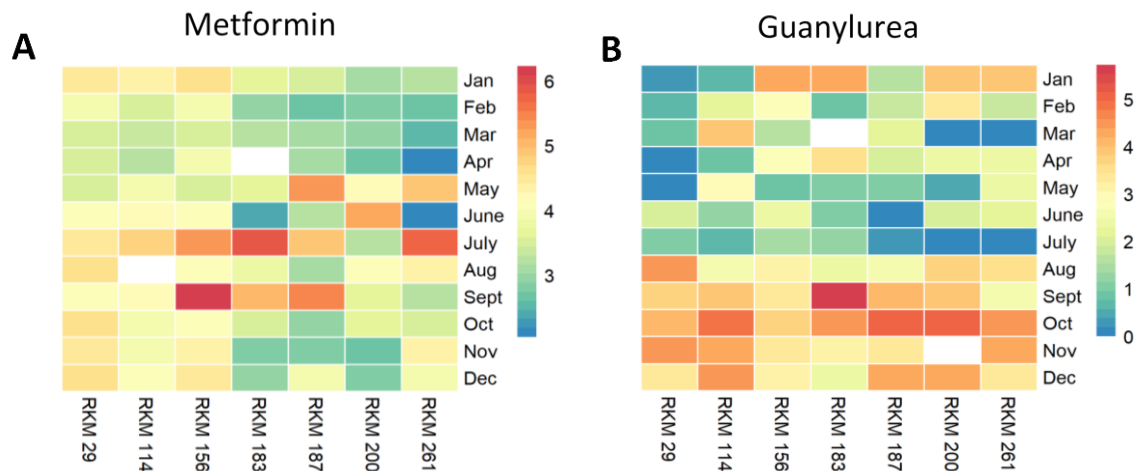
Figure 2.6. Heatmap showing average metformin (A) and guanylurea (B) concentrations along the lower Columbia River for each month. All data is shown on a transformed ln(1+x) scale.

51

2.3.3. *PCA of River Data*

Principal component analyses (PCA) reduced data dimensionality in order to consider effects of environmental conditions on metformin and guanylurea levels in the Columbia River. PCA of year-round environmental river data, including river discharge, percent oxygen saturation, CDOM, precipitation, temperature, turbidity, and chlorophyll, resulted in two principal components that explained >75% of the cumulative variation in the dataset. Variables associated with river flow (i.e., river discharge, CDOM, percent oxygen saturation, and turbidity) were most closely related to the first principal component, while variables associated with season (i.e., precipitation, temperature, and chlorophyll) varied the most along the second principal component. Five river variables, including river discharge, percent oxygen saturation, turbidity, CDOM, and precipitation, explained the most variation in the principal components for sites upstream of the Willamette-Columbia confluence (River km 156) (Figure 2.7A). The same river variables, excluding turbidity, explained the most variation in the principle components for sites downstream of the Willamette (Figure 2.7B).
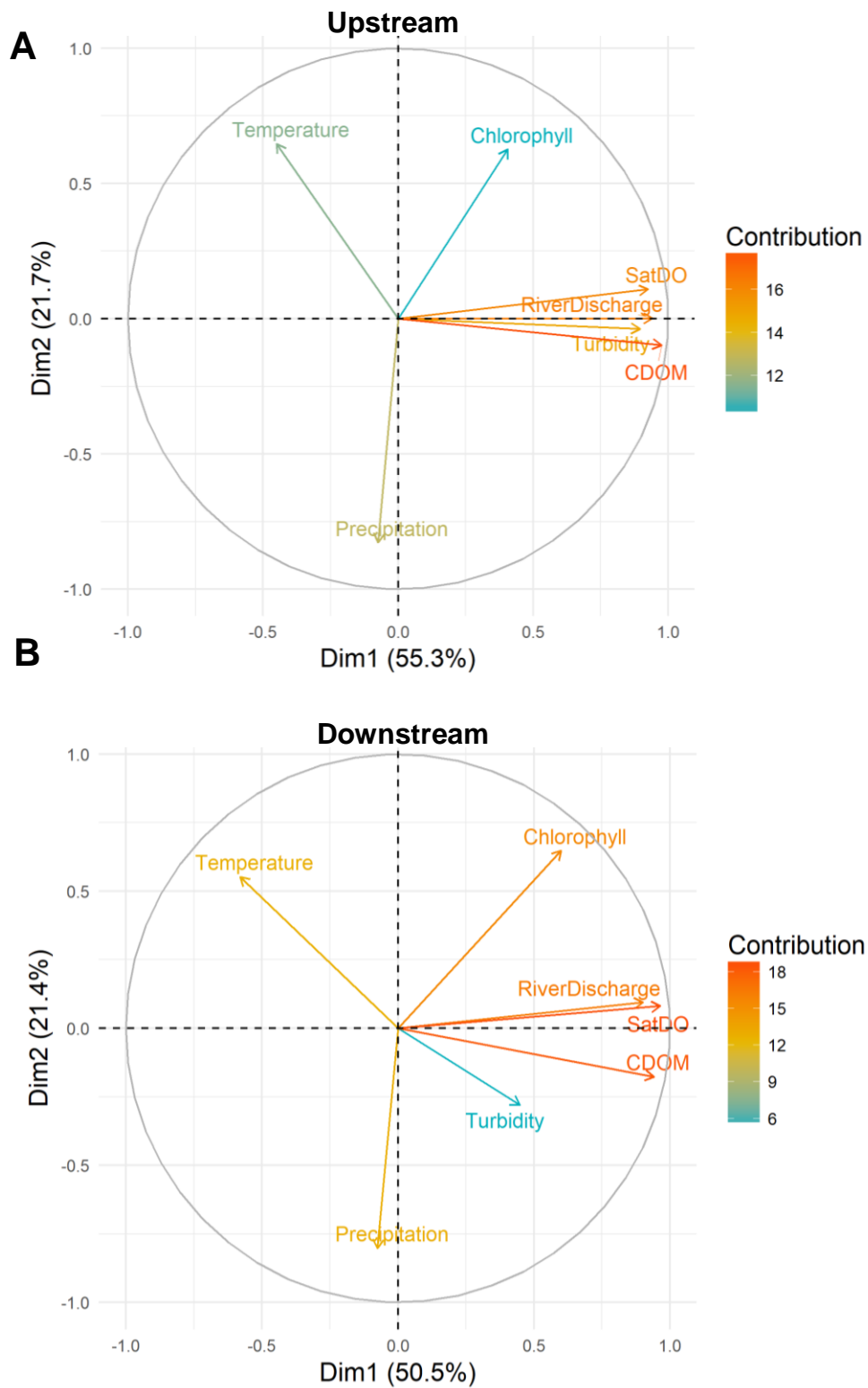
Figure 2.7. Biplot of PCA performed on river variable data associated with river water samples (A) upstream or (B) downstream of the Willamette-Columbia confluence (i.e., river km 156). Redder arrows indicate higher contribution to the first principal component.

2.3.4. GAM Model Performance

River condition variables partially explained trends in metformin concentrations in the Columbia River (Table 2.5, Figure 2.8). R^2 values associated with GAM models describing metformin patterns at sites upstream of the Willamette-Columbia confluence suggested that only ~23% of the total error in the concentration data was explained by respective upstream river predictors. However, R^2 values of metformin GAM models for sites downstream of the confluence indicated almost 50% of the total error in the data was explained by respective downstream river predictors. Both downstream and upstream metformin concentrations were best predicted by river discharge. River discharge and CDOM smooth terms exhibited high collinearity (>0.9) in the downstream model. Overall, GAM models suggested that metformin had a stronger relationship with seasonal river variables downstream of the Willamette River confluence (Table 2.5).

Table 2.5. Best-fit model comparison for GAM models predicting metformin concentrations upstream and downstream of the Willamette-Columbia confluence**.** Smooth functions are represented by "s()". The best model is compared against two high performing GAM models and best-fit linear model for comparison of fit. The best model (in bold) was chosen based on the lowest AIC value.

Response variable	Model	GCV	R^2	AIC
US Metformin	**ln(C+1) = s(RD) + s(PRECIP)**	**0.832**	**0.226**	**158.2**
US Metformin	ln(C+1) = s(RD) + s(CDOM)	0.860	0.192	160.2
US Metformin	ln(C+1) = s(RD)	0.874	0.171	161.3
US Metformin	ln(C+1) = CDOM + PRECIP	0.946	0.095	166.5
DS Metformin	**ln(C+1) = s(RD) + s(CDOM)**	**0.207**	**0.444**	**61.2**
DS Metformin	ln(C+1) = s(RD)	0.209	0.436	61.6
DS Metformin	ln(C+1) = s(SATDO) + s(CDOM)	0.218	0.471	62.6
DS Metformin	ln(C+1) = RD	0.207	0.439	61.2
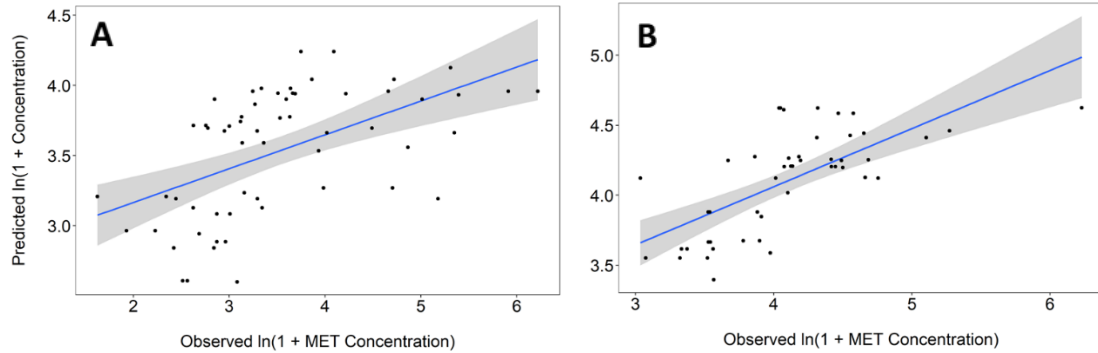
Figure 2.8. Performance of best-fit GAM models predicting metformin concentrations upstream (A) and downstream (B) of the Willamette-Columbia confluence. High spread around the best-fit line indicates partial predictive power for both models.

Similarly, river condition variables partially explained trends in guanylurea concentrations in the Columbia River (Table 2.6, Figure 2.9). R^2 values of guanylurea GAM models indicated ~50% of the total error in the data was explained by their respective river predictors. Guanylurea concentrations both downstream and upstream of the Willamette-Columbia confluence were best predicted by CDOM and precipitation; however, downstream sites were also best predicted by river discharge and upstream sites were also best predicted by percent oxygen saturation. River discharge and CDOM smooth terms exhibited high collinearity (>0.9) in the downstream model, while oxygen saturation and CDOM smooth terms exhibited high collinearity (>0.9) in the upstream model. Overall, GAM models suggested that there was a stronger relationship between guanylurea and river flow downstream of the Willamette River confluence (Table 2.6).

Table 2.6. Best-fit model comparison for GAM models predicting guanylurea concentrations upstream and downstream of the Willamette-Columbia confluence**.** Smooth functions are represented by "s()". The best model is compared against two high performing GAM models and best-fit linear model for comparison of fit. The best model (in bold) was chosen based on the lowest AIC value.

Response variable	Model	GCV	R^2	AIC
US Guanylurea	**ln(C+1) = s(SATDO) + s(CDOM) + s(PRECIP)**	**1.65**	**0.400**	**194.9**
US Guanylurea	ln(C+1) = s(SATDO) + s(CDOM) + s(PRECIP) + s(TURB)	1.64	0.403	194.8
US Guanylurea	ln(C+1) = s(SATDO) + s(TURB) + s(PRECIP)	1.65	0.401	195.0
US Guanylurea	ln(C+1) = RD + CDOM + PRECIP	1.68	0.271	169.4
DS Guanylurea	**ln(C+1) = s(RD) + s(CDOM) + s(PRECIP)**	**1.27**	**0.562**	**148.1**
DS Guanylurea	ln(C+1) = s(RD) + s(CDOM)	1.37	0.509	152.4
DS Guanylurea	ln(C+1) = s(RD) + s(SATDO) + s(PRECIP)	1.62	0.444	159.8
DS Guanylurea	ln(C+1) = SATDO	1.89	0.264	203
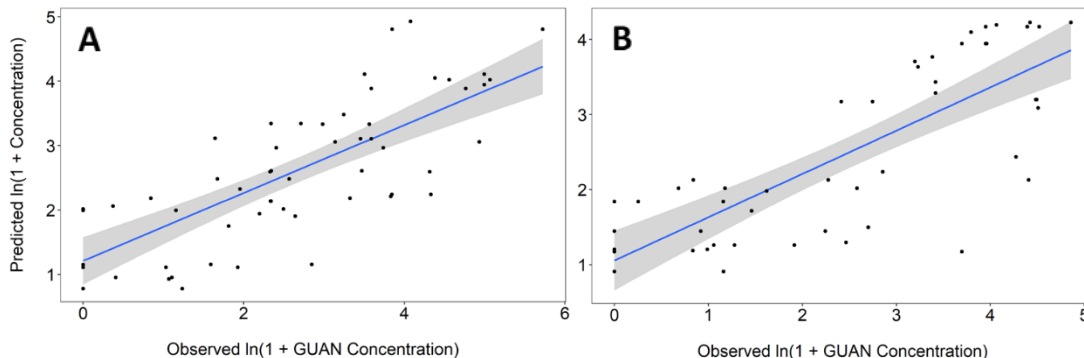
Figure 2.9. Performance of best-fit GAM models predicting guanylurea concentrations upstream (A) and downstream (B) of the Willamette-Columbia confluence. High spread around the best-fit line indicates partial predictive power for both models.

2.3.5. River Effects on Metformin Concentrations

Plots of model smooth functions describing metformin concentrations relative to the Willamette-Columbia confluence showed that metformin changed most with river discharge downstream of the Willamette River. The metformin GAM model for samples downstream of the Willamette River showed a linear inverse response to river discharge over the entire range of observed discharge rates (~3500–18,000 $m^3\,s^{-1}$) (Figure 2.10A). For samples upstream of the Willamette River, an inverse relationship between metformin response and river discharge was also observed at ~2000–8,000 $m^3\,s^{-1}$;

however, a positive relationship was observed at river discharge >8,000 m^3 s^{-1} (Figure 2.10C). Large variance in metformin concentrations across river discharge values indicated high predictive error, which may have obscured trends in response to river discharge levels for upstream sites (Figure 2.10C).

Metformin concentrations also varied inversely with CDOM downstream of the Willamette-Columbia confluence (Figure 2.10B) and inversely with precipitation upstream of the confluence; however, these effects were either very small or associated with high error (Figure 2.10D). The CDOM smooth of the downstream metformin model produced a slightly negative response in metformin concentrations (Figure 2.10B). The precipitation smooth of the upstream metformin model produced a negative response in metformin at values ranging from 0–10 mm rainfall and produced a mostly negligible response at rainfall levels >10 mm (Figure 2.10D). However, a large number of sampling events during low precipitation events produced high variance in metformin partial residuals at low predictor values, which may have obscured overall trends in response to precipitation levels for upstream sites (Figure 2.10D).
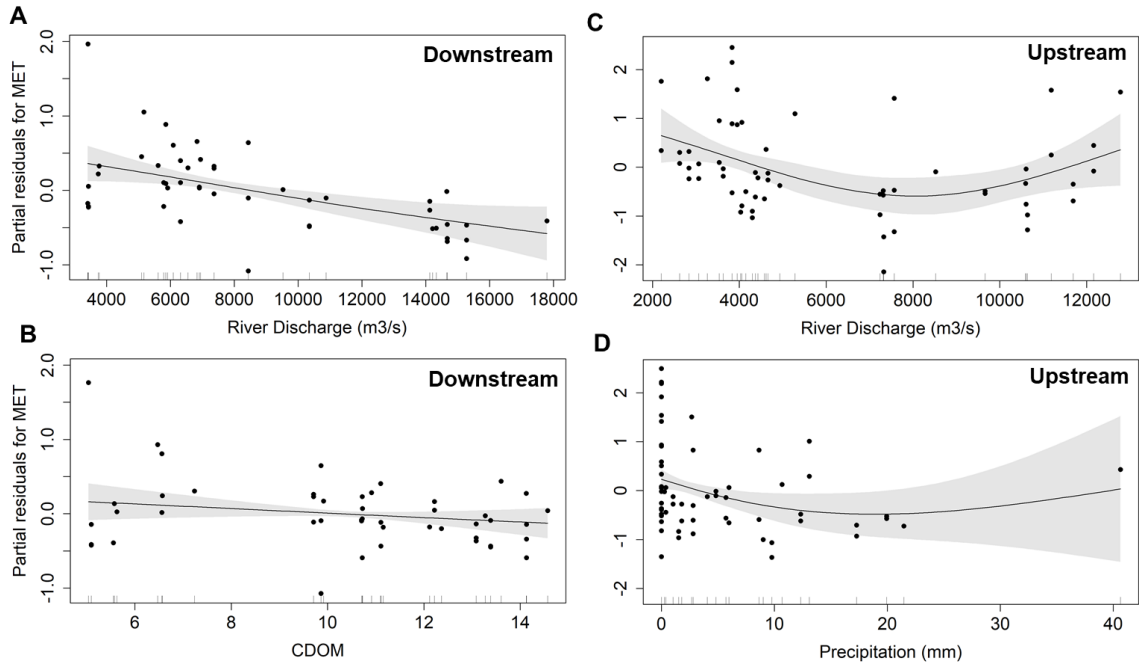
Figure 2.10. Component smooth functions for metformin GAM models based on samples taken downstream (A-B) and upstream (C-D) of the Willamette-Columbia confluence. Each plot shows the effect of a significant predictor variable given other model variables are held constant. Dots represent partial residuals of each smooth, which represent the model response that was not explained by other terms in the model. The grey shaded regions represent 95% confidence intervals.

2.3.6. *River Effects on Guanylurea Concentrations*

Similar to metformin, plots of model smooth functions describing guanylurea concentrations relative to the Willamette-Columbia confluence showed that guanylurea changed most with river discharge downstream of the confluence. An inverse relationship between guanylurea response and river discharge was observed at ~3500–10,000 $m^3 s^{-1}$ for downstream samples, with river discharge >10,000 $m^3 s^{-1}$ producing negligible response (Figure 2.11A). River discharge did not explain guanylurea concentrations upstream of the Willamette–Columbia confluence; however, oxygen saturation was associated with a negative response in guanylurea concentrations at saturation levels of 110–130% (Figure 2.11D).

Guanylurea concentrations also varied with CDOM and precipitation upstream and downstream of the Willamette–Columbia confluence. Specifically, downstream guanylurea concentrations varied directly with CDOM (Figure 2.11B) and, somewhat, with precipitation (Figure 2.11C). The CDOM smooth of the upstream guanylurea model produced a more variable response in guanylurea concentrations, with a negative response at CDOM values of ~5–7, and a positive response from CDOM values of ~7–21 (Figure 2.11E). Likewise, the precipitation smooth of the upstream guanylurea model produced a more variable response in guanylurea concentrations, with a positive response at precipitation values from ~0–6 mm and a negative response at precipitation values from ~6–21 mm (Figure 2.11F).
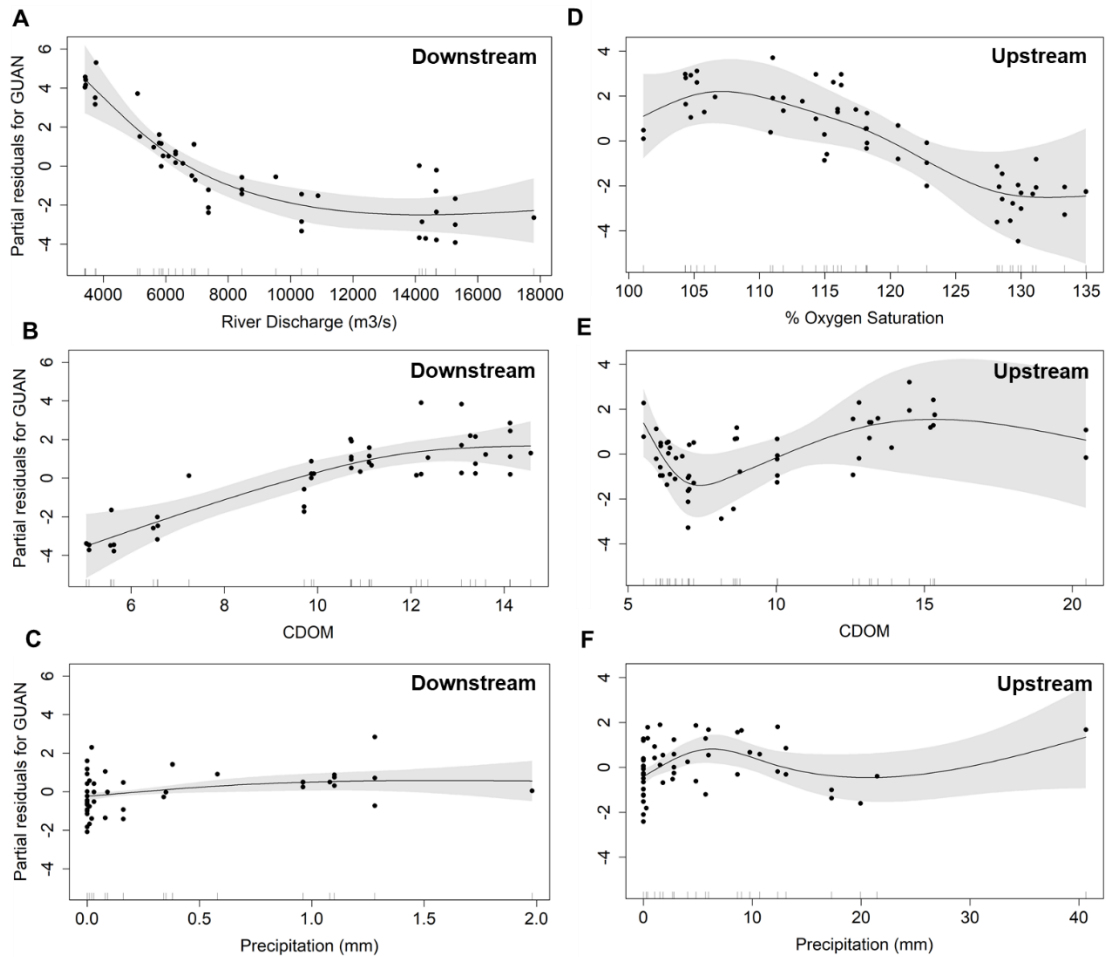
Figure 2.11. Component smooth functions for guanylurea GAM models based on samples taken downstream (A-C) and upstream (D-F) of the Willamette-Columbia confluence. Each plot shows the effect of a significant predictor variable given other model variables are held constant. Dots represent partial residuals of each smooth, which represent the model response that was not explained by other terms in the model. The grey shaded regions represent 95% confidence intervals.

2.3.7. *Sewage Source and Transformation Effects on Metformin*

Since environmental conditions failed to explain at least half of the variation in metformin and guanylurea concentrations in the Columbia River, source-driven variation was explored. Comparison of average compound concentrations at sites adjacent to sewage treatment plants at the Kalama and Hook sites revealed variable patterns based on compound, location, and season. A two-way ANOVA of metformin concentrations for

each month group at Kalama sites $(F_{(1,52)}=1.877, p=0.177)$ and Hook sites

$(F_{(1,54)}=0.615, p=0.436)$ found no main effects of location relative to the sewage pipe

(Figure 2.12A, B). Similarly, no effects were observed for guanylurea concentrations at

the Kalama site $(F_{(1,56)}=0.339, p=0.563)$ (Figure 2.12A). Some sewage pipe effects on

guanylurea were observed at the Hook site (ANOVA, $F_{(4,50)}=2.697, p=0.0411$), but a

visual inspection of upstream vs. downstream pipe trends showed this occurred only in

December (Figure 2.12B). While several sites appeared to slightly increase/decrease in

metformin or guanylurea (Figure 2.12A, B), these differences were mostly not significant

due to high standard deviation.
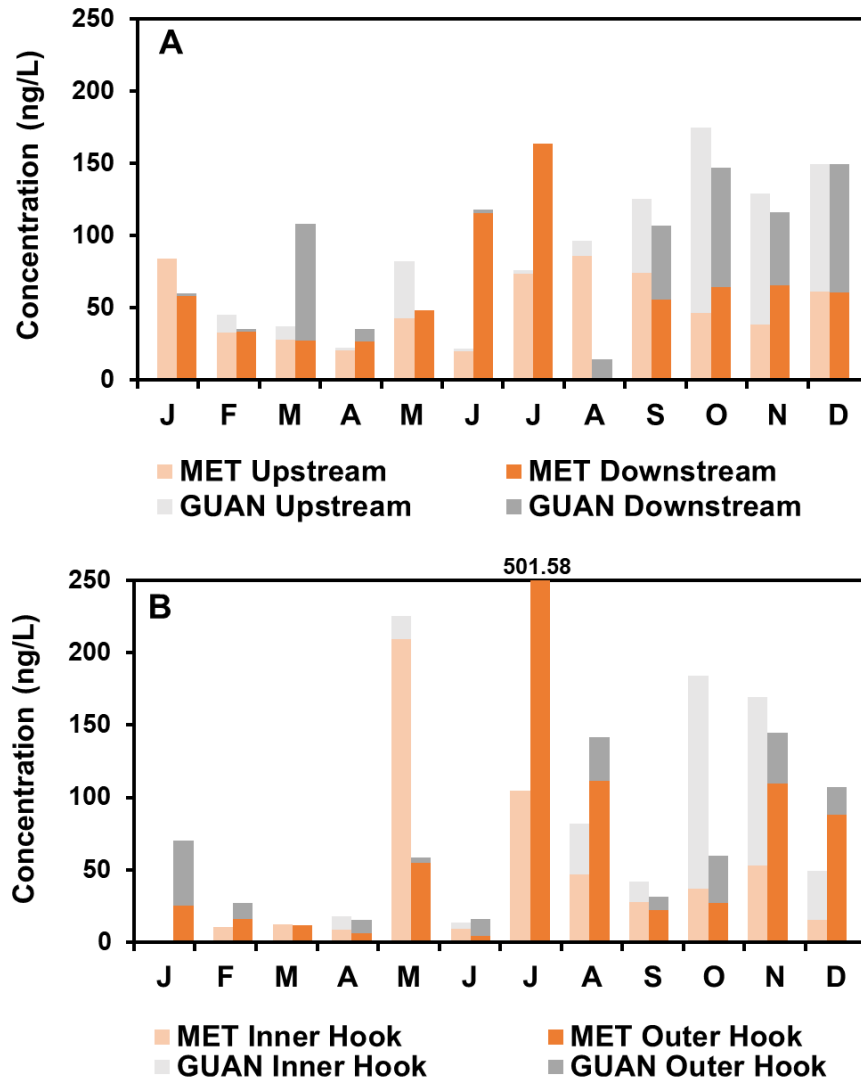
Figure 2.12. Concentrations of metformin and guanylurea at sites near sewage effluent pipes for each month group at Kalama (A) and Hook (B) locations. Adjacent bars show the compound levels upstream or shielded from effluent relative to the adjacent site receiving effluent input. January data at the Inner Hook site was unable to be collected due to frozen weather conditions (B). The number above the June bar for the Outer Hook site (B) indicates a concentration above the 0-250 ng L^{-1} range of the y-axis.

Evidence of metformin transformation along the river was explored by evaluating the percent change in metformin from the downstream-most site to respective site locations along the length of the river for each month group (Figure 2.13). With the exception of August, which showed minimal positive changes, metformin changes were mostly negative at sites upstream of River km 180 from May through September,

indicating a decreasing trend along the river during summer months. Metformin changes were mostly positive from October to December, suggesting an increasing trend along the river during autumn and early winter months. Relative to guanylurea, metformin remained unchanged from mid- to late-winter and spring months (January to April). Guanylurea changes along the river were negative from January to April and fluctuated between positive and negative changes at each site relative to the mouth of the river for the rest of the year. The variable changes along the river for the rest of the year were relatively small compared to the negative guanylurea changes along the river during the months of January through March.
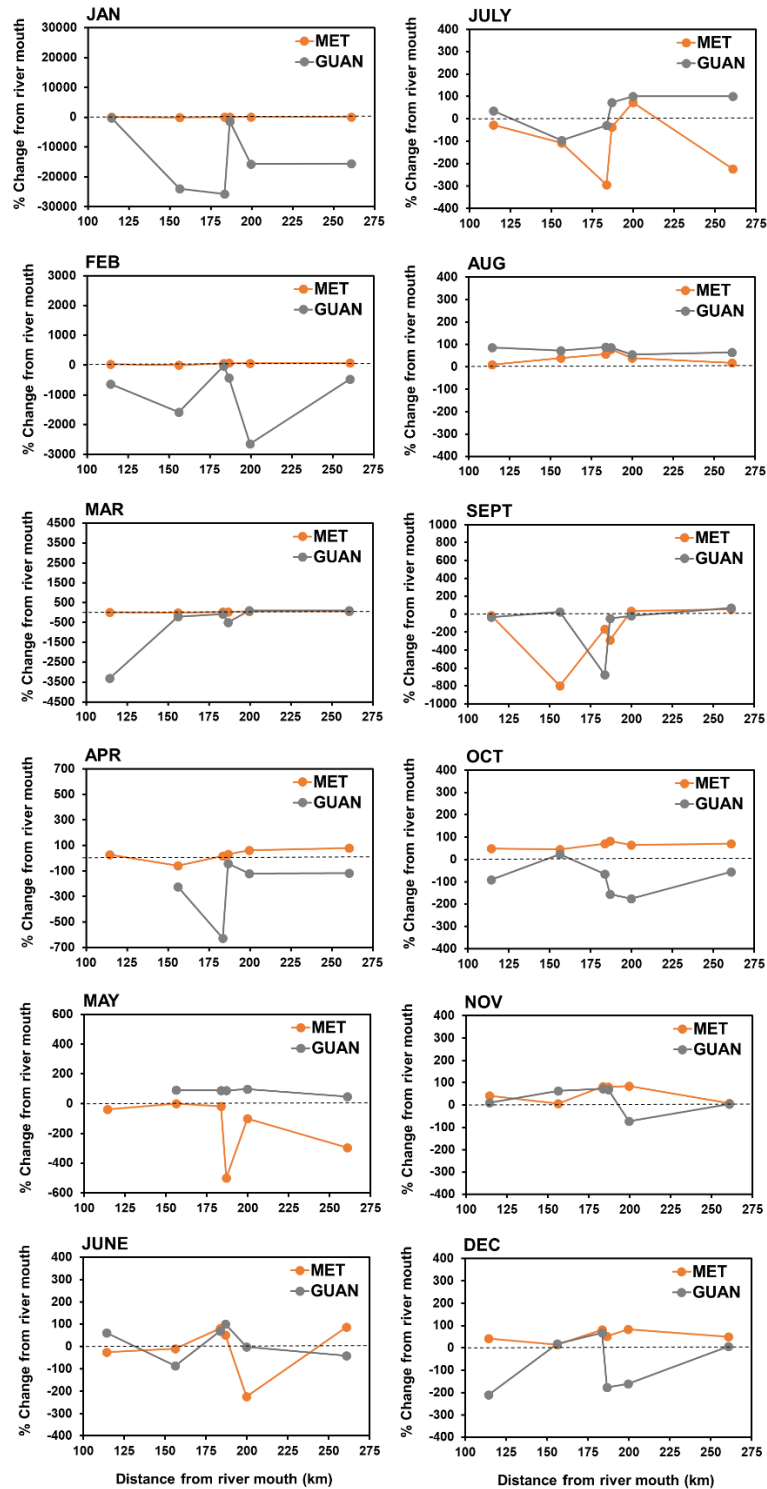
Figure 2.13. Percent change in metformin and guanylurea concentrations along the Columbia River. Percent change was calculated from the difference between average concentration at a site and the average concentration at the downstream-most site ("river mouth") (%Δ=C_{FINAL}-C_{ORIG}/C_{ORIG}). Negative values indicate a decrease. If no concentration was measured at the downstream-most site, sites were compared to the next most downstream site.

64

In order to further explore the possibility of transformation, the ratio of guanylurea to metformin (G:M) was used as a proxy for metformin breakdown. Plots of G:M showed that occurrences of guanylurea exceeding metformin were most commonly observed at sites upstream of the Willamette-Columbia confluence (River km 156), except in October and at one site in March (Table, 2.7, Figure 2.14). A two-way ANOVA testing for differences between average concentrations upstream and downstream of River km 156 at each month verified that average G:M was generally higher upstream of River km 156 ($F(1,273)=23.56$, $p<0.0001$). Temporal patterns in G:M were also present (ANOVA, $F(11,273)=15.66$, $p=0.0001$) and indicated that guanylurea exceeded metformin from September to December (Table 2.8, Figure 2.14).

Table 2.7. Average ratio of guanylurea to metfomin at year-round sampling sites along the lower Columbia River for the sampling year (Oct 2016-Sept 2017). River kilometer is a measure of distance (km) from the mouth of the river. Standard deviations are in parentheses.

Site	River km	G:M Ratio
BAT	79	0.36 (±0.5)
KD	114	0.75 (±1.8)
KU	114	0.74 (±1.0)
KPP	156	0.31 (±0.3)
CHL	183	1.19 (±2.2)
CMS	187	1.21 (±2.2)
RR	200	2.10 (±3.0)
OH	261	0.97 (±1.3)
IH	261	1.91 (±4.1)

Table 2.8. Average ratio of guanylurea to metformin at year-round sampling sites along the lower Columbia River for the sampling year (Oct 2016-Sept 2017). Standard deviations are in parentheses.

Month	G:M Ratio
January	0.86 (±1.0)
February	0.48 (±1.2)
March	0.60 (±2.2)
April	0.61 (±1.2)
May	0.04 (±0.1)
June	0.50 (±1.2)
July	0.02 (±0.1)
August	0.88 (±1.0)
September	1.10 (±2.2)
October	3.12 (±2.7)
November	2.66 (±4.6)
December	1.51 (±1.6)
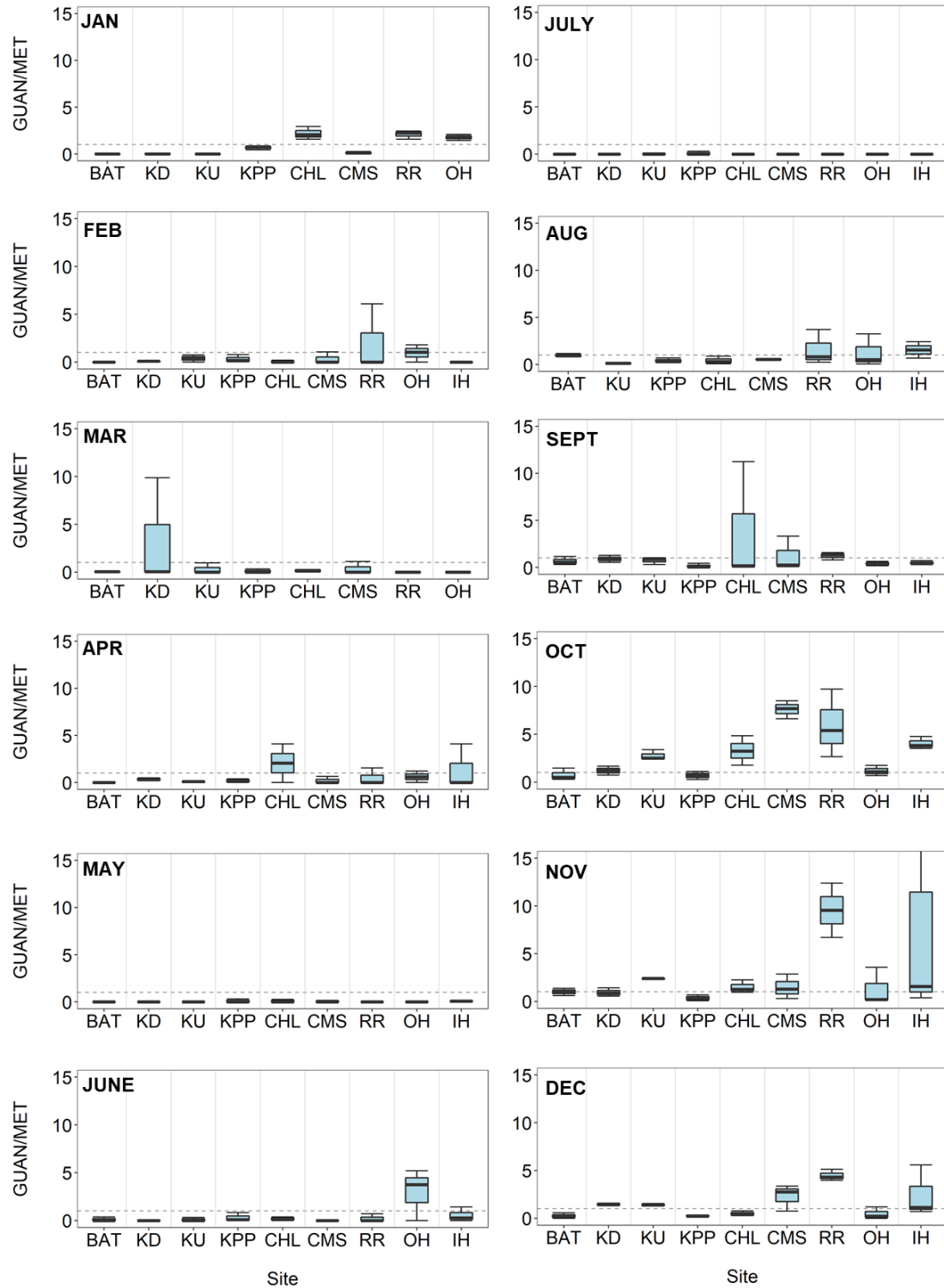
Figure 2.14. Spatiotemporal distribution of the ratio of guanylurea to metformin in the lower Columbia River. The average of triplicate samples was considered one sample point. Dots represent all sample points outside 1.5 times the interquartile range.

Possible environmental effects on metformin transformation upstream and downstream of the Willamette-Columbia confluence were analyzed by GAM models. Concentration ratio data were best predicted by temperature and CDOM. Similar to the prior GAM models on individual compound data, river variable smooth predictors best explained the total error in downstream G:M ratio data (Table 2.9).

Similar to the guanylurea models, the downstream G:M GAM model indicated a strong inverse relationship between G:M and river discharge values between ~3500–10,000 m^3 s^{-1} (Figure 2.15A), while the upstream model indicated no relationship between river discharge and guanylurea concentrations upstream of the Willamette-Columbia confluence. Also similar to guanylurea models, the upstream G:M GAM model showed an inverse trend with percent oxygen saturation; however, partial residuals were often outside the confidence bands of the smooth predictors (Figure 2.15D).

Other significant predictors included precipitation, which had a largely positively relationship to G:M values in both downstream and upstream models. However, ratios in upstream samples associated with precipitation values >6 mm showed an unchanging or inverse relationship between G:M and precipitation. The downstream G:M GAM model also indicated a slightly positive relationship with CDOM, which leveled off after CDOM values of 1.

Table 2.9. Best-fit model comparison for GAM models predicting the ratio of guanylurea to metformin. Smooth functions are represented by "s()". The best model is compared against two high performing GAM models and best-fit linear model for comparison of fit. The best model (in bold) was chosen based on the lowest AIC value.

Response variable	Model	GCV	R²	AIC
US G:M	**$C^{1/3}$ = s(SATDO) + s(PRECIP)**	**0.232**	**0.322**	**81.3**
US G:M	$C^{1/3}$ = s(SATDO) + s(CDOM) + s(PRECIP)	0.232	0.323	81.3
US G:M	$C^{1/3}$ = s(CDOM) + s(PRECIP)	0.241	0.295	83.6
US G:M	$C^{1/3}$ = SATDO	0.254	0.174	87.1
DS G:M	**$C^{1/3}$ = s(RD) + s(CDOM) + s(PRECIP)**	**0.091**	**0.486**	**21.7**
DS G:M	$C^{1/3}$ = s(RD) + s(CDOM) + s(PRECIP) + s(TURB)	0.090	0.520	20.2
DS G:M	$C^{1/3}$ = s(RD) + s(CDOM) + s(TURB)	0.095	0.490	22.8
DS G:M	$C^{1/3}$ = RD + CDOM + PRECIP	0.108	0.346	30.3
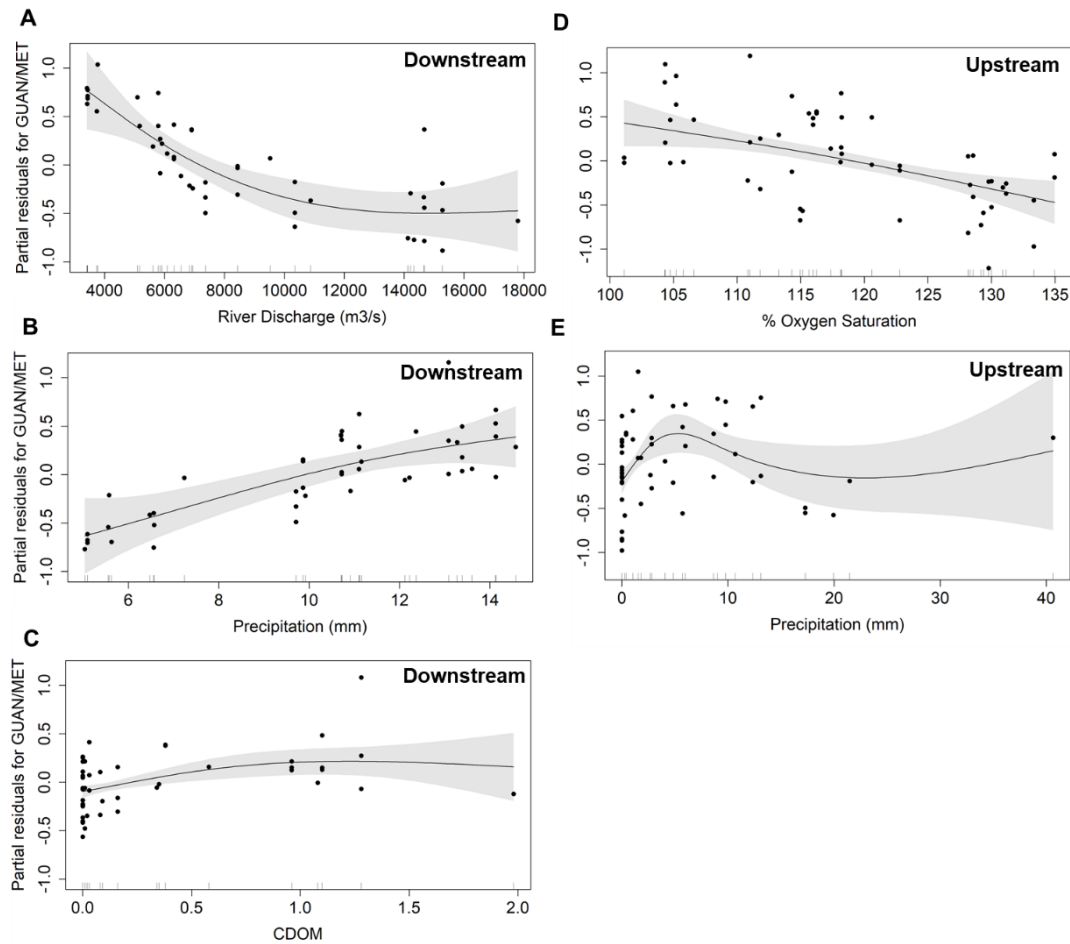
Figure 2.15. GAM model component smooth functions for the ratio of guanylurea to metformin based on samples taken downstream (A-C) and upstream (D-E) of the Willamette-Columbia confluence. Each plot shows the effect of a significant predictor variable given other model variables are held constant. Dots represent partial residuals of each smooth, which represent the model response that was not explained by other terms in the model. The blue shaded regions represent 95% confidence intervals.

2.3.8. *A Brief Investigation of Sorption*

Potential vial cap contamination issues observed in the LC-MS/MS runs prompted a short investigation into the sorption of metformin on Columbia River sediment. Acetonitrile (ACN) extractions of baked and unbaked river sediment spiked with metformin showed very poor recovery of 1 µg mL^{-1} metformin spikes. Each treatment had different recoveries of metformin (ANOVA, $F_{(2,8)}=49.30$, $p=0.0002$), with only 0.7% of the metformin spike recovered in baked sediment and only 3.4% in the unbaked sediment (Figure 2.16). No un-spiked unbaked sediment samples were processed for comparison of baseline river sediment metformin levels.
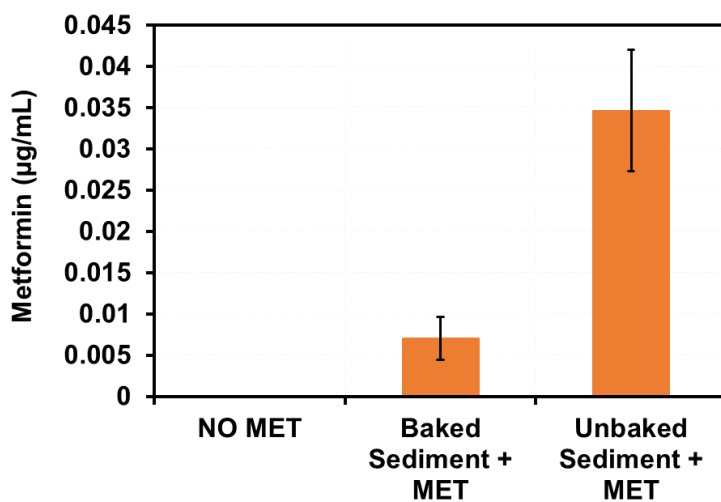
Figure 2.16. Acetonitrile extraction results of metformin-spiked Columbia River sediment. Bars represent (left to right) metformin concentrations in ACN extracts from unspiked, baked sediment; metformin-spiked, baked sediment; and metformin-spiked, unbaked sediment.

2.4. Discussion

2.4.1. *Metformin as a CEC in the Lower Columbia River*

Metformin was detected and quantified in the lower Columbia River at levels comparable to concentrations found in streams (ng L^{-1}),[13,46,162,165,223] and sewage effluent (μg L^{-1}).[51,160,167,223] The breakdown product of metformin, guanylurea, was also simultaneously detected at concentrations typically lower than metformin. Both metformin and guanylurea exhibited high variation in concentration along the river and across sampling months, but outliers were not beyond the range of stream concentrations found in other studies.[162,223] With a few exceptions in May and August, metformin levels inversely tracked the annual pattern of the freshet, with lowest levels in high-flow spring months (Feb-Apr) followed by highest levels in low-flow summer months (July-Sept). Guanylurea concentrations tended to track precipitation, with highest concentrations observed during low-flow/high-precipitation periods (Oct–Dec). Seasonal environmental factors only partially explained variation in metformin and guanylurea, but an exploration of alternative sources and particle-level interactions provided preliminary evidence for metformin distribution and behavior in a high-volume river system.

It should be noted that 2016–2017 was an exceptionally high precipitation year, with a relatively high river discharge and high average rainfall.[229] Thus, metformin concentrations observed in this study may be lower than the average surface water concentrations observed in normal or low precipitation years within the lower Columbia River.

2.4.2. *Influence of River Discharge on the Distribution of Metformin*

Seasonal river discharge patterns best explained metformin concentrations downstream of the Willamette-Columbia confluence. The data suggest that input to the lower Columbia from the Willamette River explain spatial trends in metformin concentration. Sites downstream of River km 156 had elevated metformin concentrations relative to upstream sites, suggesting that inputs from the Willamette River provide an important source of metformin. River discharge and CDOM accounted for approximately half of the variation in downstream metformin concentrations. The low levels of metformin observed at high discharge fluxes reflected effects of dilution from water volume during high-flow months. Since the CDOM effect was so small, and since CDOM was found to be highly collinear with river discharge, discharge could be considered the dominant river variable affecting metformin concentrations in the Columbia River downstream of the Willamette.

The relationship between river condition and metformin concentrations upstream of the Willamette-Columbia confluence was less clear than the relationship observed for downstream sites. While low discharge was generally associated with higher metformin concentrations reflecting river dilution effects, upstream river discharge effects were associated with a high degree of predictive error. Thus, metformin concentrations upstream of the Willamette-Columbia confluence may be less significantly influenced by single sources than metformin concentrations downstream of the confluence. Rather, the variable trend between metformin concentrations and river discharge may reflect the significance of multiple small sources of metformin to the Columbia River before the river receives a large influx of metformin from the Willamette River.

Low precipitation was generally associated with higher metformin concentrations in this upstream section, which suggests that the effects of multiple small sources may be higher during drier periods. However, the methods employed by this study may have failed to capture precipitation effects since environmental data were recorded only at the time of sampling, which often coincided with times of low rainfall despite high average monthly precipitation. Moreover, potential lag time between a precipitation event and its effects on the river may have obscured effects of precipitation observed in this study.

Overall, the clearer relationship between river discharge and metformin downstream of the Willamette-Columbia confluence relative to upstream indicates a strong relationship between large riverine sources and metformin concentrations. The Willamette River is the thirteenth largest river by volume in the United States and a major tributary of the Columbia River that accounts for ~15% of total Columbia River discharge.[180] From its source in the mountains south of Eugene, OR, the mainstem Willamette flows 187 miles north and forms a watershed that drains an area containing 70% of the population of Oregon.[230] With so many inputs from local population, sewage treatment, and runoff, the Willamette River likely delivers high concentrations of metformin to the Columbia River. However, while other studies have found trace levels of pharmaceuticals and endocrine-disrupting compounds in the Willamette River, metformin has not been measured.[200,222] Future research should monitor monthly metformin levels and river conditions at the mouth of the Willamette and other tributaries into the Columbia River in order to elucidate the contribution of riverine inputs to total metformin concentrations.

2.4.3. *Influence of River Discharge on the Distribution of Guanylurea*

Similar to metformin, seasonal river discharge best explained guanylurea concentrations downstream of the Willamette-Columbia confluence. The low levels of guanylurea observed at high discharge fluxes reflected effects of dilution from water volume during high-flow months. Moreover, high CDOM values downstream of the confluence were associated with high guanylurea concentrations, and high precipitation values were very slightly associated with high guanylurea concentrations. However, as with metformin data, precipitation effects were likely obscured by sampling methods, which were limited to downstream sampling times during mostly periods of low precipitation that did not account for high monthly average precipitation. Additionally, CDOM collinearity with river discharge made it difficult to isolate CDOM effects. Thus, river discharge could be considered the dominant river variable affecting guanylurea concentrations in the Columbia River downstream of the Willamette.

Upstream guanylurea concentrations were not explained by river discharge. Rather, low guanylurea concentrations were associated with periods of high percent oxygen saturation and intermediate CDOM values, and high guanylurea concentrations were associated with periods of intermediate precipitation. The reasons behind these trends are unknown since very little is known about guanylurea as a chemical compound in the environment; however, since high precipitation was associated with the upstream sampling period from October to December during which guanylurea concentrations were highest, these data suggest a connection between rainfall and high guanylurea levels in the Columbia River. Studies have shown that rainfall dramatically increases contaminant loading into receiving surface waters by increasing surface and groundwater

runoff.[70,231] With a historical annual rainfall reaching to over 110 in, the Columbia watershed experiences strong precipitation patterns throughout the year.[232] Since guanylurea is a breakdown product of multiple agricultural, munitions, and industrial compounds which might also be in the environment,[169–171] it is expected that periods of high precipitation would be associated with higher occurrence of guanylurea in the river.

Indeed, multiple results from this study provide evidence for non-point sources of guanylurea in the Columbia River. The lack of spatial variation in guanylurea along the river indicates diffuse sources. The negative relationship between discharge and guanylurea concentrations downstream of the Willamette–Columbia confluence tapers off sooner than was observed with metformin, suggesting that the highest discharge values were associated with delivering more non-river (i.e., terrestrial or groundwater) sources of guanylurea to the river. Furthermore, elevated guanylurea levels from October to December at the Inner Hook site (a small area shielded from local sewage effluent and mostly surrounded by land) indicated higher guanylurea input from terrestrial sources during high precipitation periods.

Overall, the clearer relationship between river discharge and guanylurea downstream of the Willamette-Columbia confluence relative to upstream provides further evidence in support of the significant effect of the Willamette River on the overall metformin and guanylurea concentrations of the Lower Columbia River. Nonpoint sources (e.g., septic, landfill leachate, agricultural runoff, groundwater) picked up by precipitation may be an important driver of guanylurea concentrations upstream of the confluence, but this study was unable to elucidate these effects.

2.4.4. *Additional Sources and Evidence of Metformin Transformation*

Surprisingly, it was found that sewage inputs did not increase metformin levels, but these results were possibly skewed by high river flows. Sites directly downstream from wastewater effluent pipes mostly did not have elevated metformin or guanylurea concentrations relative to sites directly upstream or shielded from the pipes. Given that metformin and guanylurea have been measured at high levels ($\mu g\ L^{-1}$) in sewage effluent in other studies,[51,167,223] the lack of sewage effect on metformin levels was unexpected, but not improbable given the relatively higher river discharge and mixing rates of the Columbia River. Related confounding factors were the broad sampling radius relative to the sewage pipes and relatively lower effluent discharge volume which, in conjunction with high river flow and mixing, may have quickly diluted any elevated metformin concentrations from effluent. These results provide further evidence in support of discharge-driven metformin levels in the river and explains the lack of significant local metformin variation along the river. Since it is known that metformin enters the environment largely via wastewater,[159,163,164,233] it is likely that metformin concentrations are driven by the combined input of multiple sewage sources into the river. These results also suggest illustrate the difficulty in measuring small point sources in such a high-volume water system; future research should measure the effects of Columbia River discharge on effluent dilution at varying distances from effluent pipes.

This study could not confirm metformin transformation within the Columbia River. From May to September, metformin mostly decreased from each site to the downstream-most site, thereby indicating possible transformation during these months. During the same period, guanylurea varied between increasing and decreasing from each

site to the downstream-most site, but absolute changes in guanylurea were very small relative to absolute metformin changes due to the low guanylurea concentrations during these months. Thus, metformin transformation into guanylurea was either very low or not occurring. In support of this idea, G:M values mostly did not increase in the season from June to September when the only evidence of transformation along the river was observed; this indicates minimal production of guanylurea relative to the decreased metformin concentration in the summer season. Moreover, metformin levels at each site in the following season (Oct–Dec) did not decrease along the river, and generally higher levels of guanylurea at each site relative to the downstream-most site indicated an influx of guanylurea from non-point sources. These data suggest that metformin transformation may be occurring in the river at low levels, but that metformin sources and environmental variables are stronger drivers of metformin and guanylurea variability in the Columbia River. This conclusion is also supported by model predictions of high river discharge associated with low G:M values in sites downstream of the Willamette-Columbia confluence, which suggest the dominant influence of river flow in controlling metformin and guanylurea concentrations in the river, rather than transformation. However, given that river variables were less effective at explaining upstream G:M values, transformation of metformin might better account for metformin variations upstream of the Willamette River relative to downstream sites.

2.4.5. *Inferences from Water Analysis Methods*

River water analyses by LC-MS/MS with direct injection successfully enabled low-level detection and quantification of metformin and guanylurea without solid phase

extraction. This study found metformin and guanylurea detection levels akin to other studies[13] with higher guanylurea recovery due to successful implementation of ^{15}N-labelled guanylurea internal standard. However, high variability was periodically encountered throughout the sampling year, with river water samples showing large sporadic spikes in metformin concentrations.

Metformin variability among river water samples cannot be fully explained by sampling methods or contamination. The vial cap contamination issues that were observed in the standard curves do not apply to the samples, since separate vials that had not touched sediment were used to collect river water and field blanks. Since 1 L jars were sometimes used to collect sediment, it could be argued that field blank contamination and sample variability was caused by metformin sorption to the cap of the 1 L grab sample jars, similar to the standard curve contamination from the dilution vial caps. If this were true, 11–80 ng metformin would be required to be present in the Milli-Q field jar. However, even if 1 µg sediment residue was stuck to the jar cap from previous sediment collection in the same jar, at least 11 µg metformin would have to adsorb to the particulate residue, resist removal by extensive acid and methanol washing, and then completely desorb into Milli-Q. This level of contamination is highly unlikely, since field jars only contained natural sediment and were not spiked with metformin, and since metformin may strongly adsorb to particulate matter even in the presence of a desorption solvent like acetonitrile (ACN). Thus, field blank contamination was likely not due to sediment contamination of jar or vial caps.

Although some variability could have been introduced in the data processing steps, for example during the integration of peaks subject to varying degrees of baseline

drift—a commonly observed source of error in high performance liquid chromatography[234,235]—visual inspection of the individual peaks showed no obvious peak tailing, splitting, or fronting. Moreover, peaks associated with high values were indeed much larger than peaks associated with lower values, and internal standards were comparable in terms of peak height and area. Since error due to instrumentation methods was unlikely given that patterns in elevated metformin levels between samples were random and blanks interspersed with long sample runs did not show evidence of sample carryover, it is very likely that the variability observed in this data set is real. Sources of this variability should be investigated further in future studies.

One line of further investigation involves examination of the importance of metformin speciation and its potential effect on particle interactions. Observations in this study suggest that chemical speciation and related physicochemical interactions may explain variation between sample replicates. The metformin contamination issues that appeared after cleaning and reusing sediment-exposed lab vials and field jars indicated possible interaction effects between metformin and particulate matter in the river. As a highly soluble and polar species, metformin likely does not sorb to organic matter in sediments and soils via hydrophobic interactions.[236] However, as a cationic species at the pH of typical river samples (pH 7-8), metformin may sorb to negatively charged soil and sediment surfaces via ionic interactions.[237] The sorption behavior of cationic species to clay minerals is often complex,[238] as demonstrated by conflicting and limited experimental data on metformin K_{oc} (organic carbon-water partition coefficient) values versus measured metformin levels in sediment[24,140,141,160,223,237,239] For instance, a 2002 USGS study on the distribution of PPCPs between water and sediment found that

pharmaceuticals, including metformin, with low predicted partitioning coefficients were unexpectedly found at higher concentrations in sediment than surface water.[24] These discrepancies may be explained by the idea that single parameter K_{ow} sorption models may be unreliable for K_{oc} estimations of polar compounds since they do not account for both nonpolar (van der Waals) and polar (electron) interactions between sorbent and sorbate.[25] Indeed, metformin has been detected at levels up to 140 ng g^{-1} in sediment.[160] Moreover, a recent study on the adsorption of metformin to montmorillonite clay particles found "a great affinity of metformin towards the clay mineral",[142] and another recent study has found metformin to act as a cationic partner toward DNA.[240] Based on this information, it is plausible that the sediment residues on vials caps used in this study may have caused trace variation in metformin quantification.

Ionic sorption also presents an explanation for the metformin variability observed in river water samples. Cation exchange capacity of particles is directly related to particle surface area.[201,241] Sample collection in this study took place in shallow water on beaches or rocky shorelines where greater particle capture was likely to occur. The filter size used for river water samples in this study was not large enough to remove particles <0.7 µm which have greater surface area ratios than larger particles;[241] thus, the measured metformin concentrations may have actually been a summation of surface water and colloidal concentrations. Furthermore, this study utilized a known desorption agent, acetonitrile (ACN), for the solvent gradient during HPLC separation, which could have desorbed compounds on unfiltered particles during LC-MS/MS analysis. Given the trace levels of metformin or guanylurea in river water (ng L^{-1}), only a small amount of desorption would be necessary to drastically skew quantification. This author encourages

future field experiments to explore metformin sorption to colloids and establish

environmentally relevant metformin K_{oc} values for different sediment types.

CHAPTER 3: EFFECTS OF METFORMIN ON PHYTOPLANKTON PHOTOSYNTHESIS AND GROWTH

3.1. Introduction

There is ample evidence that pharmaceuticals and personal care products (PPCP) are present in waterways throughout North America,[46,48,50,160,166] yet the ecological effects of pharmaceutical compounds are poorly known. Of particular concern is the lack of ecotoxicity data associated with metformin, despite its high prescription rate and correspondingly high occurrence in wastewater influent and surface waters of North America and Europe.[13,46,50,51,160] As an unmetabolized bioactive compound that is persistent in the environment, metformin has the potential to affect aquatic organisms in unpredictable ways that need to be elucidated for environmental risk assessment.

Of the limited research on metformin ecotoxicity, there have been possible effects on endocrine disruption, growth, and mortality, however, effects on the lower aquatic food web (i.e., algae) remain unknown.[140] Tank experiments exposing fathead minnows to metformin at wastewater-relevant levels (40 µg L^{-1}) found significant upregulation of messenger ribonucleic acid (mRNA) encoding the egg-protein vitellogenin,[31] with a significantly stronger estrogenic effect on juvenile fish.[242] Some crop plants, such as carrots, preferentially uptake metformin at the expense of growth.[243] Recent work even correlates metformin use and glucose homeostasis with compositional and functional shifts in gut microbial assemblages.[244] Perhaps relatedly, metformin also has bacteriostatic (i.e., negative growth) effects via disruption of the folate cycle and suppressed methionine production.[175] Metformin toxicity tests have been performed on

other organisms, such as zebrafish, chironomids, and zooplankton, but only at high concentrations testing for acute toxicity.[140]

The effects of metformin on eukaryotic microbes remains unknown. This constitutes a critical knowledge gap since microbes carry out key biochemical functions that influence energy flow through aquatic food webs. In particular, algae form the foundation of aquatic food webs through primary production and can provide an entry point for lipophilic (high K_{ow}) organic contaminants.[96,245] Direct toxic effects of PPCPs on algae have also been observed, but effects vary according to species and drug.[8,40,246–248] Since metformin has a low K_{ow} value,[249] the compound has a low bioaccumulation factor and is more likely to alter food web dynamics and nutrient processing through direct toxicity to algal communities.[40,250]

Given its role as an AMPK-activator, metformin likely influences cell metabolism broadly among eukaryotes. AMPK is a member of the highly conserved eukaryotic protein kinase family that includes SnRK1 (SNF1-related protein kinase 1) in plants.[251] AMPK activation reduces anabolic processes (e.g., synthesis of fatty acids, proteins) and increases catabolic processes (e.g., glycolysis).[147] Likewise, SnRK1 activation in plants signals oxidative stress and reduces carbon/energy consumption.[252] Specifically, SnRK1 activates genes that limit photosynthesis, biosynthetic processes, and overall energy supply to match cellular activity to stressful conditions (e.g. less light, nutrient deprivation).[253] Recently, genes for SnRK1 have been found in eukaryotic algae.[254] Consequently, metformin may activate the AMPK homolog, SnRK1, in eukaryotic algae to signal oxidative stress and reduce cellular quotes of carbon.

Since metformin has the potential to alter food web dynamics through allosteric changes in algal metabolic activity, the second objective of this project was to determine the effects of metformin on phytoplankton photosynthesis and growth. Specifically, freshwater and marine phytoplankton cultures were spiked to a range of environmentally and sewage relevant metformin concentrations and measured for changes in photosynthetic activity and cell growth. It was expected that higher metformin doses would inhibit photosynthetic activity and cell growth in all algal cells. The effect of metformin on algae could be used to inform fundamental questions concerning the toxicity of metformin to photosynthetic eukaryotes and other AMPK/SnRK1/SNF1 containing eukaryotes. On a larger scale, this study has particular relevance to estimating overall environmental risk associated with metformin, including energy transfer in the food web, and additional relevance to applied problems such as biotreatment of wastewater[255] and biofuel production.[256]
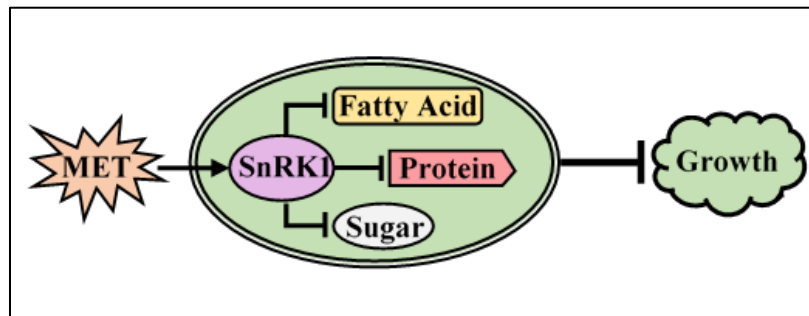
Figure 3.1. Illustration of the hypothetical effects of metformin on an algal cell. It is proposed that metformin causes a reduction in photosynthesis, biosynthetic processes, and cell growth by activating a stress response through the energy-regulating AMPK homolog SnRK1.

3.2. Methods

3.2.1. Media and Materials

All glassware used in media preparation and culturing was cleaned according to the USGS National Water-Quality Assessment (NAWQA) protocols in order to eliminate trace organic and inorganic contaminants.[225] Sampling, culturing, and filtration equipment was also sterilized by autoclaving.

Freshwater WC media[257] and ESAW (enriched seawater, artificial water) media[258,259] was prepared in 4 L Nalgene™ narrow-mouth polycarbonate bottles. Freshwater WC media was prepared by adding nutrient, vitamin, and metal constituents to Milli-Q and adjusting to a pH of 7.70-7.80. ESAW media was prepared by adding nutrients to Milli-Q, which was bubbled overnight with air before adding metal and nutrient constituents and adjusting to a pH of ~8.20. Prepared media was filtered through EMD Millipore™ (Temecula, CA) 0.45 µm mixed cellulose ester filter membranes with an EMD Millipore™ borosilicate glass 1 L vacuum flask, 300 mL funnel, and base with a silicon plug and aluminum clamp. Filtered media was stored at 4 °C in sterilized 4 L Nalgene™ narrow-mouth polycarbonate bottles until use in experiments.

Experimental cultures were grown in 250 mL Erlenmeyer flasks with glass wool plugs. Samples were taken with sterilized micropipette tips. PAM fluorometer samples were aliquoted, diluted, and dark-adapted in disposable borosilicate glass culture tubes. Coulter counter samples were aliquoted into polystyrene counter cups and diluted with Isoton II® phosphate-buffered saline diluent (Beckman Coulter, Indianapolis, IN). Samples for filtering were aliquoted into amber 40 mL glass vials and filtered using Whatcom™ 0.7 µm GF/F filters which were previously combusted at 450 °C for at least 4

h. Filtering equipment consisted of EMD Millipore™ borosilicate glass 125 mL vacuum flasks, 15 mL funnels, and bases with a silicon plug and aluminum clamp. Filtered samples were aliquoted into 1.5 mL (12x32mm) Thermo Scientific™ amber borosilicate glass SUN-SRI™ standard opening autosampler vials.

Similar to river water samples, separation of metformin and guanylurea in filtered phytoplankton samples was attained using a Synergi™ Hydro-RP LC Column (250 x 4.6 mm, 4 µm, 80 Å; Phenomenex, Torrance, CA). All mobile phase solvents were made in the laboratory: Solvent A consisted of 0.1% formic acid in water, and Solvent B consisted of 0.1% formic acid in acetonitrile. A ThermoFisher™ (Waltham, MA) BetaBasic™ C8 Javelin guard column (10 x 2.1 mm, 1.5µm) minimized column contamination from particulate matter in samples.

3.2.2. *Culture Conditions*

Two different experimental organisms were chosen to model potential effects of metformin on freshwater and estuarine algal species, respectively. Due to physiological similarity to land plants (i.e., SnRK1 pathways), short doubling times, and general use as model organisms in PPCP toxicology tests,[246,260–264] *Chlorella vulgaris* was used for initial toxicity assays probing for effects of metformin on algal photosynthesis and growth. *C. vulgaris* is a small (2-10 µm) unicellular freshwater alga that belongs to the phylum Chlorophyta, which include eukaryotic green algae and land plants. Since diatoms account for over half the algal composition of the Columbia River and estuary,[265,266] *Thalassiosira weissflogii* was used as an environmentally relevant approximation for effects of metformin on algae found along the river water sample sites

in this study. *T. weissflogii* is a relatively large (4-32 µm) marine unicellular diatom which belongs to the Heterokonta, a group that includes algae ranging from kelp to diatoms.

Experimental batch cultures were grown using stock cultures of phytoplankton and freshly prepared media. Freshwater *C. vulgaris* cultures isolated from the Columbia River were grown in standard WC media and marine *T. weissflogii* cultures (purchased from the National Center for Marine Algae and Microbiota) were grown in ESAW media. Each experimental flask received 100 mL media with an amount of stock culture to achieve a starting average culture density that would provide a lag phase of at least two days (~17,000 cells mL^{-1} for *C. vulgaris*, ~3500 cells mL^{-1} for *T. weissflogii*). All cultures were incubated at 18℃ under a 12:12 light:dark cycle in a walk-in environmental chamber equipped with full spectrum lighting (~191±18 µmol photons m^{-2} s^{-1}).

3.2.3. *Experimental Design*

Since toxic effects of CECs in unicellular organisms can range from inhibition of growth to reduced photosynthesis or enzyme activity,[267–269] triplicate batch cultures were exposed to a range of concentrations of metformin during exponential growth and compared against a triplicate control. Each batch culture was grown to mid-exponential phase and then spiked with a solution of metformin in media to achieve the target concentrations of metformin in culture. Target treatment amounts corresponded to environmentally relevant levels at ~1 µg L^{-1}, wastewater levels at 10-100 µg L^{-1}, and levels probing for biochemical effects (i.e., SnRK1 activation) at ~500 µg L^{-1}. In order to simulate the amount of metformin that would be encountered per cell in a natural river

setting at the tested levels, spike amounts were based on the product of the simulated

metformin concentration and the average culture density at the time of the spike, divided

by an approximation of the average algal cell density in the Columbia River from 2011-

2014 (~4000 cells mL^{-1}).[265] An additional flask for each treatment and control was used

to record pH over the course of the experiment.

Samples were taken at 0, 1, 3, and 5 h following the spike, and then every 24 h for

four days. Coulter Counter and PAM fluorometer samples were taken at each time point.

An additional 1 mL sample pooled over the triplicate treatments were taken at 0, 5, and

96 h. These samples were filtered and frozen at -20 °C for future LC-MS/MS analysis in

order to quantify the amount of metformin in each culture over the course of the

experiment. Directly following the 96-h time point, 1 mL of each triplicate treatment was

added to 100 mL WC or ESAW media to make four post-experiment cultures to test for

recovery of algae.

3.2.4. Instrumentation

Cells counts were measured at each time point using a Beckman Coulter© Model

Z2 particle counter (Beckman Coulter, Indianapolis, IN). The Coulter Counter was set to

inject and count the number of cells in 1 mL of saline-diluted culture sample. Optimal

size ranges were based off distribution of cells from trial measurements for each species.

The CUVETTE version of the Walz WATER-PAM (Pulse-Amplitude-

Modulation) chlorophyll fluorometer (Heinz Walz GmbH, Germany) was used to

measure the photosynthetic efficiency of algal cultures. WinControl-2 software with a

PAM-Control unit recorded fluorometer data. The PAM Light Curve program was used

to measure the fluorescence of cells exposed to a saturating light pulse followed by increasing levels of actinic light intensity covering the wavelength range of photosynthetically active radiation (400-700 nm).

Metformin and guanylurea in filtered phytoplankton samples were separated using a Shimadzu Prominence® HPLC system using two binary pumps (Shimadzu LC-20AD XR Prominence® LC pumps) and gradient elution on the reverse-phase column. Analytes were identified, detected and confirmed using an AB Sciex® QTRAP 5500 mass spectrometer (Applied Biosystems/MDS Sciex Instruments, Concord, ON, Canada) in conjunction with Analyst 1.6.2 software. All LC-MS/MS parameters matched parameters used to process river water samples (Table 2.2), except with a smaller injection volume of 10 µL to account for high density culture matrices.

3.2.5. *Sample Processing and Calculations*

Coulter Counter Samples

All samples taken for Coulter counting were diluted in 9-18 mL saline diluent before measuring. Cell counts from diluted Coulter samples (N_{CC}) were used with the known injection volume, sample:diluent ratio, and culture volume at time of sampling to calculate culture density (cells mL^{-1}) and the total number of cells in culture ($N_{culture}$).

[1] $N_{sample} = (N_{CC})^{-1}(V_{diluent} + V_{sample})$

[2] $\text{culture density (cells } mL^{-1}) = (V_{sample})^{-1}(N_{sample})$

[3] $N_{culture} = (\text{culture density})(V_{culture})$

PAM Fluorometry Samples

All samples taken for PAM fluorometry were diluted to 3 mL with WC or ESAW media. Daily measurements of a test culture determined the optimal ratio of sample to diluent media to avoid fluorescence detection errors (i.e., overflow error). Diluted samples were dark adapted for 30 min to fully oxidize Photosystem II and maximize fluorescence potential upon light saturation. Dark-adapted samples were also exposed to 10 s of far-red light just before PAM measurements to process remaining intersystem electrons through excitation of Photosystem I and oxidation of the plastoquinone pool.[270–272] A 4-min light curve was recorded for each dark-adapted sample.

PAM fluorescence measurements were used to quantify photosynthetic parameters during the light curve. Light saturation of the cells was measured by maximum fluorescence (F_m) from the initial saturating pulse and subsequent fluorescence peaks (F_m') from the stepwise actinic pulses. The PAM software subtracted maximum fluorescence values from minimum fluorescence values (F_o or F) at each light pulse to calculate photosynthetic parameters over the course of the light curve (Table 3.1, Figure 3.2). Specifically, the relative electron transport rate (rETR), maximum quantum yield (F_v/F_m), light saturation (E_k) and photoinhibition constant (β), and nonphotochemical quenching (NPQ) were calculated as proxies for the photosynthetic ability of algal cells.[273,274]

Name	**Parameter**	**Equation**	**Description**
Maximum fluorescence	F_m F'_m	Direct measurement	*Fluorescence when PSII reaction centers are closed and plastoquinone pool is reduced*
Minimum fluorescence	F_o F	Direct measurement	*Fluorescence when PSII reaction centers are open and plastoquinone pool is oxidized*
Maximum quantum yield of PSII	$\Phi PSII_{max}$	$\dfrac{F_v}{F_m}$ or $\dfrac{F_m - F_o}{F_m}$	*Efficiency of dark-adapted PSII to absorb light*
Effective quantum yield of PSII	$\Phi PSII$	$\dfrac{F'_v}{F'_m}$ or $\dfrac{F'_m - F}{F'_m}$	*Efficiency of PSII in the presence of light to absorb light*
Relative electron transport rate	ETR	$\Phi PSII \times PAR \times 0.5 \times 0.84$	*Rate of electron movement in the photosynthetic ETC*
Electron transport efficiency	α	Initial slope of light curve	*Efficiency of electron transport in the photosynthetic ETC*
Minimum saturating irradiance	E_k	$\dfrac{ETR_{max}}{\alpha}$	*Onset of light saturation*
Nonphotochemical quenching	NPQ	$\dfrac{F_m - F'_m}{F'_m}$	*Excitation dissipated by heat*

Table 3.1. Photosynthetic parameters measured or calculated by PAM fluorometer.
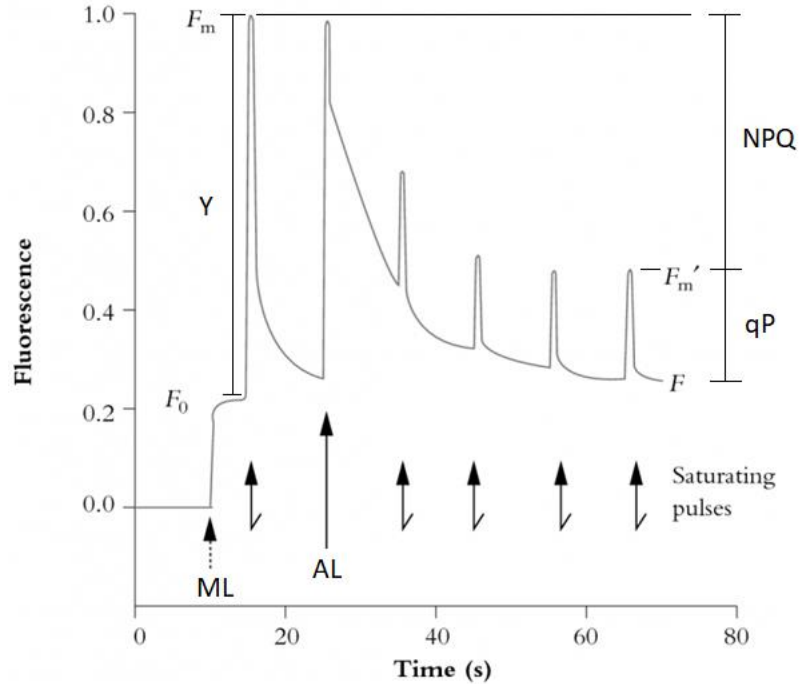
Figure 3.2. Kinetics of fluorescence in photosynthetic cells in response to the PAM fluorometer Light Curve program. A measuring light (ML) records minimum fluorescence values (F_o and F) without inducing photosynthesis. An initial saturating pulse induces maximum fluorescence (F_m) while subsequent actinic pulses induce fluorescence peaks (F_m'). Minimum and maximum fluorescence values are used to calculate photosynthetic parameters (Y, ETR, qP, qN, NPQ) over the course of the light curve to determine overall photosynthetic efficiency of a sample. Figure modified from Atwell 2010.

Metformin Analysis

Filtered samples taken for measuring metformin concentration in cultures were thawed at room temperature on the day of LC-MS/MS analysis. Samples at higher metformin concentrations were diluted 1:500 in mineral water to increase peak resolution.

Chromatographic analysis was performed using MultiQuant™ Software (Version 3.0). Metformin and guanylurea were quantified based on peak integration of chromatograms using the internal standard (IS) method. A linear baseline fit was used for all peak integrations.

The actual concentration of metformin and guanylurea was calculated from a standard curve of measured area ratios (analyte area/IS area) versus expected concentration ratios (analyte concentration/IS concentration). The standard curve encompassed the predicted range of analyte concentrations in culture treatments (0-1000 µg L^{-1}). Standard solutions capturing this concentration range were processed with each sample batch to establish a standard curve with each run. Data from a standard sample was used in the standard curve if the concentration calculated from the measured area ratio was within 20% of expected values. A singlet six-point linear standard curve with a 1/x weighting factor was established with each run.

Standards were prepared by dilutions of metformin and guanylurea. A primary stock solution of 10 mg mL^{-1} 1:1 metformin/guanylurea in mineral water was diluted to working stock solutions of 1250 ng L^{-1}. Calibration solutions ranging from 0-1000 µg L^{-1} were made by pipetting appropriate amounts of working stock solution into mineral water to reach a final volume of 1 mL calibration solution for each concentration.

Internal standard solutions of deuterated metformin and ^{15}N-labelled guanylurea were prepared the week of the LC-MS/MS runs. Solid stock material of 1 mg was previously dissolved in 1 mL Milli-Q, sealed, and frozen at -20 °C, up to 8 months. In the week of the run, a serial dilution of the 1 mg mL^{-1} stock solution in mineral water yielded a working solution of 998 ng mL^{-1}. All samples and standard solutions received 2 µL each of metformin and guanylurea IS working solution just before LC-MS/MS injection to get a final IS concentration of 10,000 ng L^{-1}.

3.2.6. Statistics

Non-linear regression was used to fit curves to cell count and ETR data. Curve fitting for PAM ETR data was achieved using Microsoft® Excel® Solver, while curve fitting for growth data was performed using GraphPad Prism (version 7.04 for Microsoft® Windows®, GraphPad Software, La Jolla, California). Resulting models were used to estimate parameters of cell growth and photosynthetic efficiency. Means and standard deviations of each parameter of interest were calculated across replicates and compared between treatments and time points using two-way repeated-measures ANOVAs, in which each time point was considered a within-factor condition and each treatment was considered a between-factor condition. All statistical analyses of growth and PAM data were performed using Microsoft® Excel® 2016 or GraphPad Prism.

Cell count data for short-term post-spike measurements were plotted against time and fitted with an exponential growth equation [4] to measure growth effects of metformin from 0-5 h after the spike. The number of cells at time t (N_t) was described by the initial number of cells (N_0) and the specific growth rate (μ).

[4] $\quad N_t = N_o\, e^{\mu t}$

Cell count data for the long-term post-spike measurements (0-96 h) were plotted against time and fitted with the Weibull growth curve model [5][275] to measure growth effects of metformin from 0-96 h after the spike. The number of cells at time t (N_t) was described by the initial and maximum number of cells (N_0, N_{max}), the specific growth rate (μ), and the time corresponding to the point of inflection (δ). Resulting best-fit models were used to compare overall differences in growth patterns between control and treatment cultures.

$$[5] \quad N_t = N_{max} - (N_{max} - N_0)e^{(-(\mu t)^\delta)}$$

The specific growth rate was also directly calculated from measured cell counts [6] and averaged for each treatment at each time point. Average specific growth rates of treatments were plotted against time and compared between control and treatment cultures using a two-way ANOVA.

$$[6] \quad \mu = \frac{(\ln N_n - \ln N_1)}{(t_n - t_1)}$$

ETR data were fitted with the Platt photosynthetic model [7].[276] Electron transport of cells exposed to PAR was estimated by best-fit values for ETR_s (ETR_{max} in the absence of photoinhibition), electron transport efficiency (α), and photoinhibition (β) parameters. Resulting models were used to compare average α and β parameter values among treatments at each time point. Likewise, maximum ETR in the presence of photoinhibition (ETR_{max}), maximum quantum yield of PSII (Φ_{max}), and minimum saturating irradiance (E_k) were calculated from predicted ETR and parameter values and compared among treatments at each time point [8].

$$[7] \quad ETR_{PAR} = ETR_s \times \left(1 - e^{-\alpha*PAR/ETR_s}\right) \times e^{-\beta*PAR/ETR_s}$$

$$[8] \quad E_k = \frac{ETR_{max}}{\alpha}$$

Additionally, NPQ and quantum yield (F_v/F_m, Φ) data were compared between treatments by calculating the percentage with respect to the control value at each time point. Two-way repeated-measures ANOVAs were used to determine significant differences in mean NPQ and Φ percentage values between treatments and time points,

however, each time point was considered a separate group and concepts of trend were ignored for these analyses.

3.3. Results

3.3.1. *Metformin Variation within Cultures*

Initial metformin concentrations for low, intermediate, and high dose *C. vulgaris* treatments were measured as 1 µg L^{-1}, 80 µg L^{-1}, and 500 µg L^{-1}, respectively. Initial concentrations in *T. weissflogii* cultures were 1 µg L^{-1}, 60 µg L^{-1}, and 400 µg L^{-1}. Each culture was within 20% error of the reported dose concentrations.

Comparison of metformin levels in cultures at the time of the spike versus after 5 h and 96 h indicated possible degradation of metformin by *T. weissflogii* diatoms and variable responses by *C. vulgaris*. Metformin concentrations of *T. weissflogii* cultures at low, intermediate, and high doses decreased by ~16%, 22%, and 15% after 96 h, respectively. However, metformin concentrations in all *C. vulgaris* treatments showed variable and inconsistent decreases and increases relative to initial spike levels after 5 and 96 h.

Possible matrix effects were observed in algal cultures, with greater effects in *C. vulgaris* cultures. Quantification of metformin in media blanks revealed no metformin in *T. weissflogii* ESAW blanks and metformin concentrations 10x below lowest dose amount in *C. vulgaris* WC media (~100 ng L^{-1}). Samples from intermediate and high dose *C. vulgaris* treatments required 500-fold dilution to enable peak separation and quantification. Moreover, considerable peak-tailing in successfully separated chromatogram peaks was observed in most *C. vulgaris* and *T. weissflogii* culture samples.

3.3.2. *Effects of Metformin on Phytoplankton Growth*

Optimal size range for cultures was estimated from cell count distribution as 2.5-5.125 µm for *C. vulgaris* and 7.0-16.5 µm for *T. weissflogii*. Growth models for treatments after 96 h were best fit by Weibull growth equations with specific growth rate and inflection point parameters listed in Table 3.1. Growth models for treatments after 5 h were best fit by exponential growth equations with specific growth rate parameters listed in Appendix Table 3A.

Metformin exposure over 5 h did not affect cell density or growth rate in *C. vulgaris* and *T. weissflogii* cultures. All 5 h exposure data for density and growth in algal cultures is summarized in Appendix Table 3A, 3B and Appendix Figure 3A. A two-way ANOVA did not find any differences in *T. weissflogii* culture density between treatments and time ($F_{(18,48)}$=0.588, P=0.891). Similarly, *C. vulgaris* culture density did not differ between treatments ($F_{(3,8)}$=1.92, p=0.205), but significant interaction effects between concentration and exposure time were observed ($F_{(24,64)}$=2.304, p=0.004). Specifically, the intermediate dose (80 µg L^{-1}) cultures were less dense than the control cultures over the 5 h of exposure (Tukey HSD, p<0.05 for each time point); however, this difference was consistent at each time point which indicated culture variation rather than treatment effects. There were no observed differences in culture growth rate in *T. weissflogii* treatments ($F_{(9,24)}$=0.890, p=0.548). A two-way ANOVA suggested that culture growth rate varied between treatments and time in *C. vulgaris* cultures ($F_{(9,24)}$=4.885, p=0.0009), but a post-hoc Tukey HSD test revealed that the only deviation from control levels occurred 24 h after the spike in high-dose 500 µg L^{-1} cultures (p<0.0001), after which growth rate returned to initial levels.

Metformin exposure above environmentally relevant levels reduced the culture density of *C. vulgaris* after 96 h (Figure 3.3B) but not growth rate (Figured 3.3D). A two-way ANOVA revealed significant interaction effects on cell density between treatments and time in *C. vulgaris* cultures (ANOVA, $F_{(27,72)}=17.3$, $p<0.0001$). Investigation with post-hoc Tukey HSD tests showed that cultures grown under intermediate (80 µg L^{-1}) and high (500 µg L^{-1}) metformin conditions had lower cell density relative to control cultures after 96 h of exposure (Table 3.2). A close inspection of differences at each experimental time point revealed that high concentration effects manifested ~48 h after exposure (Figure 3.3B). Average *C. vulgaris* growth rates differed between treatments and time ($F_{(12,32)}=3.29$, $p=0.004$), but a post-hoc Tukey HSD test showed that this result was an artifact of the abnormal starting growth rate of the intermediate dose cultures; average growth rates of low and high dose *C. vulgaris* cultures were not different from control culture growth rates at any time point. Minimal effects on cell growth rates were confirmed by full recovery of post-experiment cultures made from high dose treatment cultures. Weibull growth models with consistent growth rate parameter values between treatments and relatively higher inflection point (δ) parameter values for high dose treatments also supported minimal metformin effects on growth rate and significant metformin effects on culture density (Table 3.3).

Conversely, metformin treatments did not alter the growth or cell density of *T. weissflogii* cultures (Figure 3.3A, C). The cell density of *T. weissflogii* cultures exposed to metformin for 96 h did not differ from control cultures (Table 3.2). Furthermore, cell density of *T. weissflogii* cultures did not change relative to control cultures for any dose or time point following the spike (ANOVA, $F_{(21,56)}=0.262$, $p=0.999$). Likewise,

average growth rate did not change relative to control cultures after 96 h of exposure

(Table 3.3) or at any previous time point (ANOVA, $F_{(12,32)}=0.318$, $p=0.981$).

Table 3.2. Comparison of average cell density and specific growth rate between control and treatment cultures at the time of the spike (0 h) versus 96 h after the spike. P-values ≤0.05 indicate significant difference between control and treatment cultures.

Species	Time After Spike (h)	Treatment	Average Cell Density (cells/mL)	p-value	Average Growth Rate (cells/mL)	p-value
T. weissflogii	0	Control	112638 (±30485)		0.043 (±0.01)	
		1 µg/L	116603 (±11207)	0.991	0.054 (±0.01)	0.386
		60 µg/L	104874 (±21966)	0.941	0.048 (±0.005)	0.885
		400 µg/L	114348 (±16120)	0.999	0.044 (±0.005)	0.999
	96	Control	240122 (±4795)		0.0073 (±0.003)	
		1 µg/L	240464 (±6885)	>0.9999	0.0085 (±0.004)	0.998
		60 µg/L	233820 (±4643)	0.967	0.0038 (±0.002)	0.962
		400 µg/L	236860 (±7574)	0.995	0.0048 (±0.0009)	0.985
C. vulgaris	0	Control	6263237 (±689367)		0.045 (±0.006)	
		1 µg/L	5401901 (±929268)	0.443	0.044 (±0.008)	0.998
		80 µg/L	4646916 (±913273)	**0.031**	0.031 (±0.004)	0.007
		500 µg/L	6368082 (±977601)	0.998	0.043 (±0.008)	0.969
	96	Control	19124196 (±1042799)		0.0046 (±0.003)	
		1 µg/L	18288604 (±435686)	0.470	0.0039 (±0.004)	0.998
		80 µg/L	17240617 (±441835)	**0.008**	0.0032 (±0.003)	0.984
		500 µg/L	11413068 (±962604)	**<0.0001**	0.0049 (±0.005)	1.000

Table 3.3. Comparison of growth curve model fit and predicted growth parameters for control and treatment cultures after 96 h of metformin exposure. Growth curves were fit with Weibell growth curve models.

Species	Treatment	R2	Specific Growth Rate (µ)	AVG Resid Error (S)	Growth Curve Inflection Point (δ)	AVG Resid Error (S)	Max # Cells (Nmax)	AVG Resid Error (S)
T. weissflogii	Control	0.965	0.011	0.001	2.31	0.381	231819	12440
	1 µg/L	0.964	0.011	0.001	2.16	0.372	231194	14754
	60 µg/L	0.965	0.011	0.001	2.63	0.432	228431	10306
	400 µg/L	0.974	0.011	0.001	2.18	0.316	233951	12307
C. vulgaris	Control	0.989	0.006	0.000	3.60	0.312	20335407	1056483
	1 µg/L	0.992	0.006	0.000	3.74	0.285	19973798	1005521
	80 µg/L	0.984	0.006	0.000	4.03	0.399	17570065	741154
	500 µg/L	0.976	0.008	0.000	4.82	0.629	10391342	272356
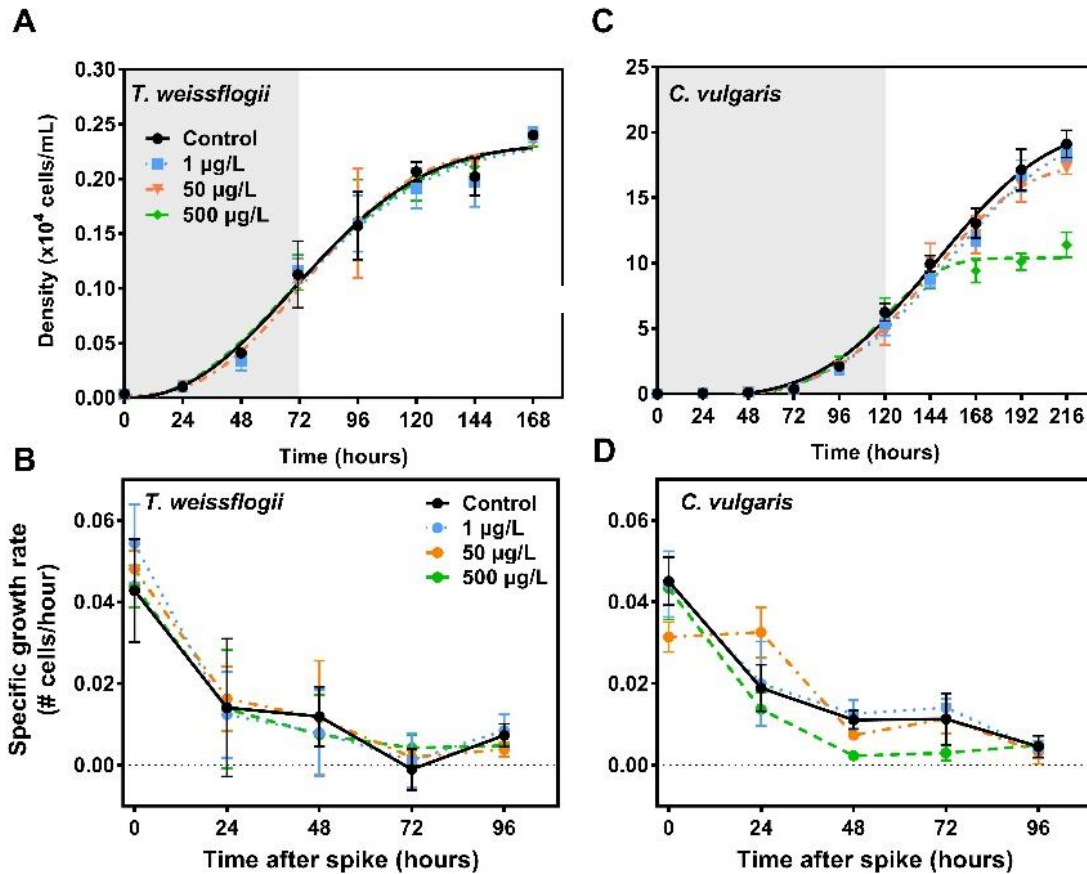
Figure 3.3. Average algal culture density (A, B) and specific growth rates (C, D) in response to different levels of metformin exposure over a 96 h period. Grey areas in A and B indicate pre-spike growth.

3.3.3. Effects of Metformin on Phytoplankton Photosynthesis

Metformin largely did not alter photosynthetic ability of *C. vulgaris* and *T. weissflogii* cultures over 5 h of exposure. Trends in ETR_{max} over 5 h of growth under metformin are shown in Figure 3.4, while all 5 h exposure data for photosynthetic parameters in algal cultures is summarized in Appendix Table 3C and Appendix Figure 3B. A two-way ANOVA did not find significant effects of metformin treatment and time on ETR_{max} ($F_{(12,32)}=0.435$, $p=0.937$), or photosynthetic parameters α ($F_{(12,32)}=0.436$, $p=0.936$), β ($F_{(12,32)}=0.635$, $p=0.797$), Φ ($F_{(12,32)}=1.09$, $p=0.401$), and E_k

$(F_{(12,32)}=1.09$, $p=0.402$) in *T. weissflogii* cultures within 5 h of the metformin spike. These cultures exhibited differences in NPQ_{max} between treatments $(F_{(3,8)}=8.854$, $p=0.0064$), but there were no interaction effects between treatment and time $(NPQ_{max}(F_{(12,32)}=0.343$,$p=974$) indicating each treatment varied similarly over time. *Chlorella vulgaris* cultures also did not differ with metformin treatment and time for ETR_{max} $(F_{(12,32)}=0.830$, $p=0.620$) and NPQ_{max} $(F_{(12,32)}=0.567$,$p=852$), α $(F_{(12,32)}=1.845$, $p=0.082$), Φ $(F_{(12,32)}=0.488$, $p=0.907$), and E_k $(F_{(12,32)}=1.405$, $p=0.215$) over the 5 h period, but significant effects of time and treatment were observed for average β $(F_{(12,32)}=3.224$, $p=0.004$). A follow-up inspection of single effects showed that average β for the lowest dose treatment (1 µg L^{-1}) only varied from the control directly following the spike (Tukey HSD, $p<0.0001$) and 5 h after the spike (Tukey HSD, $p=0.023$). Average β for the 500 µg L^{-1} treatment varied from the control at each time point following the spike (Tukey HSD, $p<0.05$ for each time point), but the same trend was also found directly before metformin exposure (Tukey HSD, $p<0.0001$) and did not change over the 5 h of metformin exposure.

The highest exposure level of metformin (500 µg L^{-1}) reduced photosynthetic performance in *C. vulgaris* cultures over 96 h of exposure (Table 3.4, Figure 3.4B). There was significant interaction between treatment and time on ETR_{max} in *C. vulgaris* (two-way ANOVA, $F_{(12,32)}=38.91$, $p<0.0001$). Cultures dosed to 80 µg L^{-1} and 500 µg L^{-1} metformin concentrations showed a significant reduction in ETR_{max} relative to cultures without metformin starting 24 h after metformin exposure (Tukey HSD, $p= 0.0065$, $p<0.0001$). The ETR_{max} of 500 µg L^{-1} cultures decreased at each time point until hitting baseline levels at 96 h, with the highest rate of decline occurring between 48-72 h of

exposure (Table 3.4, Figure 3.4B). A post-hoc Tukey test showed that ETR_{max} of cultures treated with low (1 µg L^{-1}) and intermediate (80 µg L^{-1}) metformin concentrations did not significantly differ from control cultures for the first 72 h following the metformin spike; however, ETR_{max} for 80 µg L^{-1} cultures were significantly lower than control cultures after 96 h of exposure (Tukey HSD, p=0.007; Table 3.4).

Other photosynthetic parameters of *C. vulgaris* cultures were altered by high metformin doses over 96 h of exposure (Table 3.4, Figure 3.5B). A two-way ANOVA found significant interaction effects between treatment amount and time for each average estimated parameter determined by the Platt photosynthetic models, including α ($F_{(12,32)}=40.02$, p<0.0001), β ($F_{(12,32)}=16.13$, p<0.0001), E_k ($F_{(12,32)}=12.62$, p<0.0001), Φ ($F_{(12,32)}=157.9$, p<0.0001), and NPQ_{max}($F_{(12,32)}=15.6$,p<0.0001). All estimated photosynthetic parameters for *C. vulgaris* cultures dosed to 500 µg L^{-1} were significantly different from control cultures by 96 h of metformin exposure (Tukey HSD, p<0.0001).

Specifically, α, ETR_{max}, E_k, and Φ for the highest dose treatments (500 µg L^{-1}) decreased relative to the control, while β increased. While average α values for control and other treatment cultures remained at ~3.3 µmol $photons^{-1}$ m^{-2} s^{-1}, α values for the highest dose treatments (500 µg L^{-1}) decreased from 0.33 to 0.15 µmol $photons^{-1}$ m^2 s^{-1} over the 96 h experiment period (Tukey HSD, p=0.0029). Average E_k values for 500 µg L^{-1} treatments were lower than control values starting 24 h after the spike (Tukey HSD, p=0.0003) and decreased from 885 to 263 µmol photons m^{-2} s^{-1} over the 96 h of metformin exposure. Average β values for high dose treatments (500 µg L^{-1}) were already above control levels at the time of the spike (Tukey HSD, p<0.0001), but this

difference increased steadily from ~10 to 15 µmol photons^{-1} m^{-2} s^{-1} up to 96 h following the spike. Values of β for control and other treatment cultures remained around 6-8 µmol photons^{-1} m^2 s^{-1} at each time point. Values of Φ decreased from ~0.7 to 0.3 µmol photons^{-1} m^2 s^{-1} starting 48 h (p=0.0005) after the spike.

The NPQ$_{max}$ of *C. vulgaris* cultures varied more over time than other photosynthetic parameters. Values of NPQ$_{max}$ in high dose cultures (500 µg L^{-1}) increased relative to the control for the first 48 h, but peaked at ~0.9 before quickly decreasing below control levels by 96 h (Tukey HSD, p=0.0123). Similarly, NPQ$_{max}$ of intermediate dose cultures (50 µ L^{-1}) also increased after 48 h and reached levels of ~0.9 by 96 h (Tukey HSD, p<0.0001).

Metformin treatments did not alter ETR$_{max}$ or other photosynthetic parameters of *T. weissflogii* cultures (Figure 3.4A, 3.5A). Specifically, the ETR$_{max}$ of *T. weissflogii* cultures did not change relative to control cultures for any metformin treatment or time point following the spike (ANOVA, $F_{(12,32)}$=0.306, p=0.983). Similar to ETR$_{max}$, a two-way ANOVA did not find significant interaction effects between treatment and time for average estimated parameters determined by Platt photosynthetic models, including α ($F_{(12,32)}$=0.147, p=0.999), β ($F_{(12,32)}$=1.688, p=0.1167), E$_k$ ($F_{(12,32)}$=0.751, p=0.693), Φ ($F_{(12,32)}$=0.311, p=0.982), and NPQ$_{max}$($F_{(12,32)}$=0.412, p=9.48). Average β values of pre-spike 500 µg L^{-1} cultures were lower than control β values on the day of the spike (Tukey HSD, p=0.013, but this difference was not observed at any time point following metformin exposure.

Table 3.4. Comparison of average photosynthetic parameters (α, β, ETRmax, and Ek) estimated by ETR light curve models at the time of the spike (0 h) versus 96 h after the spike. Overall goodness of fit (R2), average residual error (S), and p-value associated with each parameter are shown for each treatment. P-values ≤0.05 indicate significant difference between respective control and treatment cultures at that timepoint. P-values for individual treatments were obtained using two-way ANOVAs with post-hoc Tukey HSD tests.

Species	Time After Spike (h)	Treatment	R2	S	α	p-value	β	p-value	ETRmax	p-value	Ek	p-value	φPSII	p-value	NPQ	p-value
T. weissflogii	0	Control	0.97	9.35	**0.33** (±0.008)		**8.63** (±3.4)		**151.6** (±14)		**706.1** (±52)		**0.660** (±0.01)		**1.03** (±0.1)	
		1 µg/L	0.97	8.86	**0.33** (±0.009)	0.983	**8.18** (±0.5)	0.952	**150.6** (±6.3)	1.000	**722.8** (±22)	0.989	**0.663** (±0.01)	1.000	**1.12** (±0.1)	0.963
		60 µg/L	0.95	12.45	**0.31** (±0.003)	0.987	**7.43** (±0.7)	0.522	**152.1** (±4.8)	>0.9999	**695.6** (±67)	0.997	**0.669** (±0.01)	0.991	**1.05** (±0.1)	>0.999
		400 µg/L	0.97	10.21	**0.16** (±0.01)	0.865	**5.82** (±0.6)	**0.013**	**150.2** (±24)	0.999	**764.7** (±114)	0.678	**0.678** (±0.02)	0.933	**1.11** (±0.2)	0.973
	96	Control	0.99	2.54	**0.11** (±0.01)		**8.9** (±0.6)		**62.5** (±2.8)		**566.3** (±69)		**0.485** (±0.04)		**2.03** (±0.3)	
		1 µg/L	0.96	4.53	**0.12** (±0.02)	0.982	**10.56** (±1.2)	0.243	**59.4** (±9.8)	0.994	**506.9** (±25)	0.668	**0.484** (±0.9)	>0.9999	**2.11** (±0.6)	0.977
		60 µg/L	0.97	3.76	**0.12** (±0.02)	0.977	**10.37** (±1.0)	0.346	**64.8** (±5.6)	0.997	**554.8** (±47)	0.996	**0.494** (±0.04)	0.989	**2.24** (±0.2)	0.720
		400 µg/L	0.98	2.91	**0.11** (±0.01)	>0.9999	**9.77** (±0.2)	0.750	**62.6** (±8.0)	>0.9999	**557.7** (±20)	0.998	**0.507** (±0.02)	0.880	**2.00** (±0.5)	0.989
C. vulgaris	0	Control	1.00	6.13	**0.33** (±0.003)		**5.56** (±0.2)		**313.1** (±12)		**958.1** (±34)		**0.693** (±0.007)		**0.311** (±0.05)	
		1 µg/L	0.99	7.77	**0.34** (±0.01)	0.187	**7.31** (±0.6)	**0.001**	**295.1** (±14)	0.178	**858.3** (±71)	**0.022**	**0.697** (±0.009)	0.972	**0.352** (±0.12)	0.948
		80 µg/L	0.99	9.35	**0.33** (±0.0002)	1.000	**5.97** (±0.1)	0.759	**319.9** (±4.8)	0.863	**976.6** (±15)	0.943	**0.697** (±0.009)	0.978	**0.372** (±0.10)	0.847
		500 µg/L	0.99	9.07	**0.34** (±0.01)	0.622	**9.45** (±0.4)	**<0.0001**	**298.4** (±14)	**<0.0001**	**885.1** (±36)	0.137	**0.695** (±0.005)	0.999	**0.386** (±0.08)	0.753
	96	Control	0.98	7.32	**0.33** (±0.008)		**6.76** (±0.2)		**224.7** (±18)		**681.3** (±40)		**0.659** (±0.01)		**0.421** (±0.17)	
		1 µg/L	0.99	6.81	**0.33** (±0.009)	0.998	**8.02** (±0.4)	**0.019**	**229.4** (±11)	0.948	**700.2** (±51)	0.940	**0.663** (±0.01)	0.957	**0.365** (±0.13)	0.880
		80 µg/L	0.99	4.31	**0.31** (±0.003)	0.287	**7.67** (±0.2)	0.137	**194.5** (±4)	**0.007**	**619.5** (±16)	0.257	**0.660** (±0.006)	0.998	**0.962** (±0.15)	**<0.0001**
		500 µg/L	1.00	3.41	**0.16** (±0.01)	**<0.0001**	**16.16** (±0.1)	**<0.0001**	**40.8** (±3)	**<0.0001**	**263.2** (±3)	**<0.0001**	**0.337** (±0.01)	**<0.0001**	**0.176** (±0.01)	**0.012**
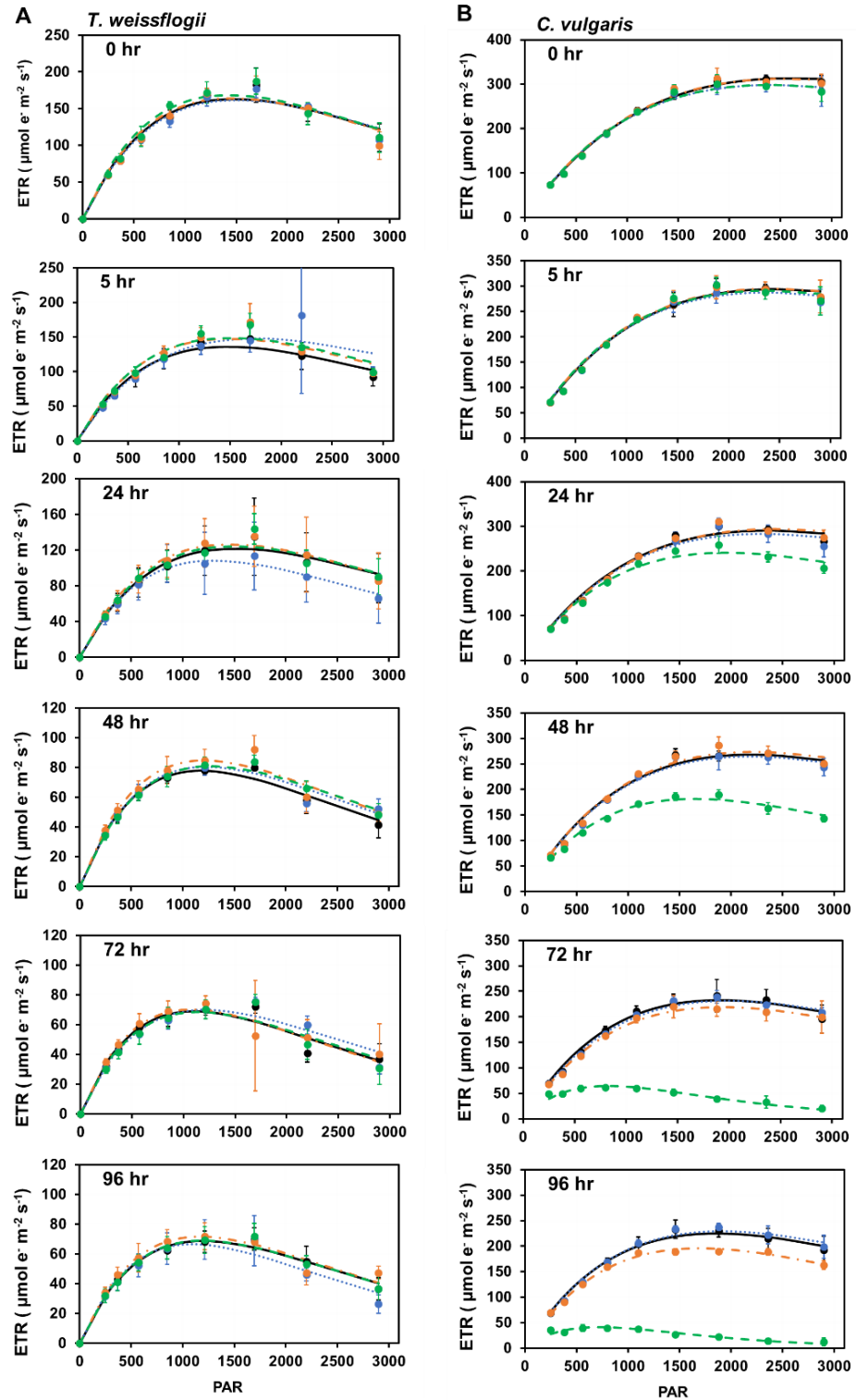
Figure 3.4. Rapid light curves showing relative electron transport rate (ETR) of *C. vulgaris* and *T. weissflogii* cultures over 96 h exposure to metformin. Different lines indicate different metformin spike amounts: 0 µg/L (black solid), 1 µg/L (blue dotted), 50 µg/L (orange dotted-dash), and 500 µg/L (green dash).
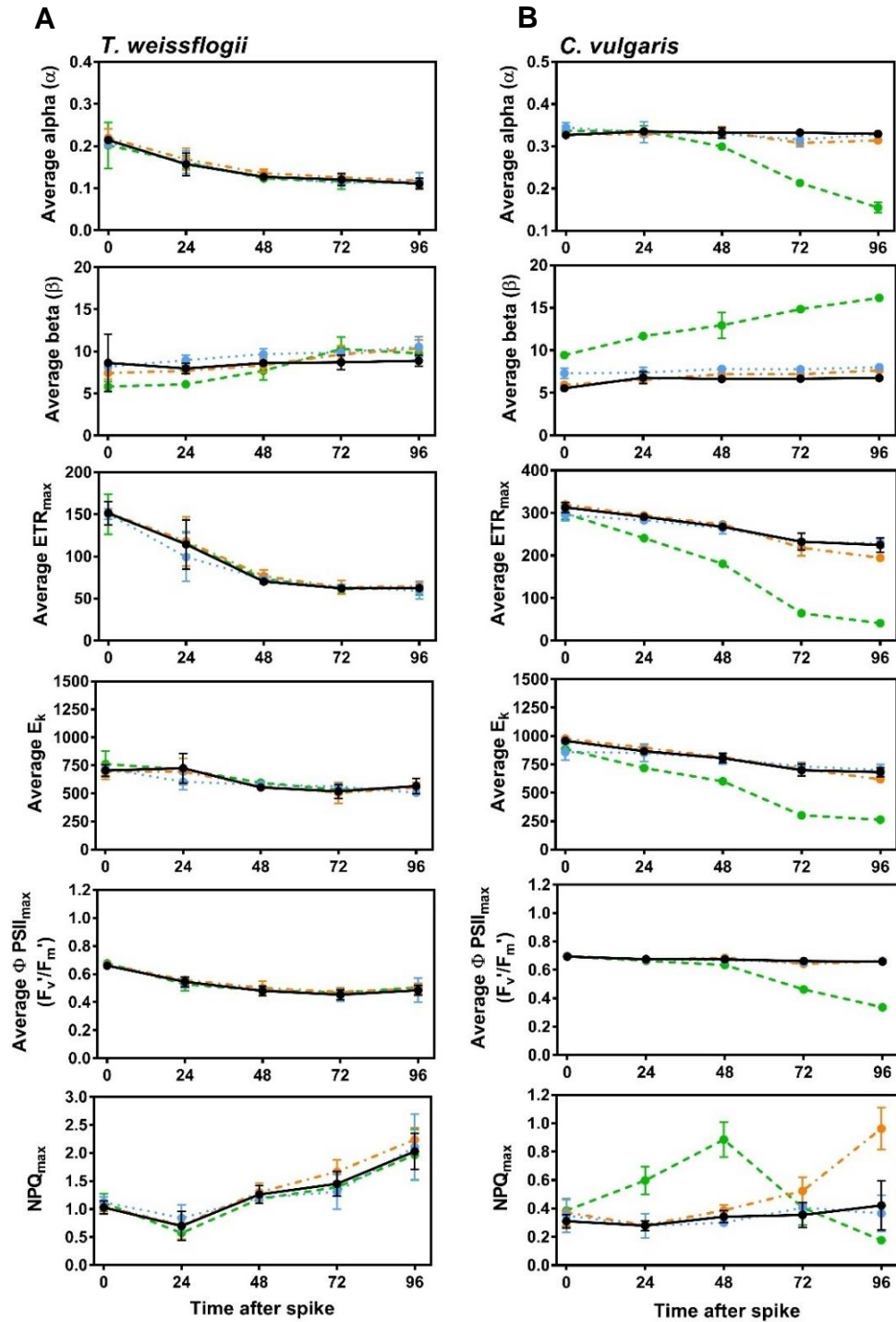
Figure 3.5. Effects of metformin on photosynthetic parameters of *T. weissflogii* (A) and *C. vulgaris* (B) over 96 h of exposure. Parameters include electron transport efficiency (α), photoinhibition (β), maximum relative electron transport rate (ETR_{max}), minimum saturating irradiance (E_k), maximum quantum yield (Φ), and nonphotochemical quenching (NPQ). All parameters were estimated by best-fit light curve models fitted with the Platt equation. Lines indicate different spike amounts: 0 µg/L (black solid), 1 µg/L (blue dotted), 50 µg/L (orange dotted-dash), and 500 µg/L (green dash).

3.4. Discussion

3.4.1. *Overview of Metformin Algal Toxicity*

While other studies have only investigated metformin toxicology at single doses,[31,242] or at high dose ranges (mg L^{-1}),[28,277] this study provides the first evidence for environmentally relevant effects of metformin on algae. Based on the known fast growth rates of *C. vulgaris*[278] and *T. weissflogii*,[279] algal cells were exposed to metformin treatments over the majority of their lifespan, and, therefore, observed responses in this study may indicate sublethal effects. Overall, algal response to metformin depended on dose, exposure time, and species. If experimental metformin levels are representative of actual exposure levels, metformin likely does not pose a risk to algal growth and photosynthesis in high-flow rivers and streams. However, negative photosynthetic effects in response to long-term (days) metformin exposure at effluent levels suggests possible implications for algal sewage treatment methods and lower trophic levels in slow-moving water systems.

3.4.2. *Metformin as a Photosynthetic Inhibitor*

Metformin impaired *C. vulgaris* photosynthetic ability at high doses (500 μg L^{-1}) and long-term intermediate doses (50 μg L^{-1}), but did not affect *T. weissflogii* photosynthesis at any dose. High dose (500 μg L^{-1}) metformin effects on *C. vulgaris* were dependent on exposure time with increasingly reduced electron transport rate (ETR$_{max}$) and efficiency (α) after each 24-h period, and almost no electron transport occurring after 96 h. Beyond reduced electron transport, *Chlorella* cultures exhibited an overall lower capacity for light capture, with an increase in the photoinhibition constant (β), lower

levels pertaining to the onset of light saturation (E_k), and overall lower PSII efficiency of light absorption. Moreover, intermediate doses (80 µg L^{-1}) showed the beginning of similar photosynthetic inhibition by 72 h of exposure. This is particularly apparent from nonphotochemical quenching (NPQ_{max}), which showed intermediate dose cultures tracking the same trends as high dose cultures after a 48-h delay. Based on these observations, environmentally relevant metformin levels may elicit negative responses in some phytoplankton species after extended periods of exposure (days). These results may be especially relevant for slow-moving bodies of water, such as lakes, where algae around sewage effluent are more likely to remain in a concentrated zone of metformin exposure. In order to elucidate long-term algal responses at lower dose levels, continuous cultures should be used to extend the exposure time beyond 96 h without the accumulation of cell products.

High doses of metformin reduced the carrying capacity (K) of *C. vulgaris* cultures. Specifically, the maximum cell density (i.e., density at stationary phase) in high-dose (500 µg L^{-1}) treatments was lower than all other treatments, which confirmed reduced photosynthetic ability and reduced ability to produce sugars for sustaining highly dense populations. No effects were observed on growth rate, but this may have been a result of spiking cultures too late in exponential phase or calculating rates from cell counts with high standard deviations.

Based on these experimental data, it is proposed that metformin signals a stress response in *C. vulgaris* algae. Photosynthetic cell stress response, which is partly regulated by SnRK1 activation, is often associated with a reduction in photosynthetic activity and, subsequently, energy deprivation.[253,280] Metformin effects on *C. vulgaris*

cultures were indicative of a stress response, with reduced photosynthetic abilities related to electron transport and light capture, and reduced culture carrying capacity. Since energy sensing kinases are highly conserved between humans (AMPK) and plants (SnRK1),[281] and metformin interacts with AMPK in humans to produce stress responses,[146] the algal stress responses observed in this study provide preliminary evidence for metformin activation of SnRK1. However, due to the biochemical complexity of SnRK1 activation in plants,[280,282,283] a correlation between metformin and stress response cannot confirm SnRK1 interaction without *in vitro* kinase assays directly testing for SnRK1 activity in the presence of metformin.[284–286] Further culture tests measuring adenylate charge (AMP:ATP) and fatty acid content will also help clarify specific metformin effects on energy pathways.

High dose (500 µg L^{-1}) effects on photosynthesis and growth capacity correspond to unrealistic levels that would not be encountered in the environment or in wastewater treatment, but long-term effects of intermediate doses (80 µg L^{-1}) reveal potential effects of metformin at wastewater treatment levels. Future research should explore the effects of metformin exposure to algae in wastewater treatment plants and other enclosed water systems, with relevance to microalgae nutrient removal technology[255] and biofuel production.[256] Additionally, since a multitude of contaminants and environmental factors are acting on algal cells at any one time in the river, a seemingly innocuous metformin concentration in lab experiments may actually produce a stress response when encountered in the environment. The results from this study reveal the importance of considering dose-dependent and environmentally relevant toxicological effects of metformin and other PPCPs in laboratory studies.

3.4.3.   *Species-Dependent Response to Metformin*

Metformin may have exhibited variable effects on the experimental organisms in this study due to physiological differences between algal species. This is not surprising, since *Chlorella vulgaris* and *T. weissflogii* are phylogenetically distinct algae[287] belonging to independent groups with different physiologies, ranging from different cell walls (e.g. frustules in diatoms) to different membrane proteins[288] and chloroplast structures.[287] *Chlorella* belongs to the phylum Chlorophyta within the plant kingdom (Viridiplantae), which includes all eukaryotic green algae and land plants that utilizes chloroplasts containing chlorophyll *a* and *b* and accessory pigments *β*-carotene and xanthophylls to carry out photosynthesis. Chlorophyte chloroplasts have two membranes and contain thylakoids in many-layered grana,[287] which may serve to increase protection of the cell from photochemical damage.[289] *Thalassiosira* belongs to the Heterokonta, which includes algae, ranging from kelp to diatoms, that utilize chloroplasts containing chlorophyll *a* and *c* and the accessory pigment fucoxanthin to carry out photosynthesis. Heterokont chloroplast have four membranes and contain thylakoids in stacks of three. Overall, differential effects of metformin based on species suggested species-dependent factors that promoted or interfered with metformin action in photosynthetic cells.

Physical size and cell wall differences between *C. vulgaris* and *T. weissflogii* may alter metformin uptake. Based on estimated cell size classes in experimental cultures, the size range of *C. vulgaris* is small (2.5-5.125 µm) compared to *T. weissflogii* (7.0-16.5 µm) indicating a higher surface area to volume ratio for *Chlorella* cells and possibly faster diffusion of metformin into the cell.[16] Moreover, differences in transmembrane

proteins between Chlorophytes and Heterokonts could alter the probability of metformin uptake.

Differences in environment may also alter physicochemical interactions for metformin uptake into algal cells. Metformin has been shown to exist at lower concentrations in seawater relative to freshwater,[13] and salinity can reduce the solubility of organic compounds in marine environments by suppressing ionic interactions.[290] Thus, media effects from ESAW in *T. weissflogii* cultures may render metformin less available for diffusion into cells.

Moreover, environmental salinity may influence membrane transport of metformin. Organic cation transporters (OCTs) are the known mechanism of metformin transport across cell membranes in human cells;[291] OCTs function in ion homeostasis and facilitate electrogenic transport of organic cations into the cell.[292] Cation transporters in some plants and algae also maintain ion homeostasis by using an antiporter system to transport cations against their concentration gradients.[293,294] For instance, Chlorophytes and *Thalassiosira* haptophytes have a proton-coupled transporter, CrCAX1, which may transport Ca^{2+} and other metal cations out of the cytosol in response to salinity stress.[293] Since a marine alga must continually export Na^+ cations that are infiltrating the cell from the salty environment, the diatom *T. weissflogii* might significantly export other small cations, such as metformin, along this same cation transporter membrane system. Additionally, salinity may reduce metformin import in marine cells through ionic influences on membrane potentials and membrane protein surface charges.[295–297]

It may also be that *T. weissflogii* did not exhibit a stress response to metformin due to functional differences in SnRK1 signaling pathway members. SnRK1 is highly

conserved across plants and algae,[281] and regulatory proteins involved in the SnRK1 signaling pathway have been identified in green algae and [Thalassiosira] diatoms.[298,299] However, there is currently no evidence for the functional role of these proteins in algae.[300] Given the degree of phylogenetic difference between algal species used in this study, and the complexity of metabolic signaling pathways in eukaryotic organisms, it is plausible that multiple or alternative functions exist for SnRK1 regulatory proteins between algal species.

CHAPTER 4: CONCLUSIONS & FUTURE DIRECTIONS

This study provides the first environmental characterization of the antidiabetic drug, metformin, as a CEC in the lower Columbia River, and constitutes one of the few studies to characterize a pharmaceutical CEC (PPCP) in a high-volume river system.[18,301] Over one year of monthly water sampling along the lower Columbia River, metformin was regularly detected at levels comparable to those measured in less dynamic stream and lake systems,[13,46,96,160,166] and exhibited spatiotemporal trends driven primarily by river discharge both in space (riverine inputs) and time (flow rate). Based on average concentrations and river discharge for the entire year, the Columbia River is discharging metformin at a rate of ~51 kg d^{-1}. The breakdown product of metformin, guanylurea, often co-occurred with metformin, but evidence of diffuse sources driven by precipitation suggested that guanylurea was an overall poor indicator of *in-situ* metformin breakdown. Unexpectedly, metformin contamination from particulate residues on vial caps and general variability in the dataset provided possible evidence for metformin ionic surface sorption, which has been observed in other studies.[24,142,237]

This research also provides the first results for dose-dependent effects of metformin on algal cells, including environmentally relevant concentrations. As would be expected from activating an energy regulator (SnRK1), metformin concentrations above environmental levels induced a stress response and reduced photosynthetic activity. A delayed response to metformin concentrations at lower levels corresponding to wastewater effluent indicated that stress effects were based on dose and exposure time, with relevance for organisms in poorly-mixed environments where exposure time might be higher.

Overall, these results are consistent with the expected behavior of a polar basic cation species in a high-flow river system and an AMPK-activator in algal physiological systems. Based on the maximum river concentration measured from this study (4.6 µg L^{-1}), metformin in the Columbia River currently does not pose a risk to photosynthetic processes in algae and, thus, energy transfer to larger organisms in the river food web.[31] However, given that the Columbia River is the fourth largest river by discharge in the United States and, consequently, >87% of the largest rivers in the U.S. experience relatively lower flow amounts over the course of a year,[176] it is likely that metformin persists at higher concentrations in many rivers and streams around the country if there are similar inputs from metformin sources. Metformin concentrations may also be consistently higher in slow-moving water systems such as lakes and enclosed estuaries, especially around point sources such as sewage pipes.[50,160]

Periods of greater risk to metformin exposure can be extrapolated based on average river conditions throughout the year. Data from this study indicates that dry, low-flow seasons (July-Sept in the Columbia River) will magnify metformin concentrations due to reduced dilution effects, and increase the amount of metformin encountered by an aquatic organism during this period. Moreover, sites downstream of the Willamette-Columbia confluence (River km 156) may experience consistently higher metformin concentrations due to numerous metformin sources along the Willamette River. Thus, the concentrations and toxicological effects of metformin in the Columbia River are expected to increase during periods of drought, with possibly greater effects downstream of the Willamette-Columbia confluence.[302] Since extreme weather events are predicted to

increase with climate change,[303] the effect of metformin on the environment will likely increase with time.

If metformin sorption is occurring in the Columbia River, as suggested by the limited observations in this study, benthic organisms might be at risk of prolonged exposure to metformin. Metformin has been found in sediments at concentrations up to 140 ng g^{-1}.[160] The only information regarding effects of metformin on benthic organisms comes from the 2015 European Medicines Agency assessment report testing for metformin toxicity in chironomids, which found no observable effects below a concentration of 125,000 ng g^{-1} metformin in sediment.[140] However, other sediment-dwelling organisms are likely to be affected by metformin. For instance, benthic green algae, which belong to the same Chlorophyta division as *C. vulgaris*, are likely to exhibit reduced photosynthetic activity in response to prolonged metformin exposure on sediments. Microbial activity may also be altered since metformin has known disrupting effects on the folate cycle of some bacteria.[175] Moreover, organisms which directly ingest sediment, such as polychaetes, or incidentally ingest sediment, such as sculpin, may experience higher exposure to sediment-bound metformin moves through their digestive tracts.[21]

Combinatory effects of metformin with other pharmaceutical drugs in the environment cannot be ignored due to the risk of underestimating toxic effects.[41,304] General use of pharmaceutical drugs is on the rise,[305] which translates to more PPCPs in the environment[51] and more opportunities for mixture effects. For example, metformin is commonly prescribed with statins to reduce cardiovascular risk[306] or chemically combined with additional antidiabetic compounds for enhanced glucose control.[307,308]

Recent research shows that toxicological risks associated with CEC mixtures can have higher toxicity effects than individual CECs.[41,264,309] This general effect has been observed in algae and plants,[41,264,309] benthic invertebrates,[309] and fish.[33,310] Therefore, the toxicological risk of metformin might be higher in the presence of other CECs in the Columbia River, and future research should explore specific combinatory toxicity associated with metformin and frequently detected CECs in the river system.

Despite minimal risks at current levels, metformin concentrations in the Columbia River and other water systems are expected to increase with rising prescription rates. At the current rate of Type 2 diabetes, it is projected that 1 in 3 adults could have Type 2 diabetes in the U.S. by 2050;[311] thus, as the most popular drug for treatment of Type 2 diabetes,[138] metformin usage will likely increase with time. However, based on the average metformin concentrations in surface waters, the number of Type 2 diabetics in the Columbia River watershed would have to increase by a factor >1000x in order to produce consistently toxic levels (80 μg L^{-1}) in surface waters. Thus, toxic [algal] effects of metformin will likely be limited to sewage effluent zones and WWTP.

Future CEC research in the Columbia River should target these metformin "hotspots" along the river. This study did not detect elevated metformin levels downstream of sewage treatment sites or other sites (except an average increase at each site downstream of the Willamette River confluence) likely due to high mixing by river flow. Therefore, future research should hone in on urban and hospital WWTP sites and determine the amount of metformin being injected into the Columbia River. These concentrations could then be compared with surface water concentrations in order to elucidate point sources of metformin versus diffuse sources from runoff and groundwater.

Knowing where metformin sources in addition to how it varies in time and space will inform OECD toxicology assessments and future policy decisions regarding PPCPs.

The best strategy for mitigating future risks associated with rising metformin levels in the environment is at the source. Type 2 diabetes is unique in that it is largely preventable with healthy diet and lifestyle.[312,313] This represents a unique opportunity to encourage a medically-supported outlook for the benefit of both humans as well as the environment.[314–316]

In summary, this focused survey of metformin in a high-volume river system has revealed the dynamic behavior of metformin as a CEC in the environment in relation to its known properties as a drug. Much PPCP research consists of costly large-scale field studies,[46,49,50,96,202,216] but this project demonstrates the efficacy of a small-scale field study focused on one CEC compound. By utilizing resources for monthly monitoring of metformin concentrations rather than one large snapshot of all abundant PPCPs, the importance of river discharge and, possibly, particle interactions to metformin distribution and supply was revealed. Furthermore, toxicity tests linked these spatiotemporal patterns with possible photosynthetic repercussions in the lower food web under concentrated conditions. As a result of this research, metformin as a topic for CEC research beckons a plethora of unexplored physicochemical and toxicological research avenues, and reinforces the need to follow large-scale CEC surveys with individual characterizations of prevalent CECs.

DELIMITATIONS, LIMITATIONS, AND ASSUMPTIONS

Limitations

1. Sample size: Financial restrictions limited methods to once-a-month triplicate sampling. Given that this study already samples more frequently than previous CEC studies in the Columbia River, this might be a non-issue.

2. Sampling time: Financial and time restrictions limited sampling to a one-year period from October 2016-September 2017. As a result, interannual variability could not be assessed.

Delimitations

1. Geographic study area: Sampling was restricted to the Lower Columbia River west of the Cascades in order to simplify river variables and economize data analysis. This area was chosen due to the region's high population density and proximity to numerous urban centers, wastewater treatment plants, and agricultural sites. Since the flow from mountain snowmelt to coastal confluence was still captured, the results of this study could be generalized for downstream areas of other high-volume river systems that experience a strong annual freshet.

2. Experimental organisms: The green algae, *Chlorella vulgaris,* and diatom, *Thalassiosira weissflogii*, were chosen over other algae due to their representative physiology, ease of culturing, and convenient availability for experiments.

Assumptions

1. Metformin and guanylurea concentrations near river shores are not significantly different than metformin concentrations in the main channel.

2. Exceptionally wet river conditions during the October 2016-September 2017

   sampling period were similar enough to other high precipitation years to

   extrapolate general relationships between river variables and concentration data.

3. Response of algae to a dose of metformin in cultures is an accurate approximation

   of algae response when that same amount of metformin is encountered in the

   environment.

REFERENCES

(1)   Diamond, J. M.; Latimer, H. A.; Munkittrick, K. R.; Thornton, K. W.; Bartell, S. M.; Kidd, K. A. Prioritizing Contaminants of Emerging Concern for Ecological Screening Assessments. *Environ. Toxicol. Chem.* **2011**, *30* (11), 2385–2394.

(2)   Anderson, P.; Denslow, N.; Olivieri, A.; Schlenk, D.; Scott, G. I. *Monitoring Strategies for Chemicals of Emerging Concern (CECs) in California's Aquatic Ecosystems: Final Report and Recommendations of a Science Advisory Panel*; 2012.

(3)   Daughton, C.G., Terns, T. A. Pharmaceuticals and Personal Care Products in the Environment. *Environ. Toxicol.* **1999**, *107* (6), 907–938.

(4)   Verlicchi, P.; Al Aukidy, M.; Galletti, A.; Petrovic, M.; Barceló, D. Hospital Effluent: Investigation of the Concentrations and Distribution of Pharmaceuticals and Environmental Risk Assessment. *Sci. Total Environ.* **2012**, *430*, 109–118.

(5)   Masoner, J. R.; Kolpin, D. W.; Furlong, E. T.; Cozzarelli, I. M.; Gray, J. L. Landfill Leachate as a Mirror of Today's Disposable Society: Pharmaceuticals and Other Contaminants of Emerging Concern in Final Leachate from Landfills in the Conterminous United States. *Environ. Toxicol. Chem.* **2016**, *35* (4), 906–918.

(6)   Bernhardt, E. S.; Rosi, E. J.; Gessner, M. O. Synthetic Chemicals as Agents of Global Change. *Front. Ecol. Environ.* **2017**, *15* (2), 84–90.

(7)   Buser, H. R.; Poiger, T.; Müller, M. D. Occurrence and Fate of the Pharmaceutical Drug Diclofenac in Surface Waters: Rapid Photodegradation in a Lake. *Environ. Sci. Technol.* **1998**, *32* (22), 3449–3456.

(8)   Andreozzi, R.; Caprio, V.; Ciniglia, C.; Champdoré, M. de; Giudice, R. Lo; Marotta, R.; Zuccato, E. Antibiotics in the Environment: Occurrence in Italian STPs, Fate, and Preliminary Assessment on Algal Toxicity of Amoxicillin. **2004**.

(9)   Kim, S. D.; Cho, J.; Kim, I. S.; Vanderford, B. J.; Snyder, S. A. Occurrence and Removal of Pharmaceuticals and Endocrine Disruptors in South Korean Surface, Drinking, and Waste Waters. *Water Res.* **2007**, *41* (5), 1013–1021.

(10)   Xu, W., Zhang, G., Zou, S., Ling, Z., Wang, G., Yan, W. A Preliminary Investigation on the Occurrence and Distribution of Antibiotics in the Yellow River and Its Tributaries, China. *Water Environ. Res.* **2009**, *81* (3), 248–254.

(11)   da Silva, B. F.; Jelic, A.; López-Serna, R.; Mozeto, A. A.; Petrovic, M.; Barceló, D. Occurrence and Distribution of Pharmaceuticals in Surface Water, Suspended Solids and Sediments of the Ebro River Basin, Spain. *Chemosphere* **2011**, *85* (8), 1331–1339.

(12)   Wolschke, H.; Xie, Z.; Möller, A.; Sturm, R.; Ebinghaus, R. Occurrence, Distribution and Fluxes of Benzotriazoles along the German Large River Basins into the North Sea. *Water Res.* **2011**, *45* (18), 6259–6266.

(13)   Trautwein, C.; Berset, J. D.; Wolschke, H.; Kümmerer, K. Occurrence of the Antidiabetic Drug Metformin and Its Ultimate Transformation Product Guanylurea in Several Compartments of the Aquatic Cycle. *Environ. Int.* **2014**, *70*, 203–212.

(14) Sui, Q.; Cao, X.; Lu, S.; Zhao, W.; Qiu, Z.; Yu, G. Occurrence, Sources and Fate of Pharmaceuticals and Personal Care Products in the Groundwater: A Review. *Emerg. Contam.* **2015**, *1* (1), 14–24.

(15) Site, A. D. Factors Affecting Sorption of Organic Compounds in Natural Sorbent / Water Systems and Sorption Coefficients for Selected Pollutants . A Review Factors Affecting Sorption of Organic Compounds in Natural Sorbent Õ Water Systems and Sorption Coefficients Fo. **2001**, *187* (1).

(16) Leeuwen, C. J. van.; Vermeire, T. *Risk Assessment of Chemicals : An Introduction*; Springer, 2007.

(17) Monteiro, S. C.; Boxall, A. B. A. Factors Affecting the Degradation of Pharmaceuticals in Agricultural Soils. *Environ. Toxicol. Chem.* **2009**, *28* (12), 2546–2554.

(18) Zhao, S.; Liu, X.; Cheng, D.; Liu, G.; Liang, B.; Cui, B.; Bai, J. Temporal–spatial Variation and Partitioning Prediction of Antibiotics in Surface Water and Sediments from the Intertidal Zones of the Yellow River Delta, China. *Sci. Total Environ.* **2016**, *569–570*, 1350–1358.

(19) Oh, S.; Shin, W. S.; Kim, H. T. Effects of pH, Dissolved Organic Matter, and Salinity on Ibuprofen Sorption on Sediment. *Environ. Sci. Pollut. Res.* **2016**, *23* (22), 22882–22889.

(20) Monteiro, S. C.; Boxall, A. B. A. *Reviews of Environmental Contamination and Toxicology*; 2010; Vol. 202.

(21) ECETOC. *Soil and Sediment Risk Assessment of Organic Chemicals (ECETOC Technical Report No. 92)*; Brussels, Belgium, 2004.

(22) Hansen, P.-D. Risk Assessment of Emerging Contaminants in Aquatic Systems. *TrAC Trends Anal. Chem.* **2007**, *26* (11), 1095–1099.

(23) Boxall, A. B. A.; Rudd, M. A.; Brooks, B. W.; Caldwell, D. J.; Choi, K.; Hickmann, S.; Innes, E.; Ostapyk, K.; Staveley, J. P.; Verslycke, T.; et al. Pharmaceuticals and Personal Care Products in the Environment: What Are the Big Questions? *Environ. Heal. Perspect.* **2012**, *120* (9), 1221–1229.

(24) Furlong, E. T.; Ferrer, I.; Glassmeyer, S.; Cahill, J. D.; Zaugg, S. D.; Werner, S. L.; Kolpin, D. W.; Kryak, D. D. Distribution of Organic Wastewater Contaminants between Water and Sediment in Surface Waters of the United States. In *National Groundwater Association 3rd International Conference on Pharmaceuticals and Endocrine Disrupting Chemicals in Water*; Minneapolis, MN, 2003.

(25) Niederer, C.; Goss, K. U.; Schwarzenbach, R. P. Sorption Equilibrium of a Wide Spectrum of Organic Vapors in Leonardite Humic Acid: Modeling of Experimental Data. *Environ. Sci. Technol.* **2006**, *40* (17), 5374–5379.

(26) Fairbairn, D. J.; Karpuzcu, M. E.; Arnold, W. A.; Barber, B. L.; Kaufenberg, E. F.; Koskinen, W. C.; Novak, P. J.; Rice, P. J.; Swackhamer, D. L. Sediment-Water Distribution of Contaminants of Emerging Concern in a Mixed Use Watershed. *Sci. Total Environ.* **2015**, *505*, 896–904.

(27) Raghav, M., Eden, S., Mitchell, K., Witte, B. Contaminants of Emerging Concern

in Water. *Arroyo* **2013**, 1–12.

(28) Cleuvers, M. Aquatic Ecotoxicity of Pharmaceuticals Including the Assessment of Combination Effects. *Toxicol. Lett.* **2003**, *142* (3), 185–194.

(29) Claessens, M.; Vanhaecke, L.; Wille, K.; Janssen, C. R. Emerging Contaminants in Belgian Marine Waters: Single Toxicant and Mixture Risks of Pharmaceuticals. *Mar. Pollut. Bull.* **2013**, *71* (1–2), 41–50.

(30) Mandiki, S. N. M.; Gillardin, V.; Martens, K.; Ercken, D.; De Roeck, E.; De Bie, T.; Declerck, S. A. S.; De Meester, L.; Brasseur, C.; Van der Heiden, E.; et al. Effect of Land Use on Pollution Status and Risk of Fish Endocrine Disruption in Small Farmland Ponds. *Hydrobiologia* **2014**, *723* (1), 103–120.

(31) Niemuth, N. J.; Jordan, R.; Crago, J.; Blanksma, C.; Johnson, R.; Klaper, R. D. Metformin Exposure at Environmentally Relevant Concentrations Causes Potential Endocrine Disruption in Adult Male Fish. *Environ. Toxicol. Chem.* **2015**, *34* (2), 291–296.

(32) Wang, C.; Lin, X.; Li, L.; Lin, S. Differential Growth Responses of Marine Phytoplankton to Herbicide Glyphosate. *PLoS One* **2016**, *11* (3), 1–20.

(33) Crago, J.; Klaper, R. Place-Based Screening of Mixtures of Dominant Emerging Contaminants Measured in Lake Michigan Using Zebrafish Embryo Gene Expression Assay. *Chemosphere* **2018**, *193*, 1226–1234.

(34) Blaise, C.; Gagné, F. Ecotoxicity of Selected Pharmaceuticals of Urban Origin Discharged to the Saint-Lawrence River (Québec, Canada): A Review. *Brazilian J.* **2006**, *10* (2), 29–51.

(35) Carson, R. *Silent Spring - 40th Anniversary Edition*; Mariner: Boston, 2002.

(36) Benotti, M. J.; Trenholm, R. A.; Vanderford, B. J.; Holady, J. C.; Stanford, B. D.; Snyder, S. A. Pharmaceuticals and Endocrine Disrupting Compounds in U.S. Drinking Water. *Environ. Sci. Technol.* **2009**, *43* (3), 597–603.

(37) Stuart, M.; Lapworth, D.; Crane, E.; Hart, A. Review of Risk from Potential Emerging Contaminants in UK Groundwater. *Sci. Total Environ.* **2012**, *416*, 1–21.

(38) Richardson, S. D.; Ternes, T. A. Water Analysis: Emerging Contaminants and Current Issues. *Anal. Chem.* **2018**, *90* (1), 398–428.

(39) Moran, P. W.; Nowell, L. H.; Kemble, N. E.; Mahler, B. J.; Waite, I. R.; Van Metre, P. C. Influence of Sediment Chemistry and Sediment Toxicity on Macroinvertebrate Communities across 99 Wadable Streams of the Midwestern USA. *Sci. Total Environ.* **2017**, *599–600*, 1469–1478.

(40) Wilson, B. A.; Smith, V. H.; Frank deNoyelles, J.; Larive, C. K. Effects of Three Pharmaceutical and Personal Care Products on Natural Freshwater Algal Assemblages. **2003**.

(41) Nagai, T. Predicting Herbicide Mixture Effects on Multiple Algal Species Using Mixture Toxicity Models. *Environ. Toxicol. Chem.* **2017**, *36* (10), 2624–2630.

(42) Ding, T.; Yang, M.; Zhang, J.; Yang, B.; Lin, K.; Li, J.; Gan, J. Toxicity, Degradation and Metabolic Fate of Ibuprofen on Freshwater Diatom Navicula Sp.

J. Hazard. Mater. **2017**, *330*, 127–134.

(43) Vajda, A. M.; Barber, L. B.; Gray, J. L.; Lopez, E. M.; Bolden, A. M.; Schoenfuss, H. L.; Norris, D. O. Demasculinization of Male Fish by Wastewater Treatment Plant Effluent. *Aquat. Toxicol.* **2011**, *103* (3–4), 213–221.

(44) Guiloski, I. C.; Ribas, J. L. C.; Piancini, L. D. S.; Dagostim, A. C.; Cirio, S. M.; Fávaro, L. F.; Boschen, S. L.; Cestari, M. M.; da Cunha, C.; Silva de Assis, H. C. Paracetamol Causes Endocrine Disruption and Hepatotoxicity in Male Fish Rhamdia Quelen after Subchronic Exposure. *Environ. Toxicol. Pharmacol.* **2017**, *53* (January), 111–120.

(45) Besson, M.; Gache, C.; Bertucci, F.; Brooker, R. M.; Roux, N.; Jacob, H.; Berthe, C.; Sovrano, V. A.; Dixson, D. L.; Lecchini, D. Exposure to Agricultural Pesticide Impairs Visual Lateralization in a Larval Coral Reef Fish. *Sci. Rep.* **2017**, *7* (1), 1–9.

(46) Kolpin, D. W.; Meyer, M. T. Pharmaceuticals , Hormones , and Other Organic Wastewater Contaminants in U . S . Streams , 1999 - 2000 : A National Reconnaissance. *Environ. Sci. Technol.* **2002**, *36* (6), 1202–1211.

(47) Nilsen, E.; Rosenbauer, R.; Furlong, E.; Burkhardt, M.; Werner, S.; Greaser, L.; Noriega, M. Pharmaceuticals, Personal Care Products and Anthropogenic Waste Indicators Detected in Streambed Sediments of the Lower Columbia River and Selected Tributaries. *Phamaceuticals Horm. Groundw.* **2008**, 1–15.

(48) Boyd, G. R.; Reemtsma, H.; Grimm, D. A.; Mitra, S. Pharmaceuticals and Personal Care Products (PPCPs) in Surface and Treated Waters of Louisiana, USA and Ontario, Canada. *Sci. Total Environ.* **2003**, *311* (1–3), 135–149.

(49) Ekberg, B. M. P.; Pletsch, B. A. *Pharmaceuticals and Personal Care Products (PPCPs) in the Streams and Aquifers of the Great Miami River Basin*; Miami, 2011.

(50) Meador, J. P.; Yeh, A.; Young, G.; Gallagher, E. P. Contaminants of Emerging Concern in a Large Temperate Estuary. *Environ. Pollut.* **2016**, *213* (July 2017), 254–267.

(51) Oosterhuis, M.; Sacher, F.; ter Laak, T. L. Prediction of Concentration Levels of Metformin and Other High Consumption Pharmaceuticals in Wastewater and Regional Surface Water Based on Sales Data. *Sci. Total Environ.* **2013**, *442*, 380–388.

(52) Riley, J. Estimates of Regional and Global Life Expectancy, 1800 – 2001. *Popul. Dev. Rev.* **2005**, *31* (3), 537–543.

(53) Organization for Economic Cooperation and Development. *Health at a Glance 2013 Demographic Trends*; 2015.

(54) Rice, D. P. Living Longer in the United States: Health, Social, and Economic Implications. *J. Med. Pract. Manage.* **1986**, *1* (3), 162–169.

(55) Roser, M. Life Expectancy https://ourworldindata.org/life-expectancy (accessed Feb 26, 2018).

(56)   Weatherall, D.; Greenwood, B.; Chee, H. L.; Al., E. Science and Technology for Disease Control: Past, Present, and Future. In *Disease Control Priorities in Developing Countries*; Jamiso, D. T., Breman, J. G., Measham, A. R., Al., E., Eds.; The International Bank for Reconstruction and Development / The World Bank: Washington D.C., 2006.

(57)   Collins, F. S.; Varmus, H. A New Initiative on Precision Medicine. *N. Engl. J. Med.* **2010**, *372* (9).

(58)   *GBD 2015 Healthcare Access and Quality Collaborators, Healthcare Access and Quality Index Based on Mortality from Causes Amenable to Personal Health Care in 195 Countries and Territories, 1990–2015: A Novel Analysis from the Global Burden of Disease Study*; 2017; Vol. 390.

(59)   Compton, W. M.; Volkow, N. D. Major Increases in Opioid Analgesic Abuse in the United States: Concerns and Strategies. *Drug Alcohol Depend.* **2006**, *81* (2), 103–107.

(60)   Riggs, P. Non-Medical Use and Abuse of Commonly Prescribed Medications. *Curr. Med. Res. Opin.* **2008**, *24* (3), 869–877.

(61)   Ebele, A. J.; Abou-Elwafa Abdallah, M.; Harrad, S. Pharmaceuticals and Personal Care Products (PPCPs) in the Freshwater Aquatic Environment. *Emerg. Contam.* **2017**, *3* (1), 1–16.

(62)   Emnet, P.; Gaw, S, Northcott, G, Storey, B, Graham, L. Personal Care Products and Steroid Hormones in the Antarctic Coastal Environment Associated with Two Antarctic Research Stations, McMurdo Station and Scott Base. *Environ. Res. 136*, 331–342.

(63)   Ashton, D.; Hilton, M.; Thomas, K. V. Investigating the Environmental Transport of Human Pharmaceuticals to Streams in the United Kingdom. *Sci. Total Environ.* **2004**, *333* (1–3), 167–184.

(64)   Fent, K.; Weston, A. A.; Caminada, D. Ecotoxicology of Human Pharmaceuticals. *Aquat. Toxicol.* **2006**, *76* (2), 122–159.

(65)   Zhou, J. L.; Zhang, Z. L.; Banks, E.; Grover, D.; Jiang, J. Q. Pharmaceutical Residues in Wastewater Treatment Works Effluents and Their Impact on Receiving River Water. *J. Hazard. Mater.* **2009**, *166* (2–3), 655–661.

(66)   Holm, J. V.; Bjerg, P. L.; Rügge, K.; Christensen, T. H. Response to Comment on "Occmrence and Distribution of Phaimaceutical Organic Compounds in the Groundwater Downgradient of a Landfill (Grindsted, Denmark)." *Environ. Sci. Technol.* **1995**, *29* (12), 3074.

(67)   Oliveira, T. S.; Murphy, M.; Mendola, N.; Wong, V.; Carlson, D.; Waring, L. Characterization of Pharmaceuticals and Personal Care Products in Hospital Effluent and Waste Water Influent/effluent by Direct-Injection LC-MS-MS. *Sci. Total Environ.* **2015**, *518–519*, 459–478.

(68)   Fick, J.; Söderström, H.; Lindberg, R. H.; Phan, C.; Tysklind, M.; Larsson, D. G. J. Contamination of Surface, Ground, and Drinking Water from Pharmaceutical Production. *Environ. Toxicol. Chem.* **2009**, *28* (12), 2522–2527.

(69)   World Health Organization (WHO). *Safe Management of Wastes from Health-Care Activities*, 2nd ed.; Chartier, Y., Emmanuel, J., Pieper, U., Pruss, A., Rushbrook, P., Stringer, R., Townend, W., Wilburn, S., Zghondi, R., Eds.; WHO Library Cataloguing-in-Publication Data, 2014.

(70)   Gray, J. L.; Borch, T.; Furlong, E. T.; Davis, J. G.; Yager, T. J.; Yang, Y. Y.; Kolpin, D. W. Rainfall-Runoff of Anthropogenic Waste Indicators from Agricultural Fields Applied with Municipal Biosolids. *Sci. Total Environ.* **2017**, *580*, 83–89.

(71)   National Research Council. *Municipal Wastewater and Sludge Treatment, Use of Reclaimed Water and Sludge in Food Crop Production*; The National Academies Press: Washington D.C., 1996.

(72)   Beijer, K.; Björlenius, B.; Shaik, S.; Lindberg, R. H.; Brunström, B.; Brandt, I. Removal of Pharmaceuticals and Unspecified Contaminants in Sewage Treatment Effluents by Activated Carbon Filtration and Ozonation: Evaluation Using Biomarker Responses and Chemical Analysis. *Chemosphere* **2017**, *176*, 342–351.

(73)   Cunningham, V. L. Special Characteristics of Pharmaceuticals Related to Environmental Fate. In *Pharmaceuticals in the Environment*; Springer Berlin Heidelberg: Berlin, Heidelberg, 2004; pp 13–24.

(74)   Gracia-Lor, E.; Sancho, J. V.; Hernández, F. Simultaneous Determination of Acidic, Neutral and Basic Pharmaceuticals in Urban Wastewater by Ultra High-Pressure Liquid Chromatography-Tandem Mass Spectrometry. *J. Chromatogr. A* **2010**, *1217* (5), 622–632.

(75)   Santos, J. L.; Aparicio, I.; Alonso, E. Occurrence and Risk Assessment of Pharmaceutically Active Compounds in Wastewater Treatment Plants. A Case Study: Seville City (Spain). *Environ. Int.* **2007**, *33* (4), 596–601.

(76)   Alley, W. M.; Winter, T. C.; Harvey, J. W.; Franke, O. L. Ground Water and Surface Water: A Single Resource. *USGS Publ.* **1998**, 79.

(77)   Farré, M. la; Pérez, S.; Kantiani, L.; Barceló, D. Fate and Toxicity of Emerging Pollutants, Their Metabolites and Transformation Products in the Aquatic Environment. *TrAC - Trends Anal. Chem.* **2008**, *27* (11), 991–1007.

(78)   Xing, Y.; Chen, X.; Chen, X.; Zhuang, J. Colloid-Mediated Transport of Pharmaceutical and Personal Care Products through Porous Media. *Sci. Rep.* **2016**, *6*, 1–10.

(79)   Corada-Fernández, C.; Candela, L.; Torres-Fuentes, N.; Pintado-Herrera, M. G.; Paniw, M.; González-Mazo, E. Effects of Extreme Rainfall Events on the Distribution of Selected Emerging Contaminants in Surface and Groundwater: The Guadalete River Basin (SW, Spain). *Sci. Total Environ.* **2017**, *605–606*, 770–783.

(80)   Beausse, J. Selected Drugs in Solid Matrices: A Review of Environmental Determination, Occurrence and Properties of Principal Substances. *TrAC - Trends Anal. Chem.* **2004**, *23* (10–11), 753–761.

(81)   Heberer, T. Occurrence, Fate, and Removal of Pharmaceutical Residues in the Aquatic Environment: A Review of Recent Research Data. *Toxicol. Lett.* **2002**,

131, 5–17.

(82) Kümmerer, K. Antibiotics in the Aquatic Environment - A Review - Part II. *Chemosphere* **2009**, *75* (4), 435–441.

(83) Dias, D. A.; Urban, S.; Roessner, U. A Historical Overview of Natural Products in Drug Discovery. *Metabolites* **2012**, *2* (4), 303–336.

(84) Trosset, J. Y.; Carbonell, P. Synthetic Biology for Pharmaceutical Drug Discovery. *Drug Des. Devel. Ther.* **2015**, *9*, 6285–6302.

(85) Augsburger, L. L.; Hoag, S. W. *Pharmaceutical Dosage Forms - Tablets*; Informa Healthcare USA, 2008.

(86) Kapusta, D. Drug Excretion. In *xPharm: The Comprehensive Pharmacology Reference*; Elsevier, 2007; pp 1–2.

(87) Alavijeh, M. S.; Chishty, M.; Qaiser, M. Z.; Palmer, A. M. Drug Metabolism and Pharmacokinetics, the Blood-Brain Barrier, and Central Nervous System Drug Discovery. *NeuroRx* **2005**, *2* (4), 554–571.

(88) Bialer, M.; Doose, D. R.; Murthy, B.; Curtin, C.; Wang, S.-S.; Twyman, R. E.; Schwabe, S. Pharmacokinetic Interactions of Topiramate. *Clin. Pharmacokinet.* **2004**, *43* (12), 763–780.

(89) Graham, G. G.; Punt, J.; Arora, M.; Day, R. O.; Doogue, M. P.; Duong, J. K.; Furlong, T. J.; Greenfield, J. R.; Greenup, L. C.; Kirkpatrick, C. M.; et al. Clinical Pharmacokinetics of Metformin : Clinical Pharmacokinetics. *J. Clin. Pharmacol.* **2011**, *29* (6), 490–494.

(90) Davies, N. M.; Anderson, K. E. Clinical Pharmacokinetics of Diclofenac. Therapeutic Insights and Pitfalls. *Clin. Pharmacokinet.* **1997**, *33* (3), 184–213.

(91) Davies, N. M. Clinical Pharmacokinetics of Ibuprofen. The First 30 Years. *Clin. Pharmacokinet.* **1998**, *34* (2), 101–154.

(92) Le-Minh, N.; Khan, S. J.; Drewes, J. E.; Stuetz, R. M. Fate of Antibiotics during Municipal Water Recycling Treatment Processes. *Water Res.* **2010**, *44* (15), 4295–4323.

(93) Oulton, R. L.; Kohn, T.; Cwiertny, D. M. Pharmaceuticals and Personal Care Products in Effluent Matrices: A Survey of Transformation and Removal during Wastewater Treatment and Implications for Wastewater Management. *J. Environ. Monit.* **2010**, *12* (11), 1956.

(94) Bu, Q.; Shi, X.; Yu, G.; Huang, J.; Wang, B. Assessing the Persistence of Pharmaceuticals in the Aquatic Environment: Challenges and Needs. *Emerg. Contam.* **2016**, *2* (3), 145–147.

(95) Daughton, C. G. Cradle-to-Cradle Stewardship of Drugs for Minimizing Their Environmental Disposition While Promoting Human Health. I. Rational for and Avenues toward a Green Pharmacy. *Environ. Health Perspect.* **2003**, *111* (5), 757–774.

(96) Ebele, A. J.; Abou-Elwafa Abdallah, M.; Harrad, S. Pharmaceuticals and Personal Care Products (PPCPs) in the Freshwater Aquatic Environment. *Emerg. Contam.*

2017, *3* (1), 1–16.

(97)   Hernando, M. D.; Petrovic, M.; Fernández-Alba, A. R.; Barceló, D. Analysis by Liquid Chromatography-Electrospray Ionization Tandem Mass Spectrometry and Acute Toxicity Evaluation for β-Blockers and Lipid-Regulating Agents in Wastewater Samples. *J. Chromatogr. A* **2004**, *1046* (1–2), 133–140.

(98)   Kim, J.-W.; Ishibashi, H.; Yamauchi, R.; Ichikawa, N.; Takao, Y.; Hirano, M.; Koga, M.; Arizono, K. Acute Toxicity of Pharmaceutical and Personal Care Products on Freshwater Crustacean (Thamnocephalus Platyurus) and Fish (Oryzias Latipes). *J. Toxicol. Sci.* **2009**, *34* (2), 227–232.

(99)   Crane, M.; Watts, C.; Boucard, T. Chronic Aquatic Environmental Risks from Exposure to Human Pharmaceuticals. *Sci. Total Environ.* **2006**, *367* (1), 23–41.

(100) Jobling, S.; Williams, R.; Johnson, A.; Taylor, A.; Gross-Sorokin, M.; Nolan, M.; Tyler, C. R.; Van Aerle, R.; Santos, E.; Brighty, G. Predicted Exposures to Steroid Estrogens in U.K. Rivers Correlate with Widespread Sexual Disruption in Wild Fish Populations. *Environ. Health Perspect.* **2006**, *114* (SUPPL.1), 32–39.

(101) Brausch, J. M.; Connors, K. A.; Brooks, B. W.; Rand, G. M. Human Pharmaceuticals in the Aquatic Environment: A Review of Recent Toxicological Studies and Considerations for Toxicity Testing; Springer, Boston, MA, 2012; pp 1–99.

(102) Prichard, E.; Granek, E. F. Effects of Pharmaceuticals and Personal Care Products on Marine Organisms: From Single-Species Studies to an Ecosystem-Based Approach. *Environ. Sci. Pollut. Res.* **2016**, *23* (22), 22365–22384.

(103) Maskaoui, K.; Zhou, J. L. Colloids as a Sink for Certain Pharmaceuticals in the Aquatic Environment. *Environ. Sci. Pollut. Res.* **2010**, *17* (4), 898–907.

(104) Lee, K. E.; Yaeger, C. S.; Jahns, N. D.; Schoenfuss, H. L. Occurrence of Endocrine Active Compounds and Biological Responses in the Mississippi River - Study Design and Data, June through August 2006. *Data Ser.* **2008**, No. August, 28.

(105) Liao, P. H.; Chu, S. H.; Tu, T. Y.; Wang, X. H.; Lin, A. Y. C.; Chen, P. J. Persistent Endocrine Disruption Effects in Medaka Fish with Early Life-Stage Exposure to a Triazole-Containing Aromatase Inhibitor (Letrozole). *J. Hazard. Mater.* **2014**, *277*, 141–149.

(106) Teixeira, J. R.; Granek, E. F. Effects of Environmentally-Relevant Antibiotic Mixtures on Marine Microalgal Growth. *Sci. Total Environ.* **2017**, *580*, 43–49.

(107) Rosi-marshall, A. E. J.; Kincaid, D. W.; Bechtold, H. A.; Royer, T. V; Rosi-marshall, E. J.; Kincaid, D. W.; Bechtold, H. A.; Royer, T. V; Rojas, M.; Kelly, J. J. Pharmaceuticals Suppress Algal Growth and Microbial Respiration and Alter Bacterial Communities in Stream Biofilms Miguel Rojas and John J . Kelly Published by : Wiley on Behalf of the Ecological Society of America Stable URL : Http://www.jstor.org/stable. **2017**, *23* (3), 583–593.

(108) Peters, J. R.; Granek, E. F.; de Rivera, C. E.; Rollins, M. Prozac in the Water: Chronic Fluoxetine Exposure and Predation Risk Interact to Shape Behaviors in an

Estuarine Crab. *Ecol. Evol.* **2017**, No. August, 1–11.

(109) Huerta, B.; Margiotta-Casaluci, L.; Rodríguez-Mozaz, S.; Scholze, M.; Winter, M. J.; Barceló, D.; Sumpter, J. P. Anti-Anxiety Drugs and Fish Behavior: Establishing the Link between Internal Concentrations of Oxazepam and Behavioral Effects. *Environ. Toxicol. Chem.* **2016**, *35* (11), 2782–2790.

(110) Parrott, J. L.; Metcalfe, C. D. Nest-Defense Behaviors in Fathead Minnows after Lifecycle Exposure to the Antidepressant Venlafaxine. *Environ. Pollut.* **2018**, *234*, 223–230.

(111) *CDER (Center for Drug Evaluation and Research) Guidance for Industry: Environmental Assessment of Human Drug and Biologics Applications*; Washington D.C., 1998.

(112) *CHMP (Committee for Medicinal Products for Human Use) Guideline on the Environmental Risk Assessment of Medicinal Products for Human Use (Doc. Ref. EMEA/CHMP/SWP/4447/00 Corr 1)*; London, UK, 2006.

(113) *CVMP (Committee for Medicinal Products for Veterinary Use) VICH Topic GL6 (Ecotoxicity Phase I) Step 7: Guideline on Environmental Impact Assessment (EIAs) for Veterinary Medicinal Products–Phase I. (Doc. Ref. CVMP/VICH/592/98)*; London, UK, 2000.

(114) *CVMP (Committee for Medicinal Products for Veterinary Use) Guideline on Environmental Impact Assessment for Veterinary Medicinal Products Phase II. (Doc. Ref. CVMP/VICH/790/03-FINAL)*; London, UK, 2004.

(115) *ECETOC (European Centre for Ecotoxicology and Toxicology of Chemicals) Intelligent Testing Strategies in Ecotoxicology: Mode of Action Approach for Specifically Acting Chemicals (TR No. 102)*; Brussels, Belgium, 2008.

(116) *WHO (World Health Organization) Pharmaceuticals in Drinking Water (WHO/HSE/WSH/11.05)*; Geneva, Switzerland, 2011.

(117) *National Diabetes Statistics Report , 2017 Estimates of Diabetes and Its Burden in the Epidemiologic Estimation Methods*; 2017.

(118) World Health Organization. *Global Report on Diabetes*; 2016.

(119) Tabish, S. A. Is Diabetes Becoming the Biggest Epidemic of the Twenty-First Century? *Int. J. Health Sci. (Qassim).* **2007**, *1* (2), V–VIII.

(120) Hu, F. B. Globalization of Diabetes: The Role of Diet, Lifestyle, and Genes. *Diabetes Care* **2011**, *34* (6), 1249–1257.

(121) Unnikrishnan, R.; Pradeepa, R.; Joshi, S. R.; Mohan, V. Type 2 Diabetes: Demystifying the Global Epidemic. *Diabetes* **2017**, *66* (6), 1432–1442.

(122) Groop, L. C.; Bonadonna, R. C.; DelPrato, S.; Ratheiser, K.; Zyck, K.; Ferrannini, E.; DeFronzo, R. A. Glucose and Free Fatty Acid Metabolism in Non-Insulin-Dependent Diabetes Mellitus. Evidence for Multiple Sites of Insulin Resistance. *J.Clin.Invest* **1989**, *84* (0021–9738 SB–AIM SB–IM), 205–213.

(123) Causes of Diabetes https://www.niddk.nih.gov/health-information/diabetes/overview (accessed Feb 22, 2018).

(124) Wilcox, G. Insulin and Insulin Resistance. *Clin. Biochem. Rev.* **2005**, *26* (2), 19–39.

(125) Kahn, S. E.; Cooper, M. E.; Del Prato, S. Pathophysiology and Treatment of Type 2 Diabetes: Perspectives on the Past, Present and Future. *Lancet* **2015**, *383* (9922), 1068–1083.

(126) Olokoba, A. B.; Obateru, O. A.; Olokoba, L. B. Type 2 Diabetes Mellitus: A Review of Current Trends. *Oman Med. J.* **2012**, *27* (4), 269–273.

(127) Druet, C.; Tubiana-Rufi, N.; Chevenne, D.; Rigal, O.; Polak, M.; Levy-Marchal, C. Characterization of Insulin Secretion and Resistance in Type 2 Diabetes of Adolescents. *J. Clin. Endocrinol. Metab.* **2006**, *91* (2), 401–404.

(128) Halban, P. A.; Polonsky, K. S.; Bowden, D. W.; Hawkins, M. A.; Ling, C.; Mather, K. J.; Powers, A. C.; Rhodes, C. J.; Sussel, L.; Weir, G. C. β-Cell Failure in Type 2 Diabetes: Postulated Mechanisms and Prospects for Prevention and Treatment. *J. Clin. Endocrinol. Metab.* **2014**, *99* (6), 1983–1992.

(129) Stolar, M. Glycemic Control and Complications in Type 2 Diabetes Mellitus. *Am. J. Med.* **2010**, *123* (3 SUPPL.), S3–S11.

(130) Wu, Y.; Ding, Y.; Tanaka, Y.; Zhang, W. Risk Factors Contributing to Type 2 Diabetes and Recent Advances in the Treatment and Prevention. *Int. J. Med. Sci.* **2014**, *11* (11), 1185–1200.

(131) Krentz, A. J.; Bailey, C. J. Oral Antidiabetic Agents: Current Role in Type 2 Diabetes Mellitus. *Drugs* **2005**, *65* (3), 385–411.

(132) Sénéchal, M.; Slaght, J.; Bharti, N.; Bouchard, D. R. Independent and Combined Effect of Diet and Exercise in Adults with Prediabetes. *Diabetes, Metab. Syndr. Obes. Targets Ther.* **2014**, *7*, 521–529.

(133) WHO Collaborating Centre for Drug Statistics Methodology http://www.whocc.no/atcddd/ (accessed Feb 27, 2018).

(134) Hadden, D. R. Goat's Rue - French Lilac - Italian Fitch - Spanish Sainfoin: Gallega Officinalis and Metformin: The Edinburgh Connection. *J. R. Coll. Physicians Edinb.* **2005**, *35* (3), 258–260.

(135) Watanabe, C. K. Studies in the Metabolic Changes Induced by Administration of Guanidine Bases. *J. Biol. Chem.* **1918**, *33* (7), 253–265.

(136) Bailey, C. J. Metformin: Historical Overview. *Diabetologia* **2017**, *60* (9), 1566–1576.

(137) Schäfer, G. Guanidines and Biguanides. *Pharmacol. Ther.* **1980**, *8* (2), 275–295.

(138) Bennett, W. L.; Maruthur, N. M.; Singh, S.; Segal, J. B.; Wilson, L. M. Review Annals of Internal Medicine Comparative Effectiveness and Safety of Medications for Type 2 Diabetes : An Update Including New Drugs and 2-Drug Combinations. *Ann. Intern. Med.* **2011**, *154* (11), 602–613.

(139) Alemón-medina, R.; Chávez-pacheco, J. L.; Ramírez-mendiola, B.; García-álvarez, R. Physicochemical Stability of Three Generic Brands of Metformin in Solution. **2014**, 94–99.

(140) *Assessment Report: Linagliptin/metformin Hydrochloride (Procedure No. EMEA/H/C/002279)*; London, UK, 2015.

(141) *NDA Environmental Assessment for Canagliflozin and Metformin Fixed Dose Combination (Document No. EDMS-ERI-42522740)*; 2012.

(142) Rebitski, E. P.; Aranda, P.; Darder, M.; Carraro, R.; Ruiz-Hitzky, E. Intercalation of Metformin into Montmorillonite. *Dalton Trans.* **2018**.

(143) Viollet, B.; Guigas, B.; Garcia, N. S.; Leclerc, J.; Foretz, M.; Andreelli, F. Cellular and Molecular Mechanisms of Metformin: An Overview. *Clin. Sci.* **2012**, *122* (6), 253–270.

(144) Hur, K. Y.; Lee, M. S. New Mechanisms of Metformin Action: Focusing on Mitochondria and the Gut. *J. Diabetes Investig.* **2015**, *6* (6), 600–609.

(145) Wang, Y. W.; He, S. J.; Feng, X.; Cheng, J.; Luo, Y. T.; Tian, L.; Huang, Q. Metformin: A Review of Its Potential Indications. *Drug Des. Devel. Ther.* **2017**, *11*, 2421–2429.

(146) Zhou, G.; Myers, R.; Li, Y.; Chen, Y.; Shen, X.; Fenyk-melody, J.; Wu, M.; Ventre, J.; Doebber, T.; Fujii, N.; et al. Role of AMP-Activated Protein Kinase in Mechanism of Metformin Action Role of AMP-Activated Protein Kinase in Mechanism of Metformin Action. *J. Clin. Invest.* **2001**, *108* (8), 1167–1174.

(147) Hardie, D. G. AMP-activated/SNF1 Protein Kinases: Conserved Guardians of Cellular Energy. *Nat. Rev. Mol. Cell Biol.* **2007**, *8* (10), 774–785.

(148) Wang, S.; Song, P.; Zou, M. H. AMP-Activated Protein Kinase, Stress Responses and Cardiovascular Diseases. *Clin. Sci. (Lond).* **2012**, *122* (12), 555–573.

(149) Zou, M. H.; Kirkpatrick, S. S.; Davis, B. J.; Nelson, J. S.; Wiles IV, W. G.; Schlattner, U.; Neumann, D.; Brownlee, M.; Freeman, M. B.; Goldman, M. H. Activation of the AMP-Activated Protein Kinase by the Anti-Diabetic Drug Metformin in Vivo: Role of Mitochondrial Reactive Nitrogen Species. *J. Biol. Chem.* **2004**, *279* (42), 43940–43951.

(150) Pryor, R.; Cabreiro, F. Repurposing Metformin: An Old Drug with New Tricks in Its Binding Pockets. *Biochem. J.* **2015**, *471* (3), 307–322.

(151) Repiščák, P.; Erhardt, S.; Rena, G.; Paterson, M. J. Biomolecular Mode of Action of Metformin in Relation to Its Copper Binding Properties. *Biochemistry* **2014**, *53* (4), 787–795.

(152) Bridges, H. R.; Jones, A. J. Y.; Pollak, M. N.; Hirst, J. Effects of Metformin and Other Biguanides on Oxidative Phosphorylation in Mitochondria. *Biochem. J.* **2014**, *462* (3), 475–487.

(153) Tucker, G. T.; Casey, C.; Phillips, P. J.; Connor, H.; Ward, J. D.; Woods, H. F. Metformin Kinetics in Healthy Subjects and in Patients with Diabetes Mellitus. *Br. J. Clin. Pharmacol.* **1981**, *12* (2), 235–246.

(154) Gabr, R.; El-Sherbeni, A.; Ben-Eltriki, M.; El-Kadi, A.; Brocks, D. Pharmacokinetics of Metformin in the Rat: Assessment of the Effect of Hyperlipidemia and Evidence for Its Metabolism to Guanylurea. *Can. J. Physiol.*

Pharmacol. **2017**, *95* (5), 530–538.

(155) Hester, R. E.; Harrison, R. M. *Pharmaceuticals in the Environment.*

(156) Trautwein, C.; Kümmerer, K. Incomplete Aerobic Degradation of the Antidiabetic Drug Metformin and Identification of the Bacterial Dead-End Transformation Product Guanylurea. *Chemosphere* **2011**, *85* (5), 765–773.

(157) Markiewicz, M.; Jungnickel, C.; Stolte, S.; Białk-Bielińska, A.; Kumirska, J.; Mrozik, W. Ultimate Biodegradability and Ecotoxicity of Orally Administered Antidiabetic Drugs. *J. Hazard. Mater.* **2017**, *333*, 154–161.

(158) Markiewicz, M.; Jungnickel, C.; Stolte, S.; Białk-Bielińska, A.; Kumirska, J.; Mrozik, W. Primary Degradation of Antidiabetic Drugs. *J. Hazard. Mater.* **2017**, *324*, 428–435.

(159) Scheurer, M.; Sacher, F.; Brauch, H.-J. Occurrence of the Antidiabetic Drug Metformin in Sewage and Surface Waters in Germany. *J. Environ. Monit.* **2009**, *11* (9), 1608.

(160) Blair, B. D.; Crago, J. P.; Hedman, C. J.; Klaper, R. D. Pharmaceuticals and Personal Care Products Found in the Great Lakes above Concentrations of Environmental Concern. *Chemosphere* **2013**, *93* (9), 2116–2123.

(161) Houtman, C. J.; ten Broek, R.; de Jong, K.; Pieterse, B.; Kroesbergen, J. A Multicomponent Snapshot of Pharmaceuticals and Pesticides in the River Meuse Basin. *Environ. Toxicol. Chem.* **2013**, *32* (11), n/a-n/a.

(162) ter Laak, T. L.; Kooij, P. J. F.; Tolkamp, H.; Hofman, J. Different Compositions of Pharmaceuticals in Dutch and Belgian Rivers Explained by Consumption Patterns and Treatment Efficiency. *Environ. Sci. Pollut. Res.* **2014**, *21* (22), 12843–12855.

(163) Kosma, C. I.; Lambropoulou, D. A.; Albanis, T. A. Comprehensive Study of the Antidiabetic Drug Metformin and Its Transformation Product Guanylurea in Greek Wastewaters. *Water Res.* **2015**, *70*, 436–448.

(164) Tong, A. Z.; Ghoshdastidar, A. J.; Fox, S. The Presence of the Top Prescribed Pharmaceuticals in Treated Sewage Effluents and Receiving Waters in Southwest Nova Scotia, Canada. *Environ. Sci. Pollut. Res.* **2015**, *22* (1), 689–700.

(165) Bradley, P. M.; Journey, C. A.; Button, D. T.; Carlisle, D. M.; Clark, J. M.; Mahler, B. J.; Nakagaki, N.; Qi, S. L.; Waite, I. R.; VanMetre, P. C. Metformin and Other Pharmaceuticals Widespread in Wadeable Streams of the Southeastern United States. *Environ. Sci. Technol. Lett.* **2016**, *3* (6), 243–249.

(166) Bradley, P. M.; Journey, C. A.; Romanok, K. M.; Barber, L. B.; Buxton, H. T.; Foreman, W. T.; Furlong, E. T.; Glassmeyer, S. T.; Hladik, M. L.; Iwanowicz, L. R.; et al. Expanded Target-Chemical Analysis Reveals Extensive Mixed-Organic-Contaminant Exposure in U.S. Streams. *Environ. Sci. Technol.* **2017**, *51* (9), 4792–4802.

(167) Shraim, A.; Diab, A.; Alsuhaimi, A.; Niazy, E.; Metwally, M.; Amad, M.; Sioud, S.; Dawoud, A. Analysis of Some Pharmaceuticals in Municipal Wastewater of Almadinah Almunawarah. *Arab. J. Chem.* **2017**, *10*, S719–S729.

(168) Johnson, A.; Carey, B.; Golding, S. Results of a Screening Analysis for Pharmaceuticals in Wastewater Treatment Plant Effluents , Wells , and Creeks in the Sequim-Dungeness Area. **2004**, No. 4, 26 pgs.

(169) Perreault, N. N.; Halasz, A.; Thiboutot, S.; Ampleman, G.; Hawari, J. Joint Photomicrobial Process for the Degradation of the Insensitive Munition N-Guanylurea-Dinitramide (FOX-12). *Environ. Sci. Technol.* **2013**, *47* (10), 5193–5198.

(170) Lamparska, K.; Smith, S. S. The Genetic and Epigenetic Effects of 5-Azacytidine and Its Major Breakdown Product Guanylurea. **2015**, 28–36.

(171) Gilbert, M. D. Mechanism and Kinetics of the Dicyandiamide Cure of Epoxy Resins. *Dr. Diss. 1896-2014* **1988**, *737*.

(172) Carley, J. F.; Whittington, L. R. *Whittington's Dictionary of Plastics.*; Technomic Pub. Co, 1993.

(173) Yamazoe, F.; Imai, J. Determination of Cyanamide Derivatives in Fertilizer Containing Lime Nitrogen. *Bunseki kagaku* **1960**, *9* (10), 877–883.

(174) Hayase, T. Slowly Available Nitrogen Fertilizers. *Japan Agric. Res. Q.* **1968**, *3* (4), 1–4.

(175) Cabreiro, F.; Au, C.; Leung, K.-Y.; Vergara-Irigaray, N.; Cochemé, H. M.; Noori, T.; Weinkove, D.; Schuster, E.; Greene, N. D. E.; Gems, D. Metformin Retards Aging in C. Elegans by Altering Microbial Folate and Methionine Metabolism. *Cell* **2013**, *153* (1), 228–239.

(176) Kammerer, J. C. Water Fact Sheet: Largest Rivers in the United States. *Open-file Rep.* **1990**, 2.

(177) Dahm, C. N.; Gregory, S. V.; Kilho Park, P. Organic Carbon Transport in the Columbia River. *Estuar. Coast. Shelf Sci.* **1981**, *13* (6), 645–658.

(178) Small, L. F.; McIntire, C. D.; MacDonald, K. B.; Lara-Lara, J. R.; Frey, B. E.; Amspoker, M. C.; Winfield, T. Primary Production, Plant and Detrital Biomass, and Particle Transport in the Columbia River Estuary. *Prog. Oceanogr.* **1990**, *25* (1–4), 175–210.

(179) Horowitz, A. J.; Elrick, K. A.; Smith, J. J. Annual Suspended Sediment and Trace Element Fluxes in the Mississippi, Columbia, Colorado, and Rio Grande Drainage Basins. *Hydrol. Process.* **2001**, *15* (7), 1169–1207.

(180) Stanford, J. A.; Gregory, S. V.; Hauer, R. F.; Snyder, E. B. Columbia River Basin. In *Rivers of North America*; Benke, A. C., Cushing, C. E., Eds.; Elsevier Academic Press: Burlington, MA, 2005; p 1144.

(181) Columbia River Basin. In *Reclamation: Managing Water in the West*; U.S. Department of the Interior - Bureau of Reclamation: Denver, CO, 2016.

(182) Hamlet, A. F.; Lettenmaier, D. P. Effects of 20th Century Warming and Climate Variability on Flood Risk in the Western U.S. *Water Resour. Res.* **2007**, *43* (6), 1–17.

(183) Elsner, M. M.; Cuo, L.; Voisin, N.; Deems, J. S.; Hamlet, A. F.; Vano, J. a; Lee,

S.; Lettenmaier, D. P. Implications of 21st Century Climate Change for the Hydrology of Washington State. *Clim. Change* **2010**, *102* (1–2), 225–260.

(184) Volkman, J. M. *A River in Common: The Columbia River, the Salmon Ecosystem, and Water Policy*; 1997.

(185) Beschta, R. L.; Platts, W. S. Morphological Features of Small Streams: Significant and Function. *J. Am. Water Resour. Assoc.* **1986**, *22* (3), 369–379.

(186) Stouder, D. J.; Bisson, P. A.; Naiman, R. J. *Pacific Salmon & Their Ecosystems : Status and Future Options*; Chapman & Hall, 1997.

(187) Fresh, K. L.; Casillas, E.; Johnson, L. L.; Bottom, D. L. *Role of the Estuary in the Recovery of Columbia River Basin Salmon and Steelhead: An Evaluation of the Effects of Selected Factors on Salmonid Population Viability*; Seattle, WA, 2005.

(188) Sullivan, B.E., Prahl, F. G., Small, L. F., Covert, P. A. Seasonality of Phytoplankton Production in the Columbia River. *Geochim. Cosmochim. Acta* **2001**, *65* (7), 1125–1139.

(189) Craig, J.; Hacker, R. The History and Development of the Fisheries of the Columbia River. *Bull. Bur. Fish.* **1940**, 132–216.

(190) Rathbun, R. A Review of the Fisheries in the Contiguous Waters of the State of Washington and British Columbia. **1899**.

(191) Hamlet, A. F.; Lee, S.-Y.; Mickelson, K. E. B.; Elsner, M. M. Effects of Projected Climate Change on Energy Supply and Demand in the Pacific Northwest and Washington State. *Clim. Change* **2010**, *102* (1–2), 103–128.

(192) Bilby, R.; Hanna, S.; Huntly, N.; Al., E. Human Population Impacts on Columbia River Basin Fish and Wildlife. *Indep. Sci. Advis. Board* **2007**.

(193) National Research Council. *Managing the Columbia River: Instream Flows, Water Withdrawals, and Salmon Survival*; The National Academies Press: Washington D.C., 2004.

(194) Jay, D. A. *Climate Effects on Columbia River Sediment Transport: The Columbia River*; 2000.

(195) Chapman, D. W. Salmon and Steelhead Abundance in the Columbia River in the Nineteenth Century. *Trans. Am. Fish. Soc.* **1986**, *115* (5), 662–670.

(196) Fullerton, A. H.; Beechie, T. J.; Baker, S. E.; Hall, J. E.; Barnas, K. A. Regional Patterns of Riparian Characteristics in the Interior Columbia River Basin, Northwestern USA: Applications for Restoration Planning. *Landsc. Ecol.* **2006**, *21* (8), 1347–1360.

(197) Morace, J. L. Water-Quality Data , Columbia River Estuary, 2004-05: U.S. Geological Survey Data Series 213. **2006**, 23.

(198) Morace, J. L. Reconnaissance of Contaminants in Selected Wastewater-Treatment-Plant Effluent and Stormwater Runoff Entering the Columbia River, Columbia River Basin, Washington and Oregon, Scientific Investigations Report. **2012**, 80.

(199) *Lower Columbia River and Estuary Ecosystem Monitoring—water Quality and*

Salmon Sampling Report; Portland, OR, 2007.

(200) Alvarez, D.; Perkins, S.; Nilsen, E.; Morace, J. Spatial and Temporal Trends in Occurrence of Emerging and Legacy Contaminants in the Lower Columbia River 2008-2010. *Sci. Total Environ.* **2014**, *484* (1), 322–330.

(201) Counihan, T. D.; Waite, I. R.; Nilsen, E. B.; Hardiman, J. M.; Elias, E.; Gelfenbaum, G.; Zaugg, S. D. A Survey of Benthic Sediment Contaminants in Reaches of the Columbia River Estuary Based on Channel Sedimentation Characteristics. *Sci. Total Environ.* **2014**, *484* (1), 331–343.

(202) Nilsen, E.; Furlong, E. T.; Rosenbauer, R. Reconnaissance of Pharmaceuticals and Wastewater Indicators in Streambed Sediments of the Lower Columbia River Basin, Oregon and Washington. *J. Am. Water Resour. Assoc.* **2014**, *50* (2), 291–301.

(203) Jenkins, J. A.; Olivier, H. M.; Draugelis-Dale, R. O.; Eilts, B. E.; Torres, L.; Patiño, R.; Nilsen, E.; Goodbred, S. L. Assessing Reproductive and Endocrine Parameters in Male Largescale Suckers (Catostomus Macrocheilus) along a Contaminant Gradient in the Lower Columbia River, USA. *Sci. Total Environ.* **2014**, *484* (1), 365–378.

(204) Torres, L.; Nilsen, E.; Grove, R.; Patiño, R. Health Status of Largescale Sucker (Catostomus Macrocheilus) Collected along an Organic Contaminant Gradient in the Lower Columbia River, Oregon and Washington, USA. *Sci. Total Environ.* **2014**, *484* (1), 353–364.

(205) USEPA. *Columbia River Basin: State of the River Report for Toxics (EPA Publication No. 910-R-08-004)*; 2009.

(206) USEPA. *Columbia River Toxics Reduction Action Plan. Prepared by: U.S. Environmental Protection Agency, Region 10 and the Columbia River Toxics Reduction Working Group*; 2010.

(207) Erickson, B. E. Analyzing the Ignored Environmental Contaminants. *Environ. Sci. Technol.* **2002**, 140–145.

(208) Field, J. A.; Johnson, C. A.; Rose, J. B. What Is "emerging"? *Environ. Sci. Technol.* **2006**, *40* (23), 7105–7105.

(209) Dai, A.; Trenberth, K. E. Estimates of Freshwater Discharge from Continents: Latitudinal and Seasonal Variations. *J. Hydrometeorol.* **2002**, *3* (6), 660–687.

(210) USEPA. *Columbia River Toxics Reduction Working Group: Strategy For Measuring, Documenting And Reducing Chemicals Of Emerging Concern*; 2014.

(211) Zhou, X. F.; Dai, C. M.; Zhang, Y. L.; Surampalli, R. Y.; Zhang, T. C. A Preliminary Study on the Occurrence and Behavior of Carbamazepine (CBZ) in Aquatic Environment of Yangtze River Delta, China. *Environ. Monit. Assess.* **2011**, *173* (1–4), 45–53.

(212) Yang, Y.; Fu, J.; Peng, H.; Hou, L.; Liu, M.; Zhou, J. L. Occurrence and Phase Distribution of Selected Pharmaceuticals in the Yangtze Estuary and Its Coastal Zone. *J. Hazard. Mater.* **2011**, *190* (1–3), 588–596.

(213) Ginebreda, A.; Sabater-Liesa, L.; Rico, A.; Focks, A.; Barceló, D. Reconciling Monitoring and Modeling: An Appraisal of River Monitoring Networks Based on a Spatial Autocorrelation Approach - Emerging Pollutants in the Danube River as a Case Study. *Sci. Total Environ.* **2018**, *618*, 323–335.

(214) Wilson, B.; Zhu, J.; Cantwell, M.; Olsen, C. R. Short-Term Dynamics and Retention of Triclosan in the Lower Hudson River Estuary. *Mar. Pollut. Bull.* **2008**, *56* (6), 1230–1233.

(215) Klosterhaus, S. L.; Grace, R.; Hamilton, M. C.; Yee, D. Method Validation and Reconnaissance of Pharmaceuticals, Personal Care Products, and Alkylphenols in Surface Waters, Sediments, and Mussels in an Urban Estuary. *Environ. Int.* **2013**, *54*, 92–99.

(216) Ferrey, M. *Pharmaceuticals and Endocrine Active Chemicals in Minnesota Lakes*; 2013.

(217) Golet, E.; Alder, AC, Walter, G. Environmental Exposure and Risk Assessment of Fluoroquinolone Antibacterial Agents in Wastewater and River Water of the Glatt Valley Watershed, Switzerland. **2002**.

(218) Ellis, J. B. Pharmaceutical and Personal Care Products (PPCPs) in Urban Receiving Waters. *Environ. Pollut.* **2006**, *144* (1), 184–189.

(219) de Jongh, C. M.; Kooij, P. J. F.; de Voogt, P.; ter Laak, T. L. Screening and Human Health Risk Assessment of Pharmaceuticals and Their Transformation Products in Dutch Surface Waters and Drinking Water. *Sci. Total Environ.* **2012**, *427–428*, 70–77.

(220) Balakrishna, K.; Rath, A.; Praveenkumarreddy, Y.; Guruge, K. S.; Subedi, B. A Review of the Occurrence of Pharmaceuticals and Personal Care Products in Indian Water Bodies. *Ecotoxicol. Environ. Saf.* **2017**, *137*, 113–120.

(221) Roberts, J.; Kumar, A.; Du, J.; Hepplewhite, C.; Ellis, D. J.; Christy, A. G.; Beavis, S. G. Pharmaceuticals and Personal Care Products (PPCPs) in Australia's Largest Inland Sewage Treatment Plant, and Its Contribution to a Major Australian River during High and Low Flow. *Sci. Total Environ.* **2016**, *541*, 1625–1637.

(222) Nilsen, E.; Morace, J. Foodweb Transfer, Sediment Transport, and Biological Impacts of Emerging and Legacy Organic Contaminants in the Lower Columbia River, Oregon and Washington, USA: USGS Contaminants and Habitat (ConHab) Project. *Sci. Total Environ.* **2014**, *484* (1), 319–321.

(223) Scheurer, M.; Michel, A.; Brauch, H. J.; Ruck, W.; Sacher, F. Occurrence and Fate of the Antidiabetic Drug Metformin and Its Metabolite Guanylurea in the Environment and during Drinking Water Treatment. *Water Res.* **2012**, *46* (15), 4790–4802.

(224) Peterson, T.D., Nilsen, E., Needoba, J. A. Unpublished. **2015**.

(225) Cleaning of Equipment for Water Sampling (Ver. 2.0). In *U.S. Geological Survey Techniques of Water-Resources Investigations, Book 9*; Wilde, F. D., Ed.; 2004.

(226) *Definition and Procedure for the Determination of the Method Detection Limit, Revision 2 (EPA Publication No. 821-R-16-006)*; Rockville, MD, 2016.

(227) Childress, C. J. O.; Foreman, W. T.; Connor, B. F.; Maloney, T. J. *New Reporting Procedures Based on Long-Term Method Detection Levels and Some Considerations for Interpretations of Water-Quality Data Provided by the U.S. Geological Survey National Water Quality Laboratory (USGS Report No. 99-193)*; Reston, VA, 1999.

(228) Wetzel, R. G. *Limnology: Lake and River Ecosystem*, 3rd ed.; Academic Press: San Diego, CA, 2001.

(229) National Oceanic and Atmospheric Administration (NOAA) Northwest River Forecast Center. Water Year Summary https://www.nwrfc.noaa.gov/water_supply/wy_summary/wy_summary.php?tab=1.

(230) Facts About the Willamette River http://willamette-riverkeeper.org/basicsfacts/ (accessed Feb 19, 2018).

(231) Pitt, R.; Clark, S.; Field, R. Groundwater Contamination Potential from Stormwater Infiltration Practices. *Urban Water* **1999**, *1* (3), 217–236.

(232) Fuhrer, B. G. J.; Tanner, D. Q.; Morace, J. L.; Mckenzie, S. W.; Skach, K. A. Water Quality of the Lower Columbia River Basin : Analysis of Current and Historical Water-Quality Data through 1994 Water Quality of the Lower Columbia River Basin : Analysis of Current and Historical Water-Quality Data through 1994. **1994**.

(233) Van Nuijs, A. L. N.; Tarcomnicu, I.; Simons, W.; Bervoets, L.; Blust, R.; Jorens, P. G.; Neels, H.; Covaci, A. Optimization and Validation of a Hydrophilic Interaction Liquid Chromatography-Tandem Mass Spectrometry Method for the Determination of 13 Top-Prescribed Pharmaceuticals in Influent Wastewater. *Anal. Bioanal. Chem.* **2010**, *398* (5), 2211–2222.

(234) Dolan, J. W. Gradient Elution, Part V: Baseline Drift Problems. *LCGC North Am.* **2013**, *31* (7), 538–543.

(235) Sigma Aldrich. HPLC Troubleshooting Guide https://www.sigmaaldrich.com/united-states.html.

(236) ten Hulscher, T. E. M.; Cornelissen, G. Effect of Temperature on Sorption Equilibrium and Sorption Kinetics of Organic Micropollutants - A Review. *Chemosphere* **1996**, *32* (4), 609–626.

(237) Bäuerlein, P. S.; Mansell, J. E.; Ter Laak, T. L.; De Voogt, P. Sorption Behavior of Charged and Neutral Polar Organic Compounds on Solid Phase Extraction Materials: Which Functional Group Governs Sorption? *Environ. Sci. Technol.* **2012**, *46* (2), 954–961.

(238) Droge, S. T. J.; Goss, K. U. Sorption of Organic Cations to Phyllosilicate Clay Minerals: CEC-Normalization, Salt Dependency, and the Role of Electrostatic and Hydrophobic Effects. *Environ. Sci. Technol.* **2013**, *47* (24), 14224–14232.

(239) Mrozik, W.; Stefańska, J. Adsorption and Biodegradation of Antidiabetic Pharmaceuticals in Soils. *Chemosphere* **2014**, *95*, 281–288.

(240) Mondal, S.; Samajdar, R. N.; Mukherjee, S.; Bhattacharyya, A. J.; Bagchi, B. Unique Features of Metformin: A Combined Experimental, Theoretical, and

Simulation Study of Its Structure, Dynamics, and Interaction Energetics with DNA Grooves. *J. Phys. Chem. B* **2018**, *122* (8), 2227–2242.

(241) *Sediment/Water Interactions : Proceedings of the Fourth International Symposium*; Sly, P. G., Hart, B. T., Eds.; Springer Netherlands, 1989.

(242) Crago, J.; Bui, C.; Grewal, S.; Schlenk, D. Age-Dependent Effects in Fathead Minnows from the Anti-Diabetic Drug Metformin. *Gen. Comp. Endocrinol.* **2016**, *232*, 185–190.

(243) Eggen, T.; Lillo, C. Antidiabetic II Drug Metformin in Plants: Uptake and Translocation to Edible Parts of Cereals, Oily Seeds, Beans, Tomato, Squash, Carrots, and Potatoes. *J. Agric. Food Chem.* **2012**, *60* (28), 6929–6935.

(244) Forslund, K.; Hildebrand, F.; Nielsen, T.; Falony, G.; Le Chatelier, E.; Sunagawa, S.; Prifti, E.; Vieira-Silva, S.; Gudmundsdottir, V.; Pedersen, H. K.; et al. Disentangling Type 2 Diabetes and Metformin Treatment Signatures in the Human Gut Microbiota. *Nature* **2015**, *528* (7581), 262–266.

(245) Coogan, M. A.; Edziyie, R. E.; La Point, T. W.; Venables, B. J. Algal Bioaccumulation of Triclocarban, Triclosan, and Methyl-Triclosan in a North Texas Wastewater Treatment Plant Receiving Stream. *Chemosphere* **2007**, *67* (10), 1911–1918.

(246) Eguchi, K.; Nagase, H.; Ozawa, M.; Endoh, Y. S.; Goto, K.; Hirata, K.; Miyamoto, K.; Yoshimura, H. Evaluation of Antimicrobial Agents for Veterinary Use in the Ecotoxicity Test Using Microalgae. *Chemosphere* **2004**, *57* (11), 1733–1738.

(247) Johnson, D. J.; Sanderson, H.; Brain, R. A.; Wilson, C. J.; Solomon, K. R. Toxicity and Hazard of Selective Serotonin Reuptake Inhibitor Antidepressants Fluoxetine, Fluvoxamine, and Sertraline to Algae. *Ecotoxicol. Environ. Saf.* **2007**, *67* (1), 128–139.

(248) Harada, A.; Komori, K.; Nakada, N.; Kitamura, K.; Suzuki, Y. Biological Effects of PPCPs on Aquatic Lives and Evaluation of River Waters Affected by Different Wastewater Treatment Levels. *Water Sci. Technol.* **2008**, *58* (8), 1541.

(249) Thomas, ter laak; Kirsten, B. The Occurrence, Fate and Ecological and Human Health Risks of Metformin and Guanylurea in Water Cycle - A Literature Review. **2014**, No. January, 18.

(250) de Solla, S. R.; Gilroy, È. A. M.; Klinck, J. S.; King, L. E.; McInnis, R.; Struger, J.; Backus, S. M.; Gillis, P. L. Bioaccumulation of Pharmaceuticals and Personal Care Products in the Unionid Mussel Lasmigona Costata in a River Receiving Wastewater Effluent. *Chemosphere* **2016**, *146*, 486–496.

(251) Hedbacker, K. SNF1/AMPK Pathways in Yeast. *Front. Biosci.* **2008**, *13* (13), 2408.

(252) Tsai, A. Y.-L.; Gazzarrini, S. Trehalose-6-Phosphate and SnRK1 Kinases in Plant Development and Signaling: The Emerging Picture. *Front. Plant Sci.* **2014**, *5* (April), 1–11.

(253) Baena-González, E.; Rolland, F.; Thevelein, J. M.; Sheen, J. A Central Integrator of Transcription Networks in Plant Stress and Energy Signalling. *Nature* **2007**, *448*

(7156), 938–942.

(254) Lehti-Shiu, M. D.; Shiu, S.-H. Diversity, Classification and Function of the Plant Protein Kinase Superfamily. *Philos. Trans. R. Soc. B Biol. Sci.* **2012**, *367* (1602), 2619–2639.

(255) Rawat, I.; Gupta, S. K.; Shriwastav, A.; Singh, P.; Kumari, S.; Bux, F. Microalgae Applications in Wastewater Treatment; Springer, Cham, 2016; pp 249–268.

(256) Gupta, S. K.; Malik, A.; Bux, F. (Faizel). *Algal Biofuels : Recent Advances and Future Prospects*.

(257) Guillard, R. R. L.; Lorenzen, C. J. Yellow-Green Algae with Chlorophyllidae C12. *J. Phycol.* **1972**, *8* (1), 10–14.

(258) Harrison, P. J.; Waters, R. E.; Taylor, F. J. R. A Broad Spectrum Artificial Seawater Medium for Coastal and Open Ocean Phytoplankton. *J. Phycol.* **1980**, *16* (1), 28–35.

(259) Berges, J. A.; Franklin, D. J.; Harrison, P. J. Evolution of an Artificial Seawater Medium: Improvements in Enriched Seawater, Artificial Water over the Last Two Decades. *J. Phycol.* **2001**, *37* (6), 1138–1145.

(260) Sun, H. Q.; Du, Y.; Zhang, Z. Y.; Jiang, W. J.; Guo, Y. M.; Lu, X. W.; Zhang, Y. M.; Sun, L. W. Acute Toxicity and Ecological Risk Assessment of Benzophenone and N,N-Diethyl-3 Methylbenzamide in Personal Care Products. *Int. J. Environ. Res. Public Health* **2016**, *13* (9).

(261) Archana, G.; Dhodapkar, R.; Kumar, A. Ecotoxicological Risk Assessment and Seasonal Variation of Some Pharmaceuticals and Personal Care Products in the Sewage Treatment Plant and Surface Water Bodies (Lakes). *Environ. Monit. Assess.* **2017**, *189* (9).

(262) Rubasinghege, G.; Gurung, R.; Rijal, H.; Maldonado-Torres, S.; Chan, A.; Acharya, S.; Rogelj, S.; Piyasena, M. Abiotic Degradation and Environmental Toxicity of Ibuprofen: Roles of Mineral Particles and Solar Radiation. *Water Res.* **2018**, *131*, 22–32.

(263) Lu, T.; Zhu, Y.; Xu, J.; Ke, M.; Zhang, M.; Tan, C.; Fu, Z.; Qian, H. Evaluation of the Toxic Response Induced by Azoxystrobin in the Non-Target Green Alga Chlorella Pyrenoidosa. *Environ. Pollut.* **2018**, *234*, 379–388.

(264) Geiger, E.; Hornek-Gausterer, R.; Saçan, M. T. Single and Mixture Toxicity of Pharmaceuticals and Chlorophenols to Freshwater Algae Chlorella Vulgaris. *Ecotoxicol. Environ. Saf.* **2016**, *129*, 189–198.

(265) Tausz, C. Phytoplankton Dynamics in off-Channel Habitats of the Lower Columbia River Estuary. *Sch. Arch.* **2015**.

(266) Maier, M. A.; Peterson, T. D. Observations of a Diatom Chytrid Parasite in the Lower Columbia River. *Northwest Sci.* **2014**, *88* (3), 234–245.

(267) Mosser, J. L.; Teng, T. C.; Walther, W. G.; Wurster, C. F. Interactions of PCBs, DDT and DDE in a Marine Diatom. *Bull. Environ. Contam. Toxicol.* **1974**, *12* (6), 665–668.

(268) Doelman, P.; Haanstra, L. Effects of Lead on the Soil Bacterial Microflora. *Soil Biol. Biochem.* **1979**, *11* (5), 487–491.

(269) Hemida, S. K.; Omar, S.A.; Abdel-Mallek, A.Y. Microbial Populations and Enzyme Activity in Soil Treated with Heavy Metals. *Water. Air. Soil Pollut.* **1997**, *95* (1/4), 13–22.

(270) Egorova, E. A.; Drozdova, I. S.; Bukhov, N. G. Modulating Effect of Far-Red Light on Activities of Alternative Electron Transport Pathways Related to Photosystem I. *Russ. J. Plant Physiol.* **2005**, *52* (6), 709–716.

(271) Hill, R.; Ralph, P. J. Dark-Induced Reduction of the Plastoquinone Pool in Zooxanthellae of Scleractinian Corals and Implications for Measurements of Chlorophyll a Fluorescence. *Symbiosis (Rehovot)* **2008**, *46* (1), 45–56.

(272) Ralph, P. J.; Hill, R.; Doblin, M. A.; Davy, S. K. Theory and Application of Pulse Amplitude Modulated Chlorophyll Fluorometry in Coral Health Assessment. In *Diseases of Coral*; John Wiley & Sons, Inc: Hoboken, NJ, 2015; pp 506–523.

(273) White, E. M.; Kieber, D. J.; Sherrard, J.; Miller, W. L.; Mopper, K. Carbon Dioxide and Carbon Monoxide Photoproduction Quantum Yields in the Delaware Estuary. *Mar. Chem.* **2010**, *118* (1–2), 11–21.

(274) Figueroa, F.; Conde-Alvarez, R.; Gomez, I. Relations between Electrion Transport Rates Determined by Pulse Amplitude Modulated Chlorophyll Fluorescence and Oxygen Evolution in Macroalgae under Different Light Conditions. *Photosynth. Res.* **2003**, *75*, 259–275.

(275) Weibull, W. A Statistical Distribution Function of Wide Applicability. *Journal of applied mechanics*. 1951, pp 293–297.

(276) Platt, T.; Gallegos, C. L.; Harrison, W. G. Photoinhibition of Photosynthesis in Natural Assemblages of Marine Phytoplankton. *J. Mar. Res.* **1980**, *38*, 687–701.

(277) Kirkwood, A. *Metformin Hydrochloride - 72-Hour Acute Toxicity Test with Freshwater Green Alga, Pseudokirchneriella Subcapitata, Following OECD Guideline #201 and the Official Journal of the European Communities L220/36, Method C.3. Springborn Smithers Study No. 13751.*; 2011.

(278) Converti, A.; Casazza, A. A.; Ortiz, E. Y.; Perego, P.; Del Borghi, M. Effect of Temperature and Nitrogen Concentration on the Growth and Lipid Content of Nannochloropsis Oculata and Chlorella Vulgaris for Biodiesel Production. *Chem. Eng. Process. Process Intensif.* **2009**, *48* (6), 1146–1151.

(279) Lomas, M. W.; Lomas, M. W.; Glibert, P. M.; Glibert, P. M. Interactions between NH4+ and NO3- Uptake and Assimilation: Comparison of Diatoms and Dino‾agellates at Several Growth Temperatures. *Mar. Biol.* **1999**, *133*, 541–551.

(280) Zhang, Y.; Primavesi, L. F.; Jhurreea, D.; Andralojc, P. J.; Mitchell, R. A. C.; Powers, S. J.; Schluepmann, H.; Delatte, T.; Wingler, A.; Paul, M. J. Inhibition of SNF1-Related Protein Kinase1 Activity and Regulation of Metabolic Pathways by Trehalose-6-Phosphate. *Plant Physiol.* **2009**, *149* (4), 1860–1871.

(281) Polge, C.; Thomas, M. SNF1/AMPK/SnRK1 Kinases, Global Regulators at the Heart of Energy Control? *Trends Plant Sci.* **2007**, *12* (1), 20–28.

(282) Sugden, C.; Crawford, R. M.; Halford, N. G.; Hardie, D. G. Regulation of Spinach SNF1-Related (SnRK1) Kinases by Protein Kinases and Phosphatases Is Associated with Phosphorylation of the T Loop and Is Regulated by 5'-AMP. *Plant J.* **1999**, *19* (4), 433–439.

(283) Crozet, P.; Margalha, L.; Confraria, A.; Rodrigues, A.; Martinho, C.; Adamo, M.; Elias, C. A.; Baena-GonzÃ¡lez, E. Mechanisms of Regulation of SNF1/AMPK/SnRK1 Protein Kinases. *Front. Plant Sci.* **2014**, *5* (May), 1–17.

(284) Halford, N. G.; Hey, S.; Jhurreea, D.; Laurie, S.; McKibbin, R. S.; Paul, M.; Zhang, Y. Metabolic Signalling and Carbon Partitioning: Role of Snf1-Related (SnRK1) Protein Kinase. *J. Exp. Bot.* **2003**, *54* (382), 467–475.

(285) Shen, W.; Reyes, M. I.; Hanley-Bowdoin, L. Arabidopsis Protein Kinases GRIK1 and GRIK2 Specifically Activate SnRK1 by Phosphorylating Its Activation Loop. *Plant Physiol.* **2009**, *150* (2), 996–1005.

(286) Mohannath, G.; Jackel, J. N.; Lee, Y. H.; Buchmann, R. C.; Wang, H.; Patil, V.; Adams, A. K.; Bisaro, D. M. A Complex Containing SNF1-Related Kinase (SnRK1) and Adenosine Kinase in Arabidopsis. *PLoS One* **2014**, *9* (1).

(287) Lipscomb, D. The Eukaryote Tree of Life. In *Beyond Cladistics: The Branching of a Paradigm*; Williams, D. M., Knapp, S., Eds.; University of California Press, 2010; pp 219–240.

(288) Spetea, C.; Pfeil, B. E.; Schoefs, B. Phylogenetic Analysis of the Thylakoid ATP/ADP Carrier Reveals New Insights into Its Function Restricted to Green Plants. *Front. Plant Sci.* **2012**, *2* (January), 1–11.

(289) Goss, R.; Oroszi, S.; Wilhelm, C. The Importance of Grana Stacking for Xanthophyll Cycle-Dependent NPQ in the Thylakoid Membranes of Higher Plants. *Physiol. Plant.* **2007**, *131* (3), 496–507.

(290) Saranjampour, P.; Vebrosky, E. N.; Armbrust, K. L. Salinity Impacts on Water Solubility and *N*-Octanol/water Partition Coefficients of Selected Pesticides and Oil Constituents. *Environ. Toxicol. Chem.* **2017**, *36* (9), 2274–2280.

(291) Horie. Recent Advances in Pharmacokinetic Modeling. *Biopharm. Drug Dispos.* **2007**, *28* (3), 135–143.

(292) Koepsell, H.; Lips, K.; Volk, C. Polyspecific Organic Cation Transporters: Structure, Function, Physiological Roles, and Biopharmaceutical Implications. *Pharm. Res.* **2007**, *24* (7), 1227–1251.

(293) Pittman, J. K.; Edmond, C.; Sunderland, P. A.; Bray, C. M. A Cation-Regulated and Proton Gradient-Dependent Cation Transporter from Chlamydomonas Reinhardtii Has a Role in Calcium and Sodium Homeostasis. *J. Biol. Chem.* **2009**, *284* (1), 525–533.

(294) Luo, Y.; Reid, R.; Freese, D.; Li, C.; Watkins, J.; Shi, H.; Zhang, H.; Loraine, A.; Song, B. H. Salt Tolerance Response Revealed by RNA-Seq in a Diploid Halophytic Wild Relative of Sweet Potato. *Sci. Rep.* **2017**, *7* (1), 1–13.

(295) Shu, S.; Yuan, Y.; Chen, J.; Sun, J.; Zhang, W.; Tang, Y.; Zhong, M.; Guo, S. The Role of Putrescine in the Regulation of Proteins and Fatty Acids of Thylakoid

Membranes under Salt Stress. *Sci. Rep.* **2015**, *5* (March), 1–16.

(296) Batoulis, H.; Schmidt, T. H.; Weber, P.; Schloetel, J. G.; Kandt, C.; Lang, T. Concentration Dependent Ion-Protein Interaction Patterns Underlying Protein Oligomerization Behaviours. *Sci. Rep.* **2016**, *6* (April), 2–10.

(297) Myers, V. B.; Iverson, R. L.; Harriss, R. C. The Effect of Salinity and Dissolved Organic Matter on Surface Charge Characteristics of Some Euryhaline Phytoplankton. *J. Exp. Mar. Bio. Ecol.* **1975**, *17* (1), 59–68.

(298) Serfontein, J.; Nisbet, R. E. R.; Howe, C. J.; Vries, P. J. De. Evolution of the TSC1 / TSC2-TOR Signaling Pathway. **2014**, *3* (128), 1–7.

(299) van Dam, T. J. P.; Zwartkruis, F. J. T.; Bos, J. L.; Snel, B. Evolution of the TOR Pathway. *J. Mol. Evol.* **2011**, *73* (3–4), 209–220.

(300) Lüttge, U.; Cánovas, Francisco; Matyssek, Rainer. Progress in Botany. *Science (80-.).* **2016**, *77*.

(301) Fairbairn, D. J.; Karpuzcu, M. E.; Arnold, W. A.; Barber, B. L.; Kaufenberg, E. F.; Koskinen, W. C.; Novak, P. J.; Rice, P. J.; Swackhamer, D. L. Sources and Transport of Contaminants of Emerging Concern: A Two-Year Study of Occurrence and Spatiotemporal Variation in a Mixed Land Use Watershed. *Sci. Total Environ.* **2016**, *551–552*, 605–613.

(302) Petrovic, M.; Ginebreda, A.; Acuña, V.; Batalla, R. J.; Elosegi, A.; Guasch, H.; de Alda, M. L.; Marcé, R.; Muñoz, I.; Navarro-Ortega, A.; et al. Combined Scenarios of Chemical and Ecological Quality under Water Scarcity in Mediterranean Rivers. *TrAC - Trends Anal. Chem.* **2011**, *30* (8), 1269–1278.

(303) Herring S. C.; Hoell, A. . H. M. P. . K. J. P. . S. I. I. I. C. J. . S. P. A. E. Explaining Extreme Events of 2015 from a Climate Perspective. *Bull. Am. Meteorol. Soc.* **2016**, *97* (12), S1–S145.

(304) Kortenkamp, A.; Backhaus, T.; Faust, M. *State of the Art Report on Mixture Toxicity*; 2009; Vol. Contract N.

(305) Kantor, E. D.; Rehm, C. D.; Haas, J. S.; Chan, A. T.; Giovannucci, E. L. Trends in Prescription Drug Use Among Adults in the United States From 1999-2012. *Jama* **2015**, *314* (17), 1818.

(306) Ginsberg, H. N. Review: Efficacy and Mechanisms of Action of Statins in the Treatment of Diabetic Dyslipidemia. *J. Clin. Endocrinol. Metab.* **2006**, *91* (2), 383–392.

(307) Moses, R. G. Combination Therapy for Patients with Type 2 Diabetes: Repaglinide in Combination with Metformin. *Expert Rev. Endocrinol. Metab.* **2010**, *5* (3), 331–342.

(308) Haak, T. Combination of Linagliptin and Metformin for the Treatment of Patients with Type 2 Diabetes. *Clin. Med. Insights Endocrinol. Diabetes* **2015**, *8*, CMED.S10360.

(309) Nowell, L. H.; Moran, P. W.; Schmidt, T. S.; Norman, J. E.; Nakagaki, N.; Shoda, M. E.; Mahler, B. J.; Van Metre, P. C.; Stone, W. W.; Sandstrom, M. W.; et al.

Complex Mixtures of Dissolved Pesticides Show Potential Aquatic Toxicity in a Synoptic Study of Midwestern U.S. Streams. *Sci. Total Environ.* **2018**, *613–614*, 1469–1488.

(310) Dantzger, D. D.; Jonsson, C. M.; Aoyama, H. Mixtures of Diflubenzuron and P-Chloroaniline Changes the Activities of Enzymes Biomarkers on Tilapia Fish (Oreochromis Niloticus) in the Presence and Absence of Soil. *Ecotoxicol. Environ. Saf.* **2018**, *148* (October 2017), 367–376.

(311) Centers for Disease Control Prevention. *Diabetes 2014 Report Card*; 2014.

(312) Knowler, W. C.; Barrett-Connor, E.; Fowler, S. E.; Hamman, R. F.; Lachin, J. M.; Walker, E. A.; Nathan, D. M.; Diabetes Prevention Program Research Group. Reduction in the Incidence of Type 2 Diabetes with Lifestyle Intervention or Metformin. *N. Engl. J. Med.* **2002**, *346* (6), 393–403.

(313) Tuomilehto J., Indstrom J., Eriksson J., Valle T., H. E. & U. M. Numb Er 18 Prevention of Type 2 Diabetes Mellitus By Changes in Lifestyle Among Subjects With Impaired Glucose Tolerance. *N. Engl. J. Med.* **2001**, *344* (18), 1343–1350.

(314) de Groot, M.; Anderson, R.; Freedland, K. E.; Clouse, R. E.; Lustman, P. J. Association of Depression and Diabetes Complications: A Meta-Analysis. *Psychosom. Med.* **2001**, *63* (4), 619–630.

(315) Wanless D. Securing Our Future Gealth: Taking a Long-Term View- Final Report. **2002**, No. April.

(316) Jacobson, A. M. Impact of Improved Glycemic Control on Quality of Life in Patients With Diabetes. *Endocr. Pract.* **2004**, *10* (6), 502–508.

APPENDICES

Appendix Table 2A. Monthly metformin and guanylurea concentrations (ng L^{-1}) for year-round sites along the lower Columbia River for the entire sampling period (October 2016-September 2017). Standard deviations are in parentheses.

Month	Metformin (ng L^{-1})	Guanylurea (ng L^{-1})
October	47.4 (±35)	99.4 (±52)
November	53.3 (±48)	62.5 (±59)
December	56.2 (±42)	49.2 (±35)
January	55.6 (±32)	30.4 (±33)
February	27.1(±15)	8.5 (±17)
March	23.6 (±9)	14.9 (±53)
April	21.5 (±16)	10.9 (±21)
May	84.4 (±123)	7.2 (±23)
June	52.9 (±106)	5.0 (±7)
July	183.8 (±306)	1.1 (±3)
August	66.0 (±62)	29.7 (±29)
September	131.4 (±194)	69.3 (±168)

Appendix Table 2B. Metformin and guanylurea concentrations (ng L^{-1}) at year-round sampling sites along the lower Columbia River for the entire sampling period (October 2016-September 2017). River kilometer is a measure of the distance (km) from the mouth of the river. Standard deviations are in parentheses.

Site Abbrev.	River kilometer	Metformin (ng L^{-1})	Guanylurea (ng L^{-1})
BAT	79	69 (±38)	26 (±34.4)
KD	114	113 (±187.8)	30 (±50)
KU	114	56 (±42)	36 (±46.3)
KPP	156	112 (±170.2)	23 (±23.9)
CHL	183	67 (±163.5)	47 (±147.3)
CMS	187	97 (±225.6)	29 (±45.2)
RR	200	42 (±84.1)	42 (±53.5)
OH	261	83 (±223.7)	18 (±18.8)
IH	261	48 (±74.2)	35 (±61.3)

Appendix Table 3A. Comparison of average cell density and specific growth rate between control and treatment cultures at the time of the spike (0 h) versus 5 h after the spike. P-values ≤0.05 indicates significant difference between control and treatment cultures.

Species	Time After Spike (h)	Treatment	Average Cell Density (cells/mL)	p-value	Average Growth Rate (cells/mL)	p-value
T. weissflogii	0	Control	112638 (±30485)		0.043 (±0.013)	
		1 µg/L	116603 (±11207)	0.984	0.054 (±0.009)	0.999
		60 µg/L	104874 (±21966)	0.895	0.048 (±0.005)	1.000
		400 µg/L	114348 (±16120)	0.999	0.044 (±0.005)	>0.9999
	5	Control	150499 (±2716)		0.11 (±0.15)	
		1 µg/L	137091 (±20298)	0.621	0.02 (±0.02)	0.614
		60 µg/L	142006 (±13348)	0.868	0.14 (±0.05)	0.975
		400 µg/L	144888 (±7638)	0.957	0.11 (±0.04)	>0.9999
C. vulgaris	0	Control	6263237 (±689367)		0.045 (±0.006)	
		1 µg/L	5401901 (±929268)	0.313	0.044 (±0.008)	0.990
		80 µg/L	4646916 (±913273)	0.009	0.031 (±0.004)	0.996
		500 µg/L	6368082 (±977600)	0.997	0.043 (±0.008)	0.913
	5	Control	6314556 (±778572)		-0.002 (±0.007)	
		1 µg/L	5271563 (±870020)	0.162	-0.002 (±0.01)	0.266
		80 µg/L	4521906 (±936147)	0.003	-0.0039 (±0.005)	0.831
		500 µg/L	5765352 (±1112852)	0.687	-0.0068 (±0.03)	0.998

Appendix Table 3B. Comparison of growth curve model fit and predicted growth parameters for control and treatment cultures after 5 h of metformin exposure. Growth curves were fit with exponential growth models.

Species	Treatment	R2	Specific Growth Rate (μ)	AVG Resid Error (S)
T. weissflogii	Control	0.926	0.046	0.007
	1 µg/L	0.965	0.047	0.005
	60 µg/L	0.941	0.047	0.007
	400 µg/L	0.972	0.044	0.004
C. vulgaris	Control	0.968	0.041	0.004
	1 µg/L	0.944	0.040	0.005
	80 µg/L	0.921	0.034	0.005
	500 µg/L	0.932	0.038	0.005

Appendix Table 3C. Comparison of photosynthetic parameters (α, β, ETRmax, and Ek) estimated by ETR light curve models at the time of the spike (0 h) versus 5 h after the spike. In actuality, 0 hours represents -0.67 h, i.e. pre-spike. Overall goodness of fit (R2), average residual error (S), and p-value associated with each parameter are shown for each treatment. P-values ≤0.05 indicate significant difference between respective control and treatment cultures at that timepoint. P-values for individual treatments were obtained using two-way ANOVAs with post-hoc Tukey HSD tests.

Species	Time After Spike (h)	Treatment	R2	S	α	p-value	β	p-value	ETRmax	p-value	Ek	p-value	φPSII	p-value	NPQ	p-value
T. weissflogii	0	Control	0.97	9.35	0.21 (±0.01)		6.02 (±0.3)		303.2 (±21)		886.3 (±62)		0.622 (±0.04)		0.846 (±0.08)	
		1 µg/L	0.98	7.25	0.21 (±0.02)	1.000	7.02 (±0.4)	0.995	303.1 (±8)	>0.9999	895.1 (±45)	1.000	0.623 (±0.04)	>0.9999	0.898 (±0.09)	0.911
		60 µg/L	0.94	13.30	0.21 (±0.02)	>0.9999	6.16 (±0.2)	0.634	303.4 (±6)	0.855	943.5 (±30)	0.808	0.645 (±0.05)	0.750	0.873 (±0.10)	0.985
		400 µg/L	0.97	8.48	0.21 (±0.02)	0.995	9.63 (±0.1)	0.895	294.2 (±6)	0.955	862.2 (±8)	0.984	0.653 (±0.05)	0.514	0.963 (±0.13)	0.451
	5	Control	0.98	6.98	0.18 (±0.02)		5.61 (±0.08)		293.7 (±7)		901.2 (±4)		0.579 (±0.04)		0.478 (±0.09)	
		1 µg/L	0.91	15.82	0.17 (±0.02)	0.938	6.98 (±0.2)	0.980	287.1 (±16)	0.542	871.7 (±58)	0.044	0.581 (±0.02)	0.999	0.522 (±0.05)	0.896
		60 µg/L	0.95	11.00	0.19 (±0.02)	0.875	6.25 (±0.4)	0.958	295.2 (±22)	0.890	895.1 (±81)	>0.9999	0.612 (±0.03)	0.460	0.636 (±0.07)	0.201
		400 µg/L	0.96	9.92	0.19 (±0.02)	0.878	7.65 (±0.5)	0.664	290.8 (±17)	0.841	873.0 (±66)	0.997	0.618 (±0.03)	0.307	0.629 (±0.10)	0.237
C. vulgaris	0	Control	0.98	10.80	0.34 (±0.003)		8.75 (±3)		141.3 (±12)		681.9 (±23)		0.699 (±0.005)		0.307 (±0.06)	
		1 µg/L	0.98	11.12	0.34 (±0.008)	0.976	8.42 (±0.5)	0.149	140.8 (±11)	>0.9999	687.1 (±23)	0.997	0.698 (±0.007)	>0.9999	0.376 (±0.09)	0.948
		80 µg/L	1.00	5.75	0.32 (±0.01)	0.064	7.11 (±0.7)	0.990	152.8 (±13)	>0.9999	739.2 (±55)	0.527	0.696 (±0.015)	0.969	0.368 (±0.09)	0.847
		500 µg/L	0.99	9.98	0.34 (±0.007)	1.000	7.78 (±3)	<0.0001	148.7 (±14)	0.845	704.7 (±29)	0.939	0.697 (±0.006)	0.990	0.317 (±0.08)	0.753
	5	Control	0.99	9.37	0.33 (±0.008)		7.31 (±0.5)		126.6 (±12)		710.0 (±12)		0.672 (±0.006)		0.172 (±0.02)	
		1 µg/L	0.99	9.03	0.33 (±0.005)	0.969	7.84 (±1)	0.023	145.9 (±37)	0.929	885.3 (±283)	0.895	0.673 (±0.009)	>0.9999	0.169 (±0.02)	0.562
		80 µg/L	0.99	9.12	0.33 (±0.008)	0.950	8.00 (±1)	0.508	136.9 (±11)	0.999	712.9 (±8)	0.999	0.671 (±0.003)	0.999	0.176 (±0.07)	0.665
		500 µg/L	0.98	11.47	0.33 (±0.009)	0.778	8.88 (±0.9)	0.000	138.5 (±7)	0.993	723.2 (±40)	0.906	0.682 (±0.015)	0.474	0.224 (±0.07)	0.998

144
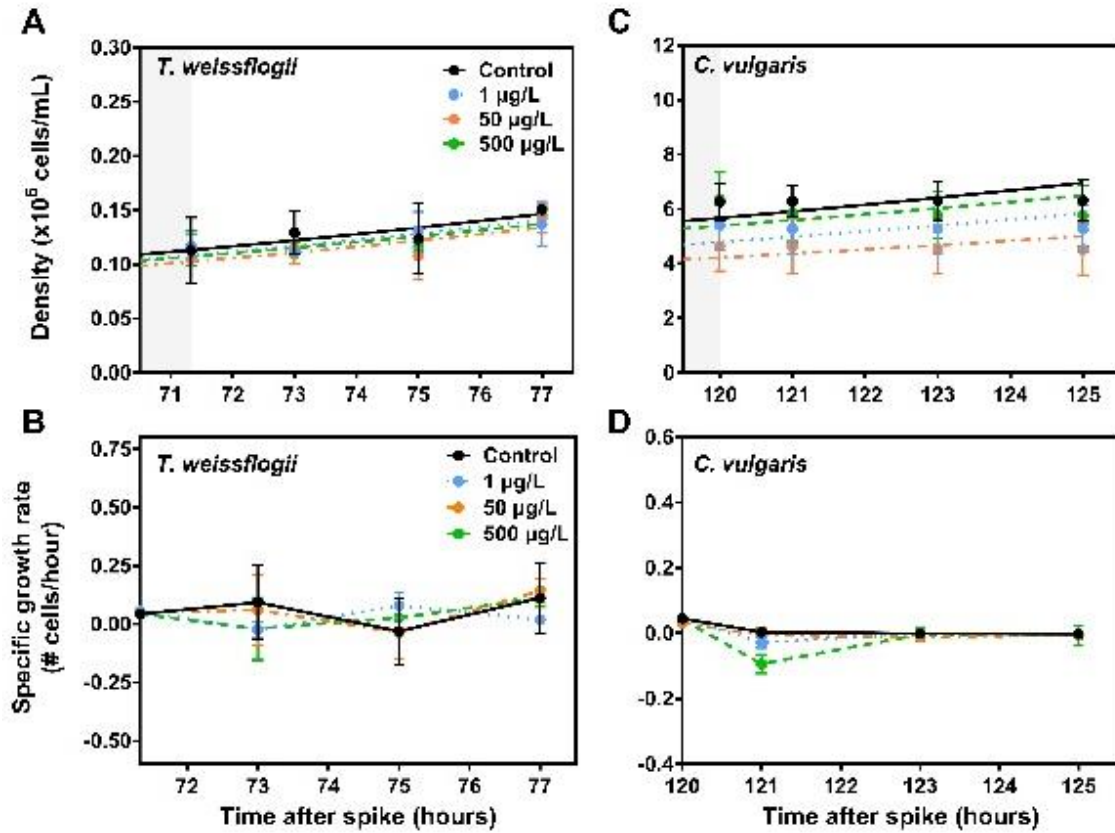
Appendix Figure 3A. Average algal culture density (A, C) and specific growth rates (B, D) in response to different levels of metformin exposure over a 5 h period. Grey areas in A and C indicate pre-spike growth.